Biological, Chemical, and Electronic Applications of Nanofibers

Luong T. H. Nguyen,* Shilin Chen, Naveen K. Elumalai, Molamma P. Prabhakaran, Yun Zong, Chellappan Vijila, Suleyman I. Allakhverdiev, Seeram Ramakrishna

With their high-surface-to-volume ratio, nanofibers have been postulated to increase interactions between nanofibrous materials and targeted substrates, which are helpful to overcome many obstacles and enhance the efficiency in a diverse number of applications. Over the past decade, many studies have been published on the fabrication of nanofibers and their applications in various fields. In this review, novel biological, chemical, and electrical characteristics of nanofibers as well as their recent status and achievements in medicine, chemistry, and electronics are analyzed. It is found that nanofibers can induce fast regeneration of many tissues/organs in medical applications and improve the efficiency of many chemical and electronics applications.

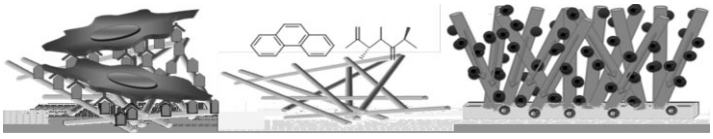

L. T. H. Nguyen
NUS Graduate School for Integrative Sciences and Engineering (NGS), National University of Singapore, 28 Medical Drive, Singapore 117456, Singapore
E-mail: hienluong@nus.edu.sg
S. Chen, N. K. Elumalai, Prof. S. Ramakrishna
Department of Mechanical Engineering, National University of Singapore, 9 Engineering Drive 1, Singapore 117576, Singapore
S. Chen, N. K. Elumalai, Dr. Y. Zong, Dr. C. Vijila
Institute of Materials Research and Engineering, A*STAR (Agency for Science, Technology and Research), 3 Research Link, Singapore 117602, Singapore
Dr. M. P. Prabhakaran
Faculty of Engineering, Center for Nanofibers and Nanotechnology, Nanoscience, and Nanotechnology Initiative, National University of Singapore, 2 Engineering Drive 3, Singapore 117576, Singapore
Dr. S. I. Allakhverdiev
Institute of Plant Physiology, Russian Academy of Sciences, Botanicheskaya Street 35, Moscow 127276, Russia, and Institute of Basic Biological Problems, Russian Academy of Sciences, Pushchino, Moscow Region 142290, Russia
Prof. S. Ramakrishna
King Saud University, Riyadh 11451, Kingdom of Saudi Arabia
E-mail: seeram@nus.edu.sg

Luong T. H. Nguyen, Shilin Chen, and Naveen Kumar Elumalai contributed equally to this work.

1. Introduction

With the development of nanotechnology during the past two decades, there have been a significantly increasing number of studies on nanofibers and their applications. The International Standards Organization (ISO) considers nanomaterials to be materials that are typically but not exclusively below 100 nm in at least one dimension. However, in informal non-wovens, textile, and other engineered fibers industries, it has been well accepted that nanofibers are fibers with diameters smaller than 1000 nm.[1] In 1992, carbon nanofibers were discovered to grow spontaneously by deposition from carbon vapor.[2] After that, many other techniques have been developed to fabricate nanofibers such as electrospinning,[3,4] self-assembly,[5,6] phase separation,[7,8] interfacial polymerization,[9,10] rapidly initiated polymerization,[11,12] template- or pattern-assisted growth,[13,14] vapor-liquid-solid growth[15,16] and hydrothermal synthesis,[17,18] etc. Due to the nanosize, nanofibers possess high-surface-to-volume ratios which help to increase interactions between the nanofibers and targeted substrates in different fields compared to other micro- to macro-size materials. Thus, using nanofibers could be a promising approach for the advanced developments in science and technology. In this

review, we aim to dissect novel characteristics of nanofibers and recent achievements in medicine, chemistry, and electronics. This will allow researchers on various fields to have an overview of the advantages of nanofibers and provide guidance for further developments of nanofibers.

2. Fabrication Methods of Nanofibers

There have been many techniques developed for the fabrication of nanofibers. Representative scanning electron microscope (SEM) images of the most popular methods are shown in Figure 1.

2.1. Electrospinning

Electrospinning is a technique using electrostatic forces to fabricate nanofibers. When a high voltage is applied to the droplet of a solution, the molecules of the solution becomes charged and an electrostatic repulsion occurs, which counteracts the surface tension of the droplet. When the high voltage increases to a critical point, a jet of the solution is erupted from the surface. As the solvent evaporates, further stretching of the charged jet under the electrostatic forces will push it into a bending instability stage. The elongation and thinning of the charged jet due to this instability lead to the formation of continuous fibers with diameters in nanoscale. Based on this principle, different electrospinning setups as well as different types of collectors have been designed to create various nanofibrous architectures.[3,4]

Properties such as the surface tension, viscosity, and density of net charges of the polymer jet highly influenced the morphology of the fibers. Solution concentration is considered as a major factor that affects the fiber size, and fiber diameter increases with increasing solution concentration.[26] The morphology of fibers has a strong correlation to solution viscosity as well as the solution concentration and temperature.[27] Lower diameter fibers were prepared by electrospinning of poly(lactic acid) (PLA) with tetraethylbenzylammonium chloride (TEBAC), whereby TEBAC increased the surface tension and electrical conductivity of the solution. Electrically induced double layer in combination with the polyelectrolytic nature of solution was also anticipated as a method for formation of high-aspect-ratio polyamide-6 nanofibers with diameters as small as 9–28 nm.[28] In many cases, randomly oriented fibers are deposited on a flat collector plate forming a non-woven mat of fibers. Another approach commonly applied is using a spinneret containing two needles to produce composite nanofibers.[29] Moreover, many different types of molecules can be incorporated into the fibers and a wide range of polymers are electrospun in varying fiber diameters ranging from <100 nm to micrometer levels using electrospinning. Controlled fiber deposition techniques are also applied for the fabrication of aligned nanofibers, on a rotation drum or a rotating rim. Using a collector designed of two conductive strips separated by a void gap of desired width, uniaxially aligned nanofibers were produced too. The alignment of the fibers could induce cell elongation and reorganize the cytoskeletal structures that regulate the cell adhesion and morphology. However, electrospinning has limitations of low productivity, as solutions are usually fed at a low rate so as to produce fibers of low diameter.

Various structural variations of the nanofibers include careful design of core-shell nanofibers, porous surface scaffolds or even multilayered fiber structures. Electrospun nanofibers of these architectures can act as drug delivery

Dr. Seeram Ramakrishna, FREng, FNAE, FAIMBE, is a professor of materials engineering at the National University of Singapore. He pioneered translucent biomaterials and devices, which are now marketed globally. He ranges among the world's topmost researchers in the field electrospinning. He authored 5 books and over 400 international journal papers, which attracted approximately 14 000 citations with an H-index of 55 and G-index of 82. He is placed 27th in the world in biocompatable materials experts by Elsevier Science. Thomson Reuters Web of Knowledge Essential Science Indicators (ESI) places him among the top 1% of materials scientists worldwide (ESI rank is 30).

Yun Zong received his B. Sc. and M. Sc. degrees in Chemistry from Wuhan University in China, and his D. Sc. from the University of Mainz in Germany. He is currently a Scientist at the Institute of Materials Research and Engineering. His current research focuses on the development of new functional colloidal nanoparticles and nanostructured hybrid materials for various applications.

Chellappan Vijila received her Ph.D. degree in physics from Anna University, Chennai, India, in 2001. From 2001 to 2002, she was with Åbo Akademi University, Turku, Finland, as a post-doctoral research fellow working on excited state dynamics of organic semiconductors using transient absorption spectroscopy techniques. In 2003, she joined with the Institute of Materials Research and Engineering, Agency for Science, Technology, and Research, Singapore, where she is currently a scientist carrying out research on organic optoelectronic devices and optical/electrical properties of organic electronic materials especially on charge transport properties using transient photoconductivity techniques.

Macromol. Mater. Eng. **2012**, DOI: 10.1002/mame.201200143

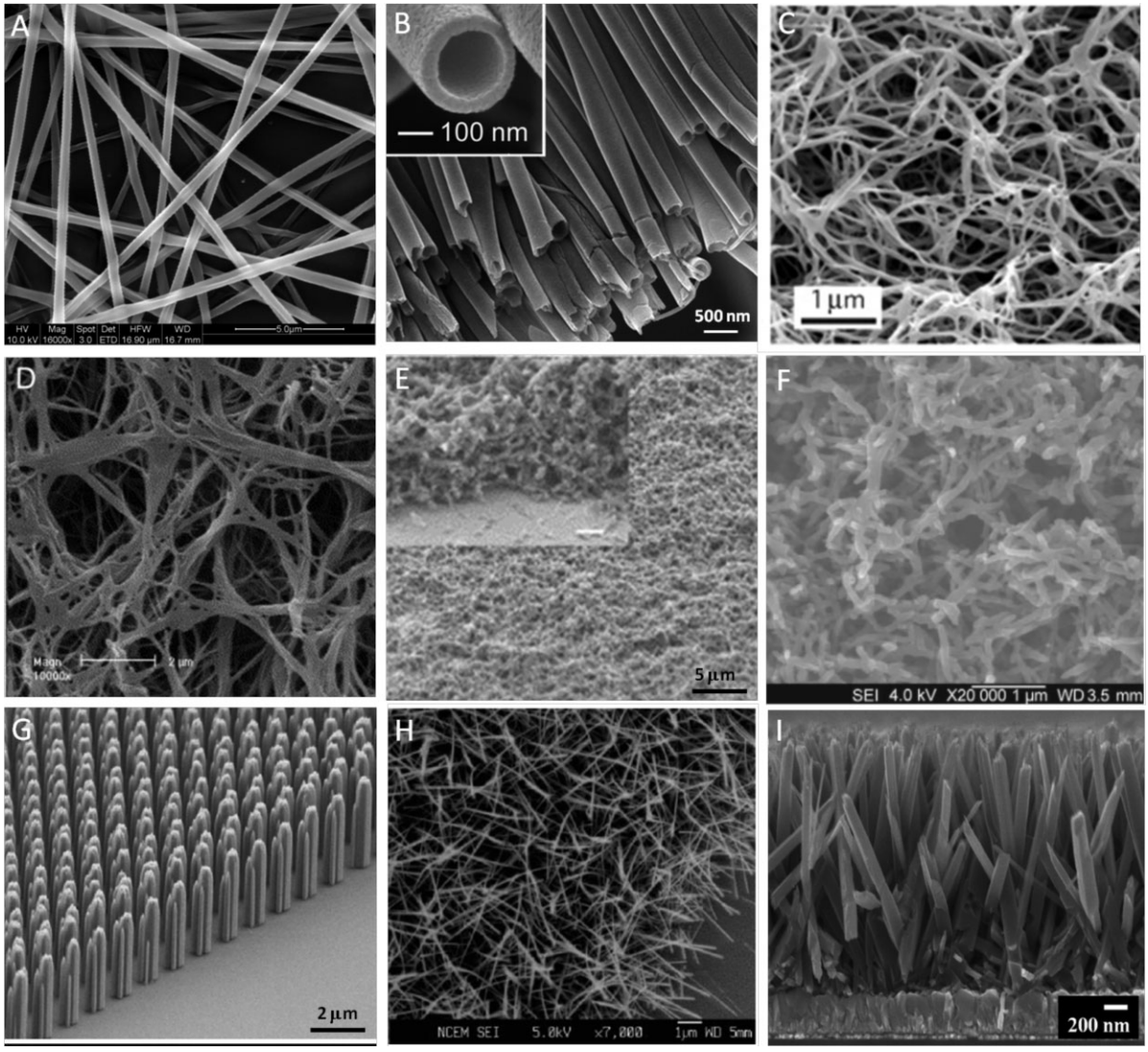

Figure 1. Representative SEM images of nanofibers fabricated by different techniques: (A) PLLA nanofibers fabricated by electrospinning, (B) TiO_2 hollow fibers fabricated by electrospinning,[19] (C) PLLA nanofibers fabricated by self-assembly,[20] (D) PLLA nanofibers fabricated by thermally induced liquid-liquid phase separation,[21] (E) Polyaniline nanofibers fabricated by interfacial polymerization,[9] (F) Polyaniline nanofibers fabricated by rapidly initiated polymerization,[22] (G) ZnO nanofibers fabricated by template assisted growth,[23] (H) ZnO nanofibers fabricated by vapor-liquid-solid liquid growth[24] and (I) TiO_2 nanofibers fabricated by hydrothermal synthesis.[25]

reservoirs for controlled and timely release of drugs, proteins, antioxidants, and other molecules to the site of tissue repair. The use of molten polymers to produce electrospun mats introduced as "melt electrospinning" is an environmentally benign process since it implies a solvent free approach.[30] Cellular infiltration within the electrospun scaffold remains a great challenge and methods such as cell electrospraying are also concurrently performed during the fabrication of a vascular conduit.[31]

Benefits of electrospinning technique are plenty, but challenges of obtaining a three-dimensional (3D) scaffold by electrospinning still remains a field of exploration. Nanofibrous and microfibrous 3D scaffolds of desired shape and size are more preferred as implantable materials compared to the electrospun 2D scaffolds. Compared to electrospinning, the major advantage of self-assembly is that it can produce fine nanofibers smaller than 10 nm and these nanofibers could be applied as injectable scaffolds for tissue regeneration. Pore sizes of 5–200 nm are insufficient for cell migration and proliferation.[32] In this respective, both electrospinning and self-assembly have one common drawback, of incapability to control the pore size and pore structure of the scaffolds. The challenge to integrate nanofibers into useful devices requires well-controlled

orientation, size, and other target characteristics of the nanofibers. Reproducibility in locating them in specific positions and orientations still remain to be faced.

2.2. Self Assembly

Self assembly is a bottom-up process in which small molecules spontaneously assemble into well-ordered nanofibers. The formation of this structure is induced by many interactions, including chiral dipole/dipole interactions, π–π stacking, hydrogen bonds, non-specific van der Waals interactions, hydrophobic forces, electrostatic interactions, and repulsive steric forces.[5] Normally, the basic molecules to fabricate nanofibers using this technique are peptide amphiphiles (PA). They consist of a dialkyl chain moiety (hydrophobic component/tail group) attached to an *N*-α-amino group of a peptide chain (hydrophilic component/head group).[6] The peptides can be self-assembled by many reagents such as acid, divalent ion, and covalent capture, etc.[5]

Bioactive sequences were introduced within PA with formation of the triple helix structure by Malkar et al.[33] and it demonstrated much similarity to the native self-assembled triple helix of the extracellular matrix (ECM). The self-assembly of PAs into nanofibers was developed by engineering of the peptide head group of the PA by controlling the pH of the solution.[34] In such a way, nanofibers of 5–8 nm in diameter with several μm lengths were developed by these researchers and it was investigated for mineralization potential, with application as primary building block for bone regeneration. With advances in this field, even the osteogenic differentiation of mesenchymal stem cells (MSCs) was possible in self-assembled PA nanofibers containing RGD peptide sequences.[35] Other methods for formation of self-assembled PAs include divalent ion induced self-assembly and drying on surface induced self-assembly.[5] Moreover, PAs can be self-assembled reversibly into nanofibers and hence it could be applied for versatile material fabrications. It produced nanofibers in high yield with low polydispersity, enabling further exploration of this method for developing "smart" biomaterial scaffolds for effective tissue regeneration.

2.3. Phase Separation

Thermally induced phase separation was commonly employed during the early days to produce porous polymeric scaffolds. The method was explored further to produce nanofibrous 3D structures from a variety of biodegradable polymers by Ma and Zhang.[7] Scaffolds with porous structure and interconnected spaces are greatly suitable for implantation, mainly because the continuous fibrous network provide interconnecting mechanical support for cell attachment, proliferation, and migration.[36] There are five basic steps in this technique: (i) polymer dissolution, (ii) phase separation and gelation, (iii) solvent extraction from the gel with water, (iv) freezing, and (v) freeze-drying under vacuum. The selection of proper solvent is considered as one of the most critical step of nanofibrous structure formation during this process. The formation of the nanofibrous structure is postulated to be caused by spinodal liquid-liquid phase separation of the polymer solutions and consequential crystallization of the polymer rich phase. The method does not require specialized instruments and it also allows for batch to batch consistency, while the architecture and scaffold properties can be controlled easily by varying the polymer concentration, gelation temperature/time, solvent, and freezing temperature.[7,8] Macroporosity was another feature that could be obtained within these scaffolds by incorporating porogens such as salt or sugars into the polymer solution during the phase separation process.[7] Such 3D macroporous structures are advantageous to the cells to absorb nutrients, receive signals, and to discard wastes. The presence of both nano- and macro-structures at the nanofiber level provide additional benefits to cell distribution and response.[8]

2.4. Interfacial Polymerization

Interfacial polymerization was developed as a template-free approach to synthesize large quantities of pure, uniform polyaniline nanofibers. Typically, an immiscible system consisting of an organic solution of aniline and an aqueous solution of ammonium peroxysulfate and acid are left to stand for some time. Nanofibers are obtained exclusively because the green polyaniline nanofibers formed in the early stages of aniline polymerization at the organic/aqueous interface diffuse into the aqueous phase, thus preventing secondary overgrowth of polyaniline on the nanofibers that produce agglomerates normally observed in traditional chemical oxidative polymerization of aniline in homogeneous aqueous systems. Pure polyaniline nanofibers are present in >95% by volume fraction of the polymer obtained with yields ranging from 6 to 10%. The nanofibers formed are typically twisted and interconnected with diameters ranging from 30 to 50 nm and length ≈500 nm to several micrometers. Doped and de-doped polyaniline nanofibers have similar morphology. Nanofiber diameters are affected by the choice of acid used, while quality and uniformity of the nanofibers are controlled by acid concentration; the higher the acid concentration, the higher the fraction of nanofibers in the final product. The type of organic solvent, monomer concentration (0.032–1.6 M) and reaction temperatures (5–60 °C) used have no effect on the size and

Macromolecular Journals
Macromol. Mater. Eng. **2012**, DOI: 10.1002/mame.201200143

morphology of polyaniline nanofibers. Polyaniline nanofibers synthesized by interfacial polymerization have a bimodal $\overline{M}_w$ distribution and a higher average $\overline{M}_w$ compared to bulk polyaniline obtained via traditional chemical oxidative polymerization.[9,10]

2.5. Rapidly Initiated Polymerization

Rapidly initiated polymerization is an alternative technique to interfacial polymerization for large-scale, template-free synthesis of pure, uniform polyaniline nanofibers. Generally, an initiator solution containing ammonium peroxydisulfate in HCl is poured into a monomer solution containing aniline in HCl all at once. The two solutions are then rapidly and vigorously mixed together for ≈15 s and left to stand for ≈1 d. Nanofibers are produced in this process because secondary overgrowth of polyaniline on nanofibers is prevented by rapid consumption of initiator molecules during the nanofiber formation phase of aniline polymerization. Polyaniline nanofibers obtained via rapidly initiated polymerization have comparable morphologies to those obtained by interfacial polymerization. The type of acid used influences the size of the polyaniline nanofibers formed, while polarity of the reaction medium affects the quality of nanofibers; the more polar the solvent, the better the quality of nanofibers. Reaction temperature and reactant concentration have no effect on nanofiber morphology.[11,12]

2.6. Template- or Pattern-Assisted Growth

This method facilitates the production of controlled arrangements of nanofibers. Porous template-based growth of nanofiber arrays can be obtained using well-established techniques such as electrochemical deposition and template filling. Various inorganic materials such as metal oxides, metals, semiconductors, and organic materials have been synthesized as nanofiber arrays using this technique.[37] The main drawback of this method can be listed as degradation of the template under longer polarizations and non-uniform pore filling for high-aspect-ratio nanostructures. Nanofibers from materials such as for NiO,[13] Cu_2O,[14] and ZnO[38] are developed using this method.

This method is basically a solution or colloidal dispersion process in which the geometric features such as diameter, density, and length of the 1D nanostructure can be controlled easily. Mesoporous metal oxides which are widely used for sensing and energy applications can be produced with well-defined and ordered porous structure by means of using surfactant as templates through sol-gel method. In specific cases, copolymer micelles is also used as templates to produce such nanostructures.[39,40] In this method, desired pore size, nanostructure morphology, size distribution, and density of pores can be obtained by selecting the appropriate template. The most commonly used template is alumina membranes which has uniform and parallel pores produced by anodic oxidation of aluminum sheets. Pore size can be controlled by chemical dissolution of the anodic oxide.[39]

2.7. Vapor-Liquid-Solid (VLS) Growth

This method is well known for synthesizing defect free one-dimensional (1D) nanostructures for a wide range of materials. The parameters of the nanofiber such as diameter, length, and composition as well as growth direction can be effectively controlled by understanding the mechanism of the VLS technique. The formation of metal nanodroplets from gaseous precursors plays a major role in the growth of nanofibers using this method. At first the dispersed metallic nanocrystals on a single crystalline substrate is melted in a tube furnace. Various process gases introduced during this process leads to the saturation of the molten metal nanodroplets which acts as catalysts resulting in the continuous precipitation of single crystalline nanofibers thereby promoting the unidirectional growth. Both hybrid and doped nanofibers can be produced using this method. Growth orientation in particular planes can be effectively controlled by appropriate substrate selection and optimizing the corresponding temperature and pressure during growth.[15,16]

The diameter of the 1D nanostructure produced in this method is controlled by altering the growth parameters by tuning the properties of the liquid alloy droplet. The preparation of the nano-sized droplets on the substrate plays a major role in 1D nanostructure growth since it determines the kinetics of supersaturation and nucleation occurring at the liquid/solid interface resulting in the axial crystal growth. Metal catalysts activate the sites where the nanofibers are to be grown and hence it determines the position of the 1D nanostructures.[41] Pressure of the source species also forms an integral role in growth rate which is directly proportional to the whisker diameter and hence the 1D nanostructures grows faster axially in whiskers of larger diameter.[41]

2.8. Hydrothermal Synthesis

This method involves the growth of the nanofibers in a heated liquid solution under pressure of 1 atm in an autoclave at a temperature of about 100–300 °C. The growth phase is dominated by the chemical decomposition during which the thermally degraded reactive ions from the precursors in the solution contribute to the growth of the nanofibers. The growth can be facilitated in a particular orientation by using appropriate catalysts which serves to

lower the surface energy. This method was first employed for growing single crystals of semiconductors which was later improvised and modified for developing other nanostructures.[42,43] Some of the metal oxide nanofibers grown using this method are In_2O_3,[44] MnO_2,[17] and Ga_2O_3.[18] The growth of the nanofibers can be controlled by manipulating the parameters such as temperature, precursor concentration, and pH, etc. The main disadvantage of this method is the low levels of crystallinity of the grown nanofibers.

In hydrothermal synthesis, the properties of the 1D nanostructures are defined by the process kinetics which in turn dependent on the parameters such as temperature and pressure in the system, duration of the synthesis, and the initial pH of the solution medium. Salts called mineralizers also play a major role in providing supercritical conditions for hydrothermal synthesis since it forms the hydrothermal solution which determines the solubility of the metal oxides to be processed.[45] Porosity of the synthesized 1D nanostructure can be controlled by selecting suitable surfactants for the targeted nanomaterial. The morphology of the metal oxide nanostructures is dependent on the surface-active agents (SAA) which has immense influence on the hydrothermal growth of oxide compounds.[46]

The advantages and disadvantages of the above fabrication methods are shown in Table 1. Electrospinning, self-assembly, and phase separation are methods usually employed for medical applications. Meanwhile, chemical applications normally used electrospinning, interfacial polymerization, and rapidly initiated polymerization as methods for the fabrication of nanofibers. Lastly, electrospinning, template- or patterned assisted growth, vapor-liquid-solid growth, and hydrothermal synthesis are generally applied in the nanofibrous fabrication of electronics. As such, it can be seen that electrospinning is the unique fabrication method which can apply to these three main applications. It is due to the fact that this method is flexible in material selection (both organic and inorganic materials) and diverse in nanofibrous architectures and nanofibrous diameters.

3. Medicine

3.1. Current Challenges in Medical Treatment

Tissue and organ failure is a major health problem, which can be caused by injury or other types of damage. In the US, the treatment of this failure accounts for approximately one half of the total annual expenditure in health care. Treatment options include transplantation (human or xenotransplantation), surgical repair, artificial prostheses, mechanical devices, and in a few cases, drug therapy. However, these methods can neither repair nor produce a long-term recovery effect on major damage in a truly satisfactory way.[47]

Over the past 30 years, tissue engineering has emerged as an alternative or complementary approach to tissue and organ reconstruction. As firstly stated by Langer and Vacanti,[48] tissue engineering is "an interdisciplinary field that applies the principles of engineering and life sciences toward the development of biological substitutes that restore, maintain, or improve tissue function or a whole organ." A distinctive feature of tissue engineering is to regenerate damaged tissues or organs of the own patient that remarkably enhance biocompatibility and biofunctionality as well as reduce immune rejection. Due to the great advantages, tissue engineering is often conceived as an ultimately ideal medical treatment.[49] The worldwide market of tissue engineering and regenerative medicine approached US$ 1.5 billion in 2008, and is projected to grow at a 16.2% compound annual rate from 2008 through 2013, approaching US$ 3.2 billion by 2013.[50]

Three basic tools utilized in tissue engineering today are cells, scaffolds, and growth factors. Although tissue-engineered products have been applied to patients, their clinical applications are still very limited. There are many challenges to overcome before the translation of scientific discoveries into treatments for millions of patients: (i) risk of rejection,[51,52] (ii) vascularization of tissue-engineered constructs,[47,51,52] (iii) lack of proper mechanical properties,[49] (iv) scaffolds able to degrade in response to remodeling progress,[51] (v) quality control of materials,[47] (vi) fundamental understanding of tissue differentiation mechanisms,[47] (vii) enhancement of production scale,[52] (viii) storage and preservation of tissue constructs,[51,52] (ix) translation of successful animal studies to humans.[51] and (x) lack of verifiable clinical data.[52] Among them, the risk of rejection of tissue-engineered constructs is a major challenge today. The inflammatory response can lead into fibrous capsule development which will inhibit tissue remodeling by limiting nutrient transport and angiogenesis.[53] The importance of nanofibers to reducing the inflammatory response and inducing fast regeneration of native tissues will be demonstrated in the following sections.

3.2. Novel Characteristics of Nanofibers in Medical Applications

Collagens are the most abundant protein in the ECM of many tissues in the body such as the bone, skin, and nerve, etc. They are present as nanofibrillar proteins with diameters in the range of 50–500 nm. ECM has several functions such as providing biomechanical strength to the tissue, serving as a biological scaffold for cells to adhere/migrate, serving as an anchor for several proteins, and

Table 1. Advantages and disadvantages of fabrication methods of nanofibers.

Fabrication method	Advantages	Disadvantages
electrospinning	nanofibers are long and continuous nanofibrous diameters are quite uniform, wide range of diameters can be fabricated flexibility in material selection various architectures can be created bulk structure can be formed	small pore size difficult to produce uniform fibers with diameters less than 50nm
self assembly	nanofibers can easily be modified and functionalized	bulk structure difficult to obtain low mechanical strength limited material selection only random and short nanofibers can be fabricated
phase separation	simple bulk structure can easily be formed large pore sizes with well-defined structures	limited material selection only random and short nanofibers can be fabricated
interfacial polymerization	one-pot reaction with no template or template-removing process required ease of scale-up production with high yield of uniform nanofibers dispersibility of nanofibers in water for environmentally friendly processing and biological applications large choice of solvents, acids, reaction temperatures, and reactant concentrations with control of nanofiber morphology via choice of acid and acid concentration	organic solvents required post-fabrication purification required
rapidly initiated polymerization	same as interfacial polymerization large choice of acids, reaction temperatures, and reactant concentrations with control of nanofiber morphology via choice of acid, reaction temperature, reaction medium, and rate of mechanical agitation environmentally friendly synthesis process because no organic solvents required, aniline monomers in spent aqueous solutions can be decomposed or recovered/reclaimed, synthesis of substituted polyaniline nanofibers possible	post-fabrication purification required
template- or pattern-assisted growth	good control of arrangement of nanofibers guided growth of nanofibers	pore filling is non-uniform for nano-structures with high aspect ratio, contamination from the template, template degradation during longer polarizations and poor crystallinity

Macromol. Mater. Eng. **2012**, DOI: 10.1002/mame.201200143

Table 1. (Continued)

Fabrication method	Advantages	Disadvantages
vapor-liquid-solid growth	defect-free 1D structures	growth material needs to form an eutectic liquid with the catalyst for efficient growth high temperatures required for processing therefore fabrication on plastic and glass substrates cannot be performed
hydrothermal synthesis	high yield	contamination of the nanostructures
	low cost	clustering and agglomeration of the nanostructures within the solution during growth
	easy fabrication	

regulating the phenotype of cells.[54] Among existing biomaterial structures, nanofibrous scaffolds can create cellular environments mimicking the nanoscale structure with complexity of the ECM. As opposed to flat surfaces, the attachment of various cell types such as the smooth muscle cells, adipose stem cells, and fibroblasts was at a rate of 50–150% higher on the nanofibers (in 15 min to 8 h period).[55–57] It has been hypothesized that, the body can recognize the biomimetic nanofibrous scaffolds as ''self'' and therefore, all of the intercellular and intracellular responses can be mimicked which help to stimulate the healing and the regeneration of tissues and organs.[58–60] Smartly designed tissue engineered scaffolds are even capable of promoting an organized deposition of ECM products from the resident cells. In a study carried out by Li et al., chondrocytes seeded on electrospun fibers of 500–900 nm produced double the amount of glycosaminoglycan in 28 d compared to the cells on microfiber (15 μm) culture.[61]

In addition, the topography of nanofibers can lead into changes in focal contacts through a phenomenon called contact guidance.[62] At the cell/matrix interface, the focal adhesions play an important role in linking the ECM on the outside to the actin cytoskeleton on the inside. The adhesion of cells to ECM causes clustering of integrins into focal adhesion complexes, and consequently activates intracellular signaling cascades into the nucleus and cytoskeleton.[63,64] Thus, the changes in focal adhesions can cause changes in cytoskeletal organization and integrin-containing adhesions.[65] These components are known to drive filopodia (or microspikes) in response to nanotopography for the specific activation of cytoskeleton- and focal adhesion-related signaling pathways.[66] Focal adhesion plaque of hMSCs on nanofibrous scaffolds had a more elongated shape than on those on smooth surfaces after 4 d of culture.[67] This elongation is associated with the cytoskeletal strengthening as well as the recruitment of focal adhesion-associated signaling molecules.[68] The guidance of filopodia by nanotopography may alter mechanical forces within the cells which can affect the interphase nucleus organization and genomic regulation.[69,70]

Moreover, due to their large surface-area-to-volume ratio, nanofibers provide more binding sites to cell membrane receptors, promote the adsorption of serum proteins and change the profile of adsorbed proteins.[62,71] The adsorption of serum fibronectin and vitronectin, which are known to mediate cell/matrix interactions, are improved significantly with nanofibrous structures.[72] As such, changes in the amount or type of adsorbed serum proteins may provide cells with a better niche to enhance cellular functions. Besides, the conformation of cellular proteins on the nanofibers may expose additional cryptic binding sites and be more favorable for cell/matrix interactions.[62,73]

The overall advantage of nanofibers over other micro- or macro-sized fibers is demonstrated in Figure 2.

3.3. In vivo Response to Nanofibers

To achieve a desired tissue/organ reconstruction, biomaterials should possess following properties: good biocompatibility, proper biodegradation, high-cellular infiltration, high vascularization, and ability to induce angiogenesis.

Macromolecular Journals
Macromol. Mater. Eng. **2012**, DOI: 10.1002/mame.201200143

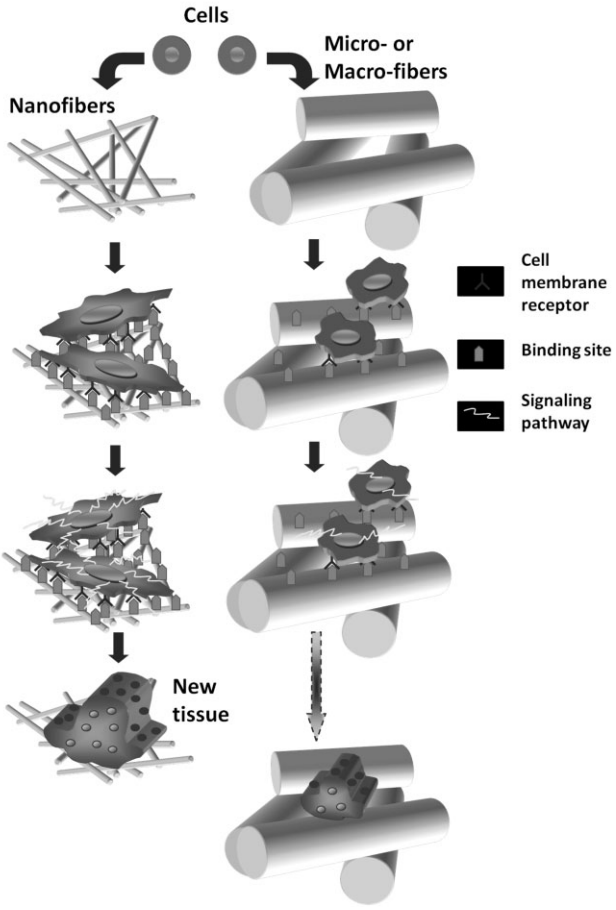

Figure 2. The advantage of nanofibers over micro- or macro-fibers. Due to high-surface-to-volume ratio, nanofibers provide more binding sites for cell membrane receptors resulting in activating more related signaling pathways, and consequently faster tissue regeneration.

In an in vivo condition, cells in distances of >200 μm from a blood vessel will suffer from hypoxia and limitation of other nutrients since this is the maximum diffusion distance.[74] So, angiogenesis and rapid vascularization of implants are essential for cell survival.[75]

3.4. Biocompatibility and Biodegradation

A biodegradable scaffold is a material capable of degraded enzymatic hydrolysis, whereby non-toxic alcohols, acids, or low-molecular-weight products are easily eliminated of the body. Meanwhile, a biocompatible scaffold is a material which elicits little or no immune response in the body and well-integrated with the targeted tissue/organ. To reduce the immune response, scaffolds should have non-thrombogenic blood compatible surfaces, and should be in harmony with the cells and environment. The antithrombogenic properties can be induced by hydrophilic/hydrophobic microdomains on the material surfaces. The biocompatibility not only depends on the type of the polymer and functional groups, but also on the structure of the scaffold surface.

Compared to thin films, nanofibrous meshes minimized host immune responses with the thickness of fibrous capsule decreased approximately 6 times.[76] Similarly, fibrous capsule was significantly reduced on nanofibrous scaffolds compared to microfibrous ones.[77] Electrospun polyhydroxyalkanoate (PHA) copolymers showed excellent biocompatibility during the course of the subcutaneous implantation, with no fibrous encapsulation, mild inflammatory responses, and the presence of thin connective tissue surrounding the scaffolds.[78] When modified with heparin, silk fibroin nanofibrous scaffolds did not induce any neutrophil and lymphocyte which indicated the minor inflammation as well as no significant rejection of this type of scaffolds.[79] Excellent biocompatibility in vivo with minor inflammatory reactions and biodegradation after 3 months of implantation was demonstrated by bi-layer PLLA/silk fibroin–gelatin nanofibrous meshes.[80] Multi-layered poly(ε-caprolactone) (PCL)/collagen nanofibrous constructs also showed good integration with surrounding tissues and neovascularization when implanted into nude mice.[81]

3.4.1. Cell Migration and Infiltration

Infiltration of cells through the polymeric scaffold is a crucial factor while utilizing nanofibrous scaffolds for tissue regeneration and nanofibrous structure could encourage migratory and remodeling behavior in comparison to smooth surface. Optimally designed pore size and high porosity of electrospun scaffolds provide sufficient space for cell migration and it enables the exchange of nutrients between the scaffold and the environment.

Periosteal cells were infiltrated when PCL nanofibers were implanted under rabbit periosteum with the infiltration extent increased from day 1 to day 7.[82] A hybrid scaffold of electrospun poly(ether urethane urea) (PEUU) and an ECM-derived scaffold resulted in a large cellular infiltrate compared to the PEUU alone.[83] In rat dermal replacement model, electrospun poly[(lactic acid)-*co*-(glycolic acid)] (PLGA) nanofibers achieved good cellular penetration, with no adverse inflammatory response and no capsule formation.[84] However, in a cylindrical shape with a inside diameter of 2 mm and a wall thickness of 200–250 μm for the implantation into the interstitial space of the rat vastus lateralis muscle, only electrospun scaffolds made from collagen showed good infiltration by interstitial and endothelial cells and the formation of functional blood vessels within 7 d.[85] Meanwhile, implants

made from gelatin, poly(glycolic acid) (PGA), PLA, and PLGA were not infiltrated to any great extent and induced fibrosis. The difference might be derived from a unique topography formed by collagen nanofibers which promoted cell migration and capillary formation. Compared to random nanofibers, aligned nanofibers were shown to increase cell infiltration, guide matrix organization, and elicit a thinner fibrous capsule.[76,86,87] Increasing scaffold porosity also promoted cellular infiltration and angiogenesis.[88] In general, electrospun nanofibers have limited cell infiltration because of their small pore sizes. It could restrict the delivery of nutrients to the cells and waste disposal, and constrains vascularization. To overcome this problem, the electrospinning technique was combined with photopatterning to create multiscale porous scaffolds.[89] Another solution was the use of ice crystals as templates to fabricate cryogenic electrospun scaffolds with large pore sizes.[90] This technique improved cell infiltration and vascularization compared to conventional electrospun scaffolds. In addition, layers of micro- and nanofibers have been proposed,[91] while methods such as salt leaching and introduction of sacrificial polymers such as poly(ethylene oxide) (PEO) were moderately successful in fabricating stable fibers with larger pore sizes suitable for cell infiltration.[92] Recruitment of endothelial progenitor cells, MSCs, and myocytes progentitor cells was achieved in vivo in a peptide nanofiber-assembled myocardium and the nanofibrous substrates enhanced vascularization and tissue regeneration.[93] Electrospun scaffolds fabricated as 3D structures similar to a "cotton ball" might overcome the current challenges and have great potential in a range of tissue engineering applications.

3.4.2. Vascularization and Angiogenesis

Vascularization is the development of proliferating capillaries, while angiogenesis is the formation of new vessels. Angiogenesis is one of the major processes required for functional tissue formation. To induce angiogenesis, nanofibers have been normally combined with inducers. In mice, supramolecular nanofibers formed by self-assembly of a heparin-binding peptide amphiphile (HBPA) and heparin sulfate-like glycosaminoglycans revealed excellent biocompatibility and developed a new vascularized tissue which demonstrated an angiogenesis-promoting potential of this material.[75] When injected into rats, IKVAV (Isoleucine-Lysine-Valine-Alanine-Valine)-containing peptide nanofibers were able to induce angiogenesis as shown by forming capillary vessels with complete walls.[94] Chemokines induced by platelet-derived growth factor (PDGF) released from nanofibers enhanced the angiogenesis in vivo.[95]

Subcutaneous injection of hepatocyte growth factor (HGF) incorporated with self-assembled PA nanofibers to mouse sub-cutis was carried out by Hosseinkhani et al, and 3 weeks post-evaluation maintained their biological activities and showed enhanced vascularization.[96] However, robust strategies for complete integration and vascularization of the engineered tissue with the host tissue are apparently lacking after implantation of the bioengineered grafts. Clinical studies to deliver vasculogenic growth factors in myocardial and peripheral limb ischemia are in its preliminary stages.[97]

Taken together, with chemical and physical modifications, nanofibers have shown their good in vivo characteristics in biocompatibility, biodegradation, cell infiltration, vascularization and angiogenesis. These properties would help to accelerate their success in targeted functional applications in medical treatment. The studies of in vivo response to nanofibers are significantly important and have to be taken into a serious consideration before the studies of functional applications (bone, cartilage, skin, nerve, heart, etc.) are performed, especially when a new material is introduced. The results of biocompatibility, biodegradation, cell infiltration, vascularization, and angiogenesis studies will provide a in-depth profile of responses of in vivo environments (animals/humans) so that researchers can modify their scaffolds accordingly. A few important properties of nanofibers that need to be considered before performing in vivo studies are biocompatibility, biodegradation, and pore sizes of the scaffolds. The biocompatibility and biodegradation normally can be determined by the chemical components of nanofibers. The nanofibers should possess a suitable biodegradable property for tissue regeneration, but it also has to maintain an appropriate mechanical property to serve as a scaffold for cellular growth and differentiation. The pore size is a key factor of nanofibrous scaffolds which determines cell migration, infiltration, and vascularization. To achieve a complete cell migration, infiltration, and vascularization, the nanofibrous scaffolds should have a pore size of 100–200 μm.

3.5. Animal Studies

Due to the novel characteristics of nanofibers, they have been studied for diverse applications in medicine. Nanofiber-based scaffolds have demonstrated their substantial support in the repair of skeletal, integumentary, nervous, and cardiovascular systems as well as the treatment of many other diseases in a broad range of animal models (from small to large animals; Table 2).

3.6. Skeletal System

Among applications of nanofiber-based scaffolds in medicine, their application in skeletal system (bone, cartilage,

Table 2. Animal studies using nanofibers.

Application	Animal model		Nanofiber-based scaffold[a)]
bone	mouse	subcutaneous	PLLA/differentiated hAFSC[98] PLLA/n-HA;[99] PEOT/PBT/calcium phosphate/MSC;[100] PCL/gelatin/n-HA/differentiated DPSC;[101] and Self-assembling PA/differentiated DPSC[102]
		intraperitoneal	P-15 peptide/ABM/MSC[103]
		tibia	PLGA/HAp/BMP-2 plasmid[104,105]
		calvaria	fibrin/n-HA/rhBMP-2;[106] and fibrin/ALP[107]
	rat	subcutaneous	PCL/HS/differentiated MSC[108] PLLA nanofibers immobilized with rhBMP-7 containing PLGA nanospheres;[21] and Self-assembling PA/bFGF combined with collagen/PGA[109]
		abdominal omentum	PCL/differentiated MSC[110]
		femur	self-assembling PA with phosphoserine residues;[111] self-assembling PA/Ti;[112] PCL/Irradiated RGD-modified alginate/rhBMP-2[113,114]
		calvaria	PLLA;[115] PCL nanofibrous mesh/PLGA membrane;[116] PLLA/DBP;[117] PCL/BG;[118] PCL/simvastatin;[119] Collagen/nBG/bFGF[120]
	rabbit	tibia	PLLA[121]
		calvaria	chitosan;[122] silk fibroin;[123] silica gel;[124] SiO_2/CaO gel;[125] and PLGA/TCP[126]
		sterna	PLLA/differentiated MSC[127,128]
cartilage	mouse	subcutaneous	p(NiPAAm-*co*-AAc)/TGF-β3/hMSC;[129] star-shaped PLLA/chondrocyte;[20] articular cartilage ECM/differentiated MSC[130]
	rabbit	subcutaneous	PLLA/cationized gelatin/chondrocyte[131]
		medial femoral condyle	p(NiPAAm-*co*-AAc)/TGF-β3/differentiated hMSC;[129] and star-shaped PLLA/chondrocyte[20]
	pig	medial femoral condyle	PCL/hMSC[132]
		medial femoral condyle and patellar groove	PCL/PCL-TCP/MSC resurfaced with PCL/collagen mesh[133]
tendon	mouse	intramuscular	PLLA/TSC[134]
skin	mouse	normal wound	chitosan/PVA;[135] PHBV/ORSC/DSC[136]
		diabetic ulcers	sNAG;[137] PCL/curcumin;[138] PCL-PEG/LPEI/DNA;[139] PCL-PEG/rhEGF [140]; and PCL-PEG/bFGF/EGF[141]
	rat	normal wound	collagen;[142] collagen/chitosan/PEO;[143] PLGA/collagen;[144] PCL, PVA, PVA/wool, PVA/Ag;[145] genipin-crosslinked silk fibroin/HBC;[146] RADA16-I self-assembling peptide;[147] and PLGA/Collagen/CD29/MSC[148]
	pig	normal wound	MDOC/gentamicin;[149,150] hyaluronic acid[151]

Table 2. (*Continued*)

Application	Animal model		Nanofiber-based scaffold[a)]
nerve	rat	peripheral (sciatic)	chitosan;[152,153] PLGA;[154] PLGA/PCL;[155] PAN-MA;[156] PLCL/PPG/sodium acetate;[157] chitosan/CG6YIGSR peptide;[158] PCLEEP/hGDNF;[159] PLLA-laminin/PLGA-NGF;[160] BD™ PuraMatrix™ peptide/Schwann cell;[161] PLCL/PPG/sodium acetate/differentiated NCSC[162]
		central (spinal cord)	polyamide/D5′ peptide;[163] RADA16-4G-BMHP1 self-assembling peptide;[164] self-assembling PA/NPC or self-assembling PA/Schwann cell;[165] PCL-PLGA nanofiber/RADA16-I-BMHP1 self-assembling peptide[166]
	hamster	central	self-assembling PA[167]
cardiac	mouse	myocardial infarction	HBPA/rhVEGF/rh-bFGF[168]
	rat	myocardial infarction	self-assembling PA/S-SDF-1(S4V);[169] self-assembling porcine myocardial ECM;[170] RAD16-II self-assembling peptide/selected MSC;[171] and RADA16 self-assembling peptide/RGDSP/MCSC[172]
	pig	myocardial infarction	self-assembling PA/bone marrow MNC[173]
vascular	mouse	subcutaneous	PLLA;[174] self-assembling PA/MSC[175]
	rat	abdominal aorta	hyaluronan;[176] PCL/Paclitaxel;[177] and PEUU/PMBU;[178] PLGA/Tacrolimus[179]
		carotid artery	self-assembling PA/nitric oxide;[180] PLLA/MSC[181]
		ischaemic hind limb	HBPA/rhVEGF/rh-bFGF[168]
	rabbit	epigastric-free flap	PLCL/collagen[182]
		aortoiliac bypass	PCL/collagen[183]
	dog	carotid artery	PLGA/MSC/EC[184]
stent	rabbit	aneurysms	PU[185]
liver	mouse	intramuscular	self-assembling PA/growth factors[186]
		spleen	self-assembling PA/hepatocyte[187]
abdominal wall	rat		PEUU;[188] PEUU/PLGA/tetracycline hydrochloride;[189] and PCL/Biteral[190]
bladder	mouse	subcutaneous	PLLA/MSC[191]
eye	mouse	ocular Surface	polyamide/LSC/MSC[192]
diabetes	mouse	islet transplatation	self-assembling PA/fibronectin/human islet[193]
hemostasis	rabbit	liver wound healing	self-assembling d-EAK16[194]
tumor	mouse	mammary fat pad	RADA16 self-assembling peptide/breast cancer cell[195]
		glioblastoma xenograft	PLGA/Paclitaxel[196]

Table 2. (*Continued*)

Application	Animal model		Nanofiber-based scaffold[a)]
drug/cell delivery	mouse	endo-tracheal	self-assembling PA/ESC[197]
	rat	intra-tracheal	calcium pyrophosphate/Dex-P[198]
suture	rat		PLLA/chitosan;[199] PLLA/CFX-Na[200]

[a)]Cells: AFSC, amniotic fluid-derived stem cell; DPSC, dental pulp stem cell; DSC, dermal sheath cell; EC, endothelial cell; ESC, embryonic stem cell; LSC, limbal stem cell; MCSC, marrow-derived cardiac stem cell; MNC, mononuclear cell; MSC, mesenchymal stem cells; NCSC, neural crest stem cell; NPC, neural progenitor cell; ORSC, epithelial outer root sheath cell; TSC, tendon stem cell. Growth factors/chemical agents: ALP, alkaline phosphatase; bFGF, basic fibroblast growth factor; BMP-2, bone morphogenetic protein-2; rhBMP-2, recombinant human bone morphogenetic protein-2; rhBMP-7, recombinant human bone morphogenetic protein-7; CFX-Na, cefotaxime sodium; Dex-P, dexamethasone phosphate; EGF, epidermal growth factor; GDNF, glial cell-derived neurotrophic factor; NGF, nerve growth factor; S-SDF-1(S4V), protease-resistant stromal cell derived factor-1; TGF-β3, transforming growth factor-β 3; VEGF, vascular endothelial growth factor. Materials: 4G, 4-glycine spacer; ABM, anorganic bone material; BMHP1, bone marrow homing motif; D5' peptide, neurite outgrowth-promoting peptide derived from tenascin-C; DBP, demineralized bone powder; EEP, ethyl ethylene phosphate; HAp, hydroxyapatite; HBC, hydroxybutyl chitosan; HBPA, heparin-binding peptide amphiphile; HS, glycosaminoglycan heparin sulfate; LPEI, linear poly(ethyleneimine); MDOC, microdispersed oxidized cellulose; nBG, nano-bioactive glass; n-HA, nano-hydroxyapatite; P-15 peptide, cell-binding domain of type I collagen; PA, peptide-amphiphile; PAN-MA, poly(acrylonitrile-*co*-methacrylate); PBT, poly(butylene terephthalate); PCL, poly(ε-caprolactone); PEG, poly(ethylene glycol); PEO, poly(ethylene oxide); PEOT, poly(ethylene oxide terephthalate); PEUU, poly(ester urethane) urea; PGA, poly(glycolic acid); PHBV, poly(3-hydroxybutyrate-*co*-3-hydroxyvalerate); PLCL, poly[(L-lactide)-*co*-caprolactone]; PLGA, poly[(lactic acid)-*co*-(glycolic acid)]; PLLA, poly(L-lactic acid); PMBU, poly[2-methacryloyloxyethylphosphorylcholine-*co*-(methacryloyloxyethyl butylurethane)]; p(NiPAAm-*co*-AAc), poly[(*N*-isopropylacrylamide)-*co*-(acrylic acid)]; PPG, poly(propylene glycol); PU, polyurethane; PVA, poly(vinyl alcohol); RGD, arginine-glycine-aspartic acid; sNAG, poly(*N*-acetylglucosamine); TCP, tricalcium phosphate; Ti, titanium.

and tendon) is the most popular. The treatment of bone defects in mouse, rat, or rabbit models have been successfully done using pure nanofibers made from synthetic/natural polymers such as PLLA,[115,121] PCL,[116] chitosan,[122] and silk fibroin;[123] or inorganic matrices such as bioactive glass (BG)[118] and silica gel.[124] Woo et al.[115] showed significant advantages of PLLA nanofibrous scaffolds over PLLA solid-walled scaffolds in critical-size calvarial defects. The nanofibrous implants produced substantially more new bone minerals, abundant collagen deposition, and strong expressions of Runx2 and bone sialoprotein (BSP) compared to the solid-walled implants. Especially, electrospun nanofibrous scaffolds have been beneficial to be employed as guided bone regeneration (GBR) membranes.[116,121–123] GBR is a standard procedure which uses membranes to protect bone defects from the ingrowth of surrounding tissues, and thus promote bone healing. The nano- to micro-pore size of nanofibrous membranes was shown to be efficient in preventing from fibrous connective tissue invasion, but allowing growth factors, nutrients, and oxygen to be penetrated into the defects, which leaded to faster bone regeneration. Not only organic matrices, nanofibers made from BG or silica gel also indicated good osteoconductivity in the treatment of calvarial defects.[118,124]

In addition to using the pure nanofibers, nanofibers have been usually combined with growth factors or other osteogenic inducers such as bone morphogenetic proteins (BMPs),[21,106,113,114] basic fibroblast growth factor (bFGF),[109,120] alkaline phosphatase (ALP),[107] demineralized bone powder (DBP),[117] hydroxyapatite (HA),[99,104,105] and tricalcium phosphate (TCP),[126] etc. to further improve bone regeneration. Nanofibers provided a sustained and prolonged release of the growth factors for bone defects. The presence of BMP-2 in nanofiber-based scaffolds resulted in consistent bony bridging for the repair of critically sized segmental bone defects.[113] Not only growth factors, but nanofibers also significantly contributed to bone formation. Although both scaffolds contain bFGF, only the scaffold with the presence of nanofibers produced a homogeneous bone formation.[109] In addition to growth factors, inorganic substances such as HA and TCP were demonstrated to be very efficient in promoting or even inducing bone regeneration when combined with nanofibers.[99,104,105,126]

When injury or other types of damage occur in the body, stem cells are hypothesized to migrate to the injured sites

and combine with local cells in the repair response. Thus, recently, stem cells have been usually incorporated into scaffolds to speed up tissue regeneration. The incorporation of MSCs,[100,103,108,110,127,128] amniotic fluid-derived stem cells (AFSCs)[98] and dental pulp stem cell (DPSCs),[101,102] etc. into nanofibous scaffolds helped to accelerate bone regeneration. The cell/scaffold composite indicated obvious in vivo hard tissue formation with a surrounded thin fibrous tissue capsule, and without any sign of tissue ingrowth.[101,102]

In cartilage tissue engineering, using nanofiber-based scaffolds also brings significant advantages to the treatment of cartilage defects. Since cartilage regeneration requires a high-cell density, nanofibers have been usually combined with cells (chondrocytes[20,131] or MSCs[129,130,132,133]) ± transforming growth factor-β3 (TGF-β3).[129] In the treatment of 7 mm full-thickness cartilage defects in a swine model, the MSC-seeded PCL nanofibers demonstrated a more complete repair in the defects compared to the acellular PCL scaffolds.[132] Nanofibrous scaffolds have been fabricated as electrospun meshes of PLLA[131] and PCL,[132,133] sponges of cartilage ECM,[130] injectable scaffolds of poly[(*N*-isopropylacrylamide)-*co*-(acrylic acid)] [p(NiPAAm-*co*-AAc)],[129] and star-shaped PLLA.[20] The nanofibrous hollow microsphere/chondrocyte construct achieved remarkably better repair of a critical-size rabbit osteochondral defect model than the chondrocyte alone.[20] As such, using nanofibers as cell carriers would be a promising approach for clinically cartilage regeneration.

As such, nanofiber-based scaffolds showed their significant achievements in skeletal tissue engineering in the presence/absence of cells/growth factors. However, it is still challenging to develop 3D hierarchical nanofibrous scaffolds with controlled porosity, pore size, fibrous dimeter, and mechanical property to further facilitate the hard tissue regeneration. Electrospun nanofibers are normally limited in pore size; whereas nanofibers fabricated by self-assembly and phase separation methods usually encounter low-mechanical property and uncontrollable fibrous diameter, respectively. Scaffolds with high porosity are necessary for efficient mass transport of nutrients, oxygen, growth factors, and waste products. To allow cell ingrowth and facilitate vascularization to avoid necrosis at the core, appropriate pore sizes (100–200 μm) must also be required. In addition, in the treatment of large bone or cartilage defects, it is important to develop biomimetic scaffolds with the osteoinduction and chondroinduction abilities by themselves, without the need for soluble inducers (or growth factors). Growth factors are generally derived from animal sources, expensive and difficult to control the optimal concentration for an efficient differentiation without side effects, so the development of osteoinductive and chonroinductive scaffolds could be a key issue to facilitate the success of clinical trials in the future.

3.7. Integumentary System

One of the most successful applications of nanofibers in medical treatment is skin regeneration. Many types of nanofibrous polymers (natural/synthetic) such as hyaluronic acid,[151] collagen,[142] collagen/PLGA,[144] chitosan/poly(vinyl alcohol) (PVA),[135] collagen/chitosan/PEO,[143] PCL,[145] genipin-crosslinked silk fibroin/hydroxybutyl chitosan (HBC)[146] and RADA16-I self-assembling peptide,[147] etc. have been shown to facilitate wound healing in animal models. Compared to an adhesive bandage, a sterilized solid hyaluronic acid, gauze with Vaseline, and an antibiotic dressing, nanofibrous hyaluronic acid was the best type of wound dressing in a large animal–pig model.[151] The nanofibers could absorb the exudates of wounds to a greater extent, allow greater air to be permeated, and help with the migration and proliferation of cells in wounds than solid hyaluronic acid, which led to faster wound healing. The nanofibrous composite of type I collagen, chitosan, and PEO was also demonstrated to be better than gauze and commercial collagen sponge wound dressing in wound healing rate.[143] Similarly, at 2 and 3 weeks after implantation, the healing in the PLGA/collagen nanofiber group was visibly faster than those of the gauze group and the commercial dressing group, with well integrated into surrounding skin (Figure 3).[144]

For the healing of acute wound infections, nanofibers have been usually loaded with antibiotics such as Ag[145] and gentamicin,[149,150] etc. Micro-dispersed oxidized cellulose (MDOC) nanofibers blended with gentamicin indicated their effectiveness in the treatment of full-thickness pig skin infections.[149,150] In addition, seeding dermal sheath cells (DSCs)/epithelial outer root sheath cells (ORSCs),[136] and MSCs[148] on nanofibrous scaffolds prior to implantation was shown to provide significantly better wound healing than the matrices alone.

Nanofiber-based scaffolds have not been only able to treat normal wounds, but also to treat diabetic ulcers which are common in patients with diabetic mellitus. They can lead to limb loss if proper treatment is delayed. Some successful approaches in animal models include poly(*N*-acetyl-glucosamine) (sNAG),[137] PCL/curcumin,[138] PCL-poly(ethylene glycol) (PEG)/linear poly(ethyleneimine) (LPEI)/DNA,[139] PCL-PEG/epidermal growth factor (EGF),[140] and PCL-PEG/bFGF/EGF.[141] The EGF nanofibers showed superior in vivo wound healing compared to the nanofibers or EGF alone.[140]

Taken together, nanofibrous scaffolds showed obvious evidences of facilitating skin regeneration in comparison with non-nanofibrous scaffolds in the pre-clinical studies.

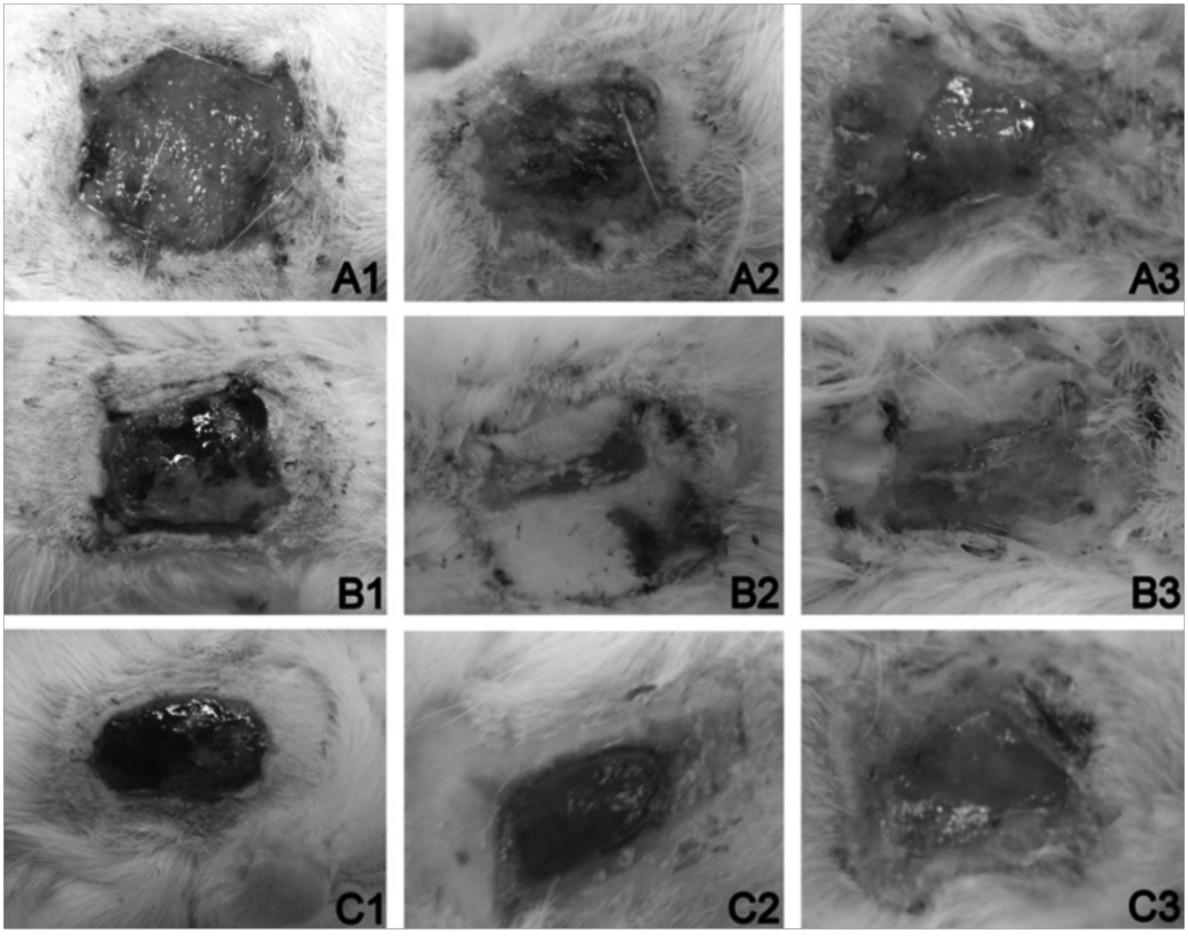

Figure 3. Appearance of wound healing at 1, 2, and 3 weeks after grafting in rat's back: (A) gauze group, (B) nanofiber group, and (C) commercial dressing group. The PLGA/collagen nanofiber showed better skin healing than others at week 2 and week 3 (Reprinted from ref.,[144] Copyright 2010, with permission from Elsevier).

The incorporation of cells into nanofibers also provided a significant improvement. In spite of those achievements, there are three major challenges still remained in this field including improving safety of the incorporated cells, angiogenesis in replacement tissue, and ease of use for cell delivery approaches. The maximum thickness of a skin graft substitute which can easily become vascularized is about 0.4 mm. Thus, with scaffolds thicker than 0.4 mm, new blood vessels cannot penetrate quickly enough to feed the epidermal layer once the scaffolds are grafted to the wound bed. In addition, nanofibrous scaffolds are expected for further development to mimic chemical components, physical structures, and mechanical properties of natural skin ECM, which are important to an efficient skin regeneration.

3.8. Nervous System

Nanofiber-based scaffolds have been applied in the treatment of peripheral (sciatic) and central nervous systems. In the peripheral nerve regeneration, most of tissue-engineered scaffolds of the last few decades make use of rigid channel guides which may lead to cell loss during patient's movement.[155] But with the ability to fabricate flexible tubular scaffolds, electrospinning technique provides a promising approach for treatment of nerve injuries. Using electrospun nanofibers made from natural and/or synthetic polymers such as chitosan,[152,153] (PAN-MA),[156] and poly[(L-lactide)-*co*-caprolactone] (PLCL)/poly(propylene glycol (PPG)/sodium acetate,[157] etc., an effective bridging of critical-size peripheral nerve gaps were made possible. Scaffolds have been usually fabricated as aligned nanofibers in order to guide and promote the regenerating nerve.[153,156,157] To further facilitate the nerve regeneration, active domains and growth factors such as CG6YIGSR peptide,[158] glial cell-derived neurotrophic factor (GDNF),[159] and laminin/nerve growth factor (NGF),[160] etc. have been loaded into the nanofibers. The efficacy of aligned PCL-ethyl ethylene phosphate (EEP)/

GDNF nanofibers was compared with aligned nanofibrous PCL-EEP tubes without GDNF and solid-walled PCL-EEP scaffolds (control) for the treatment of rat peripheral nerve injury.[159] Three months after implantation, all the rats that received nanofibrous conduits (with and without GDNF) showed a complete bridging of a 15 mm critical defect gap. Meanwhile, bridging was only 50% in the control group. Electrophysiological recovery was seen in 33 and 44% of the rats with the nanofibers alone and the nanofibers/GDNF respectively, while none was observed in the control. As such, nanofibers itself can support peripheral nerve regeneration; however, the synergistic effect of embedded growth factors significantly facilitated the recovery. In addition to growth factors, Schwann cells[161] and neural crest stem cells (NCSCs)[162] have been seeded onto the nanofibers prior to implantation to improve axonal regeneration and myelination. Alternatively a tubular scaffold to reconnect the transacted nerve stumps stuffed with a variety of materials such as gels or fibers within the lumen of the tube are also attempted to serve as a better graft for in vivo implantation and regeneration of nerve. We developed PLLA conduits in our lab with aligned PLGA nanoyarn (intra luminal guidance channel) in the lumen, and incorporated biomolecules such as laminin and NGF to determine the efficacy of the nerve graft for in vivo regeneration.[160] Implantations in rat sciatic nerve defect model showed high-functional recovery using such grafts, the conduit with aligned nanoyarn performed better than the autograft in muscle reinnervation and withdrawal reflex latency tests.

While most of nanofibers used for peripheral nervous regeneration were fabricated by electrospinning technique, the nanofibrous scaffolds employed for the treatment of central nervous system were based on injectable self-assembling peptides.[164–167] Because of the complexity of this injury, it would need injectable scaffolds to minimize damages brought to lesion sites. In the treatment of rat acute spinal cord injury, RADA16-4G-BMHP1 self-assembling peptide nanofibers were demonstrated to induce matrix remodeling, and provided physical and trophic supports to nervous tissue ingrowth.[164]

Empty bridging tubular grafts provide limited tissue-level guidance (axon mis-direction) and nerve conduits filled with intraluminal guidance channels are the most attractive option among the various nerve grafts. However factors such as the conduit collapse, maintenance of lumen space (patency of conduit), packing density of the guidance channels need careful consideration with respect to the dimension of the nanofibers and its composition. With advances in electrospinning technology, the development of new nozzle and collector configurations has led to the design of nanofibers with desired scaffold geometry, drug release, or surface properties. However challenges of mimicking every aspect of native nerve, within a bioengineered nerve graft is still questionable and the latest research direction is toward the incorporation of fibers into a hydrogel and the loading of this ''combined construct'' into a 3D conduit. Further resolving the attributes of such scaffolds for clinical applications turns even more challenging or sometimes compromising.

3.9. Cardiovascular System

Heart failure following myocardial infarction (MI) is the leading cause of death in the U.S. Since myocardical tissue lacks the ability to substantially regenerate itself following MI, tissue-engineered scaffolds are a requisite for myocardial repair. In particular, injectable nanofibrous scaffolds possess impressive advantages of mimicking the natural myocardial ECM and minimally invasive delivery. A natural myocardial ECM was de-cellularlized and self-assembled to form a nanofibrous structure with the ability to gel in vivo upon injection into rat myocardium.[170] Eleven days after the injection, they observed the migration of endothelial cells and smooth muscle cells toward the myocardial matrix, with a significant increase in arteriole formation. In addition to using a natural matrix, synthetic self-assembling peptides were mixed with autologous stem cells to repair myocardium and improve cardiac functions in both small (rat) and large (mature mini-pig) models.[171–173] It has been postulated that the efficacy of stem cell transplant is related to paracrine factors. Thus, instead of using stem cells, growth factors such as vascular endothelial growth factor (VEGF) and bFGF[168] were incorporated with HBPA to augment cardiac functions after MI or enhance vasculature following critical ischemia. Besides, self-assembling peptide nanofibers were employed to locally deliver stromal cell derived factor-1 (SDF-1),[169] a well-characterized chemokine, to drive stem cell recruitment into infracted myocardium. This is a potentially novel approach to cardiac tissue regeneration.

In addition to myocardial regeneration, cardiovascular diseases require a large number of revascularization procedures to complete the tissue regeneration process. Together with using autologous veins or arteries, biostable synthetic vascular grafts such as expanded polytetrafluoroethylene (e-PTFE) and polyethylene terephthalate (Dacron) have been utilized to replace blood vessels. However, they have encountered some specific problems as small blood-vessel diameters (<6 mm), whereby these grafts can lead to graft occlusion and thickening of the arterial wall due to their inadequate mechanical properties and biocompatibility.[201] Thus, developing novel small-diameter vascular graft is an imperative need. Nanofibrous scaffolds of PLLA,[174] hyaluronan,[176] PEUU/poly(2-methacryloyloxyethyl phosphorylcholine-*co*-methacryloyloxyethyl butylurethane) (PMBU),[178] PLCL/collagen[182] and PCL/collagen,[183] etc. showed promising

materials for the reconstruction of small blood vessels in rat and rabbit models. When implanted into rabbits to replace the inferior superficial epigastric veins, PLCL/collagen nanofibrous tubes kept the structure integrity, and showed patency for 7 weeks.[182] The PEUU/PMBU vascular grafts indicated a thin neo-intimal layer covered with endothelial cells and good anastomotic tissue integration.[178] To prevent neointimal hyperplasia, paclitaxel,[177] tacrolimus,[179] and nitric oxide[180] were blended with nanofibers. The PCL/Paclitaxel nanofibrous graft[177] showed good patency, reendothelialization, and remodeled with the autologous cells. Moreover, it reduced neointima formation until the end point of 6-month study. MSCs were also seeded on nanofibers prior to implantation to prevent thrombosis.[175,181,184] The combination of PLLA nanofibers with MSCs[181] created a vascular graft with excellent patency and unique antithrombogenic property for the treatment of small-diameter arteries.

On the other hand, using polyurethane (PU) nanofibers to cover stents was shown to be efficient in treating cerebral aneurysms.[185] One day after implantation in rabbits, complete occlusion of the aneurysms occurred with patency of the parent arteries. On day 10, the aneurysm neck was completely covered with a neointimal layer.

Designing a bioengineered graft capable of working in synchronization with the nonlinear elastic behavior of heart upon integration is a great challenge. Inadequate mechanical properties of the blood vessel implants can cause problems such as graft occlusion or arterial wall thickening. Therefore, the most important factor for designing a biomaterial graft for cardiovascular engineering is the mechanical property and structural integrity of the biomaterial. Moreover, disappointments of therapeutic angiogenesis in clinical trial necessitate the development of better multimodal research strategies for controlled delivery of angiogenic promoters, with ability to propagate electrical impulses, creating a functional myocardium.

3.10. Other Applications

In addition to numerous animal studies on the above systems, nanofibers have been applied to a diverse range of other medical treatments. Injectable self-assembling peptide nanofibers were loaded with growth factors derived from a conditionally immortalized human hepatocyte cell line[186] or hepatocytes[187] for the treatment of liver failure. The self-assembling peptide/hepatocyte construct corrected acute liver failure in mice and prolonged their survival.[187] In a rat model for abdominal wall replacement, PEUU nanofibers fabricated by a wet electrospinning technique provided a good healing with a mimic mechanical behavior as well as a substantial cellular infiltration.[188] In combination with tetracycline hydrochloride, an antibiotic, PEUU/PLGA nanofibers prevented abscess formation in a contaminated rat abdominal wall model.[189] Together with proper mechanical properties, this scaffold could be valuable to improve abdominal laparotomy management. Loading with Biteral, a model antibiotic, into PCL nanofibers also significantly eliminated post-surgery abdominal adhesions, and improved the healing of abdominal wall.[190] Besides, the construct of PLLA nanofibers and MSCs demonstrated its potential in bladder regeneration for patients with bladder exstrophy or cancer who need cystoplasty.[191] Moreover, the treatment of ocular surface injuries was shown to be successful by using polyamide nanofibers seeded with limbal stem cells (LSCs) and MSCs.[192] The scaffold/cell construct significantly inhibited local inflammatory reactions and facilitated the healing process.

Human islets embedded in fibronectin/self-assembling peptide nanofibers and transplanted into streptozotocin (STZ)-induced diabetic severe combined immunodeficiency (SCID) mice reestablished the cell/matrix interactions and maintained the islet functions in vivo for the treatment of type 1 diabetes mellitus.[193] Self-assembling d-EAK16 nanofibers also showed a rapid hemostasis of approximately 20 s in a rabbit liver wound healing model.[194] Furthermore, self-assembling peptides effectively reduced the malignant phenotype of the tumor cells in vivo in comparison with collagen type I and Matrigel.[195] An optimal paclitaxel pharmacokinetics was obtained when this drug was incorporated into PLGA nanofibers to treat malignant glioblastoma in mice.[196] Forty-one days after the treatment, the drug-loaded scaffold demonstrated significant (approximately 30-folds) tumor inhibition and significantly low-tumor proliferation index. Calcium pyrophosphate nanofibers also exhibited a controlled release of dexamethasone phosphate (Dex-P) in a pulmonary inflammation model.[198] For 42 h following a single application, the nanofibers loaded with Dex-P inhibited eosinophil and total inflammatory cell increases in bronchoalveolar lavage fluid. In addition to drug delivery, nanofibers were indicated to be an effective carrier for cell delivery. Self-assembling peptide nanofibers possessed sufficient rigidity to remain embryonic stem cells (ESCs) localized and gradually release them rather than immediately dissolving in the abdominal cavity.[197] Finally, braided nanofibers can be also applied as tissue sutures with/without antibiotics. PLLA/chitosan[199] and PLLA/cefotaxime sodium (CFX-Na)[200] exhibited comparable tensile and knot strengths to those of a commercial suture and had more preferable histological compatibility performance than commercial silk sutures.

3.11. Clinical Trials

To our best knowledge, up to now, there have been few published reports on clinical trials of nanofibers as listed

Table 3. Clinical trials using nanofibers.

Nanofiber-based scaffold	Application	Status	Reference
nitric oxide releasing nanofibrous patch	cutaneous leishmaniasis	completed phase III	[202,203]
nitric oxide releasing nanofibrous patch	diabetic ulcers	on-going phase III	[204]
bioactive borate glass nanofibers	diabetic ulcers	completed phase II	[205]
nanofibrous mesh	anti-adhesion	completed phase II	[206]

in Table 3. It might be due to the fact that nanofibers have been only studied for applications in tissue engineering/medical treatment during the past decade. In addition, many challenges as shown above are needed to be solved before moving up with clinical trials. For example, immense challenge remains in finding the accurate path that guide the axons to their target and in establishing the microenvironment to facilitate neurite outgrowth while utilizing nerve graft for clinical trials. Most of the trials have focused on skin regeneration–the simplest application, including the treatments of cutaneous leishmaniasis[202,203] and diabetic ulcers.[204,205] Phase III clinical trial of nitric oxide releasing nanofibrous patch ($\approx$3.5 μmol NO $\cdot$ cm^{-2} $\cdot$ d^{-1} for 20 d) for cutaneous leishmaniasis treatment was completed.[203] Previous pre-clinical studies and clinical trials of this material showed that the multilayer transdermal nanofibrous patch fabricated by electrospinning provided a continuous and stable nitric oxide release when administered topically without adverse events.[202] In the phase III, 3 months after the treatment starts, although the cure rate of the nanofibrous patch was only 37.1% compared to 94.8% of intramuscular meglumine antimoniate (Glucantime, 20 mg $\cdot$ kg^{-1} $\cdot$ d^{-1} for 20 d), the patients treated with the nanofibers showed a significantly lower frequency of adverse events as well as a decreased variation in serum markers. Phase III clinical trial of this material for diabetic ulcer treatment is going on.[204] Bioactive borate glass nanofibers are also under clinical trials to treat diabetic ulcers.[205] The result of phase II with twelve patients demonstrated that the material helped to heal venous stasis wounds in eight of the patients who had suffered from diabetes and not responded to other treatments. The nanofibers supported the migration of epidermal cells and facilitated the healing process. This study has been expanded and phase III clinical trial will be performed soon. In addition, nanofibers have been performed with clinical trials for anti-adhesion application.[206] The biodegradable nanofibrous membrane helped body tissues be prevented from sticking together as they heal. Further results will be obtained from the phase III clinical trial. Although there are not many clinical trials, with novel results of nanofibers as shown in pre-clinical trials, we believe that a large number of human trials on nanofibers with various applications are coming.

4. Chemistry

Much has been reported in the literature relating to chemistry done on or with nanofibers. Numerous reviews have been written on the chemistry of nanofibers synthesis,[207,208] bulk/surface modifications,[209,210] and response to environmental stimuli[211] with applications in various chemical reactions and processes.[212,213] Chemical reactions on or with nanofibers do not alter their nature. Indeed, a recent review on chemistry involving electrospun polymeric nanofibers revealed no new chemical reaction that generates any novel type of chemistry that is different from conventional ones in terms of reaction pathways, tacticities, or ligand spheres of complexes.[214] Nonetheless, the use of nanofibers in processes involving chemical reactions does confer some advantages over conventional systems. This section attempts to provide an overview on the practical applications of nanofibers in chemical processing with respect to the types of chemical processes/reactions in which nanofibers have been employed and the benefits and novel chemical functionalities that nanofibers offer over conventional processes. The applications of nanofibers in chemical processing are shown in Figure 4.

4.1. Current Challenges in Chemical Processing

While nanofibers are employed differently in various applications to address unique challenges (details of which are discussed in each respective section), the underlying issue common to all is reaction efficiency in terms of speed and yield. Heterogeneous reactions involving solids, particularly heterogeneous catalysis, are widely utilized in many industrial chemical processes. Finely divided solids in the form of particles, especially nanoparticles, are usually used in these processes because their small sizes mean high-surface areas, large number of reactive sites, and better reaction efficiency. However, aggregation and uncontrolled

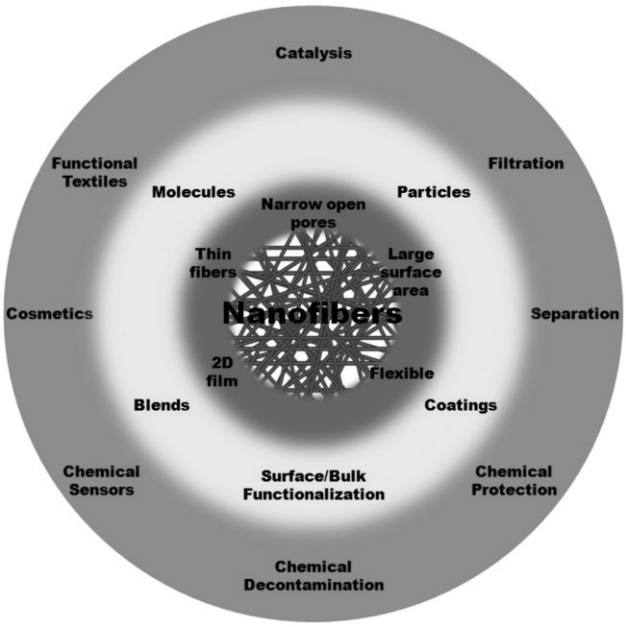

Figure 4. Nanofibrous applications in chemical processing following surface functionalization.

crystal growth during particle synthesis reduce their active surface areas resulting in loss of reaction efficiency.[214] In addition, particulates pose difficulties in handling, product purification and catalysis recovery, and are health hazards due to their powdery nature.[215,216] Packing particulates or mounting them onto porous substrates with high-surface areas ease handling, product purification, and catalyst recovery/reuse but these again lower reaction efficiency due to loss of reactive surface areas and porosities, chemical changes in the particles, and large pressure drops and moving bed phenomena in continuous flow fixed-bed processes.[215,216] Furthermore, commonly used catalyst substrates such as activated charcoal have small and narrow pores which limit reaction efficiency due to low-mass transfer.[217]

4.2. Novel Characteristics of Nanofibers in Chemical Processing

Nanofibers can be used in chemical reactions to improve reaction efficiency due to their unique morphology. The high-aspect ratio and thin diameters of nanofibers mean high-specific surface areas for chemical reactions compared to bulk materials and also for catalyst immobilization. This translates into greater number of reactive sites and hence faster reactions and higher yield in chemical reactions. Fang et al.[218] applied Au-nanoparticle-coated polyethyleneimine (PEI)/poly(vinyl alcohol) (PVA) nanofibers as catalysts in the hydrogenation of 4-nitrophenol to 4-aminophenol. 97% hydrogenation was achieved with nanofibers in 36 min compared to 72% with Au nanoparticles-coated PEI/PVA film due to higher specific surface area and porosity of the nanofibers. The open porosity of nanofiber mats also allows more efficient mass transport at reactions sites on the fibers. Zhou et al. used Pd-nanoparticles-coated carbon nanofibers in the catalytic hydrogenation of 4-carboxybenzaldehyde (4-CBA) to terephthalic acid (PTA), a raw material used in the production of poly(ethylene terephthalate) (PET) and an important industrial polymer.[217] 98.3% conversion was achieved using the fabricated catalyst compared to 90% with commercial Pd-on-activated-carbon catalyst despite a lower specific surface area in the fabricated catalyst (200 $m^2 \cdot g^{-1}$) compared to the commercial one (1000 $m^2 \cdot g^{-1}$). Analysis of surface porosity on both catalysts revealed that the commercial catalyst had mostly micropores of less than 2 nm while the fabricated catalyst had larger open pores ≈10 nm in size. Hence, the authors concluded that better catalytic performance of the Pd-nanoparticle-coated carbon nanofibers was due to their higher porosity which promoted greater mass transfer between reactants, products, and catalytic sites on the nanofibers.

The ability to macroscopically shape nanofibers and grow/deposit them onto various substrates facilitates their handling and customization for different applications. In catalytic processes, nanofibers can be employed to ease the separation of catalysts from reactants and products for product purification and catalyst recycling. For instance, Chen et al.[219] employed carbon nanofibers containing Pd nanoparticles as catalyst in the liquid-phase Sonogashria coupling reaction of iodobenzene and phenylacetylene for 10 runs. After each run, the nanofiber catalyst was retrieved by filtration, washed, and vacuum-dried before being used again for the next reaction. It was found that the catalyst showed near 100% retrieval with no change in catalytic activity after 10 runs. When mounted on an appropriate support, nanofibers can be used as reaction membranes in continuous flow processes, which is useful in large-scale industrial operations. Ag-doped zeolite Y particles coated onto the surface of Al_2O_3 nanofibers had been used as an integrated membrane in the photo-degradation of Methylene Blue in wastewater treatment with 85% permeating selectively under visible light irradiation and a flux of 200 $L \cdot m^{-2} \cdot h^{-1}$ without flux deterioration commonly encountered with non-catalytic membranes.[220]

4.3. Catalysis

Catalysis plays critical roles in the production of fuel, energy, chemicals, food, and pharmaceuticals, and in environmental remediation as well, contributing to >35% of global GDP.[221] Owing to its economic and

industrial importance, there is always on-going research to develop better catalysts to improve reaction efficiency. There has been growing interest in using nanofibers as catalysts or catalyst supports due to their unique morphology, which promises greater reaction efficiency. Table 4 provides a summary of nanofibers that have been applied in industrially relevant catalytic reactions.

4.4. Heterogeneous Catalysis

The various challenges associated with the use of catalyst particles in heterogeneous catalysis have been described. Nanofibers can offer viable solutions to these challenges because their thin fibers and open, porous morphology provide large specific surface areas on which to mount catalyst nanoparticles with minimum compromise their large reactive surface areas and mass transport, resulting in improved reaction efficiency, as discussed above. Aggregation and chemical changes to catalyst particles are avoided, uniform growth of catalyst nanoparticles on the nanofibers can be achieved and handling and separation of products and catalysts for product purification and catalyst recovery/reuse become more convenient, as pointed out earlier. Besides catalyst supports, nanofibers can be made catalytic as well by fabricating them directly from catalytic materials, thus eliminating the need for catalyst immobilization and disadvantages associated with nanoparticle use. For instance, hollow TiO_2 nanofibers were shown to have greater activity in the photo-catalytic degradation of formaldehyde, decomposing 80% of formaldehyde compared to 42% for TiO_2 nanoparticles and 50% for mesoporous TiO_2 powder.[250]

Nanofiber catalyst supports can be designed to play an active role in assisting catalytic reactions. Ledoux and coworkers[222–224] fabricated Ir nanoparticles supported on carbon nanofibers and compared their catalytic performance in the decomposition of hydrazine with commercially available Ir/Al_2O_3 catalyst for satellite propulsion. Faster hydrazine decomposition was achieved with the synthesized nanofibers compared to the commercial catalyst in terms of similar or greater thrust generated with less Ir. Good performance of the synthesized nanofibers was attributed by the authors in part to better thermal conductivity of the carbon nanofibers which reduced formation of hot spots in the catalyst compared to the commercial catalyst, in addition their higher open porosity and specific surface area. The same research group also synthesized Ni nanoparticles supported on carbon nanofibers for the catalytic oxidation of H_2S to sulfur, a process used to remove H_2S from waste gases generated by various industries.[231] Increased resistance toward catalyst deactivation was observed compared to Ni/SiC catalyst due to rapid removal of sulfur formed on the catalytic sites by the condensed water film formed on the hydrophilic surface of carbon nanofibers, in addition to increased desulfurization activity.

4.5. Homogeneous Catalysis

Homogeneous catalysis usually involves reactants and catalyst molecules in liquid medium. Stability and reactivity of catalyst molecules in the reacting medium are of relevance in homogeneous catalysis; a loss of either one would result in decreased reaction efficiency. Instability and inactivity of catalyst molecules could arise due to a variety of reasons such as temperature variation, pH variation, solvent effects, or aggregation.[214,266]

Using nanofibers to immobilize molecular catalysts in homogeneous catalysis offers several advantages over the use of free molecules. Like heterogeneous catalysis, nanofibers offer large specific surface areas for catalyst immobilization, efficient mass transport due to their open porous morphology, ease of product purification and catalyst recovery/reuse, and the possibility of continuous flow operations. Xie and Hsieh[259] investigated the catalytic activity of lipase-carrying polymer nanofibers in the hydrolysis of olive oil. While catalytic activity of lipase immobilized on nanofibers decreased 100-fold compared to free lipase, it was 6 times more than those immobilized on cast films due to higher specific surface area and porous morphology of the nanofibers. Immobilization of catalyst molecules on nanofiber surfaces also enables a certain degree of restrain on their spatial and conformational arrangements, protecting them to some extent from inactivation due to aggregation, solvent effects, and temperature or pH changes with minimum detrimental effects to their catalytic activity.[214,266] Jia et al.[263] fabricated α-chymotrypsin-coated PS nanofibers and found hydrolytic activity of the immobilized enzymes to be 65% that of free enzymes. However, this was higher compared to other forms of enzyme immobilization. Furthermore, enzyme activity of the synthesized nanofibers in non-aqueous medium was three orders of magnitude higher compared to free enzymes due to improved enzyme stability against structural denaturation; half-life of enzymes immobilized on PS nanofibers was 18-fold longer compared to free enzymes.

Many nanofiber-based catalysts have been developed and investigated for different industrial catalytic reactions. It can be generally concluded that they exhibit greater reaction efficiency due to their larger specific surface areas and open, porous morphologies, without the disadvantages commonly associated with traditional particulate catalysts. A variety of nanofiber-based catalysts have also been synthesized for similar chemical reactions or reaction types; however, comparison as to which is better is difficult due to dissimilar methods and characterization techniques employed in different studies. Many studies conducted

Table 4. Nanofibers for catalysis.

Type of reaction	Nanofiber fabrication technique	Nanofiber used[a)]
heterogeneous catalysis		
decomposition	CCVD	Ir NPs on CNFs on graphite felt[222–224]
hydrodechlorination	CCVD	Ni NPs on CNFs on SiO_2[225]
hydrogenation	CCVD, electrospinning, HDP	Au NPs-coated PEI/PVA NFs;[218] PAN-AA NFs containing Pd NPs;[226] Pd NPs-coated CNFs;[217,227] Pd NPs-coated CNFs containing Ni-Fe NPs;[228] Ru NPs-coated CNFs[229]
oxidation	CCVD, electropolymerization electrospinning, flame burning, hydrothermal synthesis, polyol reduction, template synthesis	Ag-hollandite NFs;[230] NiS_2 NPs on CNFs;[231] PANI NFs on Pt/C-coated electrodes;[232] Pt NPs or nanofibers-coated TiO_2 NFs;[233] Pt NPs-coated CNFs;[234–236] Pt NPs-coated hollow CNFs;[237] Pt NPs-coated SDS-functionalized CNFs;[238] Pt NPs-coated CNFs containing MWCNTs;[239,240] CNFs containing PtRu NPs;[239] PtRu NPs-coated CNFs;[241,242] silicotungstic acid stabilized PtRu NPs-coated CNFs;[243] PtRu NPs-coated PAMAM-functionalized CNFs;[244] $LaMnO_3$ NFs[245]
oxidative dehydrogenation	CCVD	carbon nanofilaments;[246] CNFs on carbon felt;[215,216] CNFs on lava rock[247]
oxygen reduction	CCVD, electrospinning, polyol reduction	Pt NPs-coated Nb-doped TiO_2 NFs;[248] N-doped CNFs[249]
photocatalysis	electrospinning	hollow TiO_2 NFs;[250] TiO_2 NFs[251]
proton exchange membrane fuel cell	CCVD, electrospinning, polyol reduction	sulfonated polyimide NFs in sulfonated polyimide;[252] Pt NPs-coated CNFs;[253] Pt NPs-coated CNFs on carbon fabrics[254]
chemical coupling	electrospinning	CNFs containing Pd NPs;[219] Pt-, Pd-, or Rh-coated TiO_2 or ZrO_2 NFs[255]
water gas shift	electrospinning	TiO_2 NFs containing Pt NPs[256]
homogeneous catalysis		
cell lysis	electrospinning	lysozyme-coated PCL/PLGA-*b*-PEG-NH_2 NFs[257]
hydrolysis	electrospinning	PS/PSMA NFs containing α-chymotrypsin;[258] PVA NFs containing lipase[259]
aza-Diels-Alder	CCVD, electrospinning	PS core, PPX, or PPX C-shell, NFs containing $Sc(OTf)_3$[260,261]
oxidation	CCVD, electrospinning	PAMAM-coated on inner surface of PPX nanotubes[260]
Michael addition	electrospinning	PS NFs containing prolinol-oligostyrene[262]
others	electrospinning	α-Chymotrypsin-coated PS NFs;[263] lipase-coated PANCMPC NFs;[264] lipase-coated PSU/PVP or PSU/PEG NFs[265]

[a)]AA, acrylic acid; CNFs, carbon nanofibers; CCVD, catalytic chemical vapor decomposition; HDP, homogeneous deposition precipitation; MWCNTs, multi-walled carbon nanotubes; NFs, nanofibers; NPs, nanoparticles; PAMAM, polyamidoamine; PAN, polyacrylonitrile; PANCMPC, poly[acrylonitrile-*co*-(2-methacryloyloxyethyl phosphorylcholine)]; PANI, polyaniline; PCL, poly(ε-caprolactone); PEG, poly(ethylene glycol); PEI, polyethyleneimine; PLGA, poly[(D,L-lactic acid)-*co*-(glycolic acid)]; PPX, poly(*p*-xylylene); PS, polystyrene; PSU, polysulfone; PSMA, poly[styrene-*co*-(maleic anhydride)]; PVA, poly(vinyl alcohol); PVP, poly(*N*-vinyl-2-pyrrolidone); SDS, sodium dodecylsulfate.

on the catalytic applications of nanofibers were in vitro, small-scale, and laboratory-based investigations. While these may be satisfactory for elucidating and understanding catalytic processes and evaluating materials for further development, the promising catalytic performance of nanofiber-based catalysts needs to be assessed and validated with scale-up studies in pilot plants for potential industrial applications. Besides reaction efficiency, other relevant performance parameters need to be examined in evaluating nanofiber-based catalysts for industrial catalysis. For instance, selectivity of the catalyst for the desired reaction pathway or product should be assessed. Chen et al.[230] studied the acetaldehyde and carbon dioxide selectivities of Ag-hollandite nanofibers in the catalytic oxidation of ethanol and found that acetaldehyde selectivity was almost 100% below a reaction temperature of 170 °C but any further increase in reaction temperature resulted in a drop in selectivity due to the formation of carbon dioxide. Catalyst leaching and catalytic yield after repeated runs are also major concerns in industrial catalysis. Stasiak et al.[261] investigated the loss of $Sc(OTf)_3$ catalyst from polystyrene core/poly(*p*-chloroxylylene) shell nanofibers and found that most catalyst loss occurred during the pre-washing process and initial catalysis run. Despite the low-catalyst loading after this initial leaching, catalytic activity of the nanofibers in aza-Diels-Alder reaction remained high. However, yield was significantly reduced after the 5th catalytic run. Other factors of interests in the design and characterization of nanofiber-based catalysts include catalyst poisoning, deactivation, stability under different reaction conditions, and ease of catalyst regeneration/reuse.

4.6. Filtration and Separation

Nanofibers have great potential in filtration due to their unique morphology. Their thin fibers, high-specific surface areas and narrow but open pore structures allow for high-filtration efficiency at high flux with low-pressure drop.[267,268] Filtration performance is dependent on nanofiber morphology, which can be modified easily by varying fabrication parameters.[269–271] Nanofibers have been investigated for use in particulate filtration in fluids,[272,273] aerosol,[274] and emulsion filtration[275] with promising results. This review will focus on the chemical aspects of filtration and separation using nanofibers. Table 5 provides a summary of nanofibers that have been investigated for chemical-related applications in filtration and separation.

Nanofibers made from inert materials are used solely as particulate filters. However, with chemical functionalization, nanofiber filter membranes can detoxify the filtering medium by removing molecular or ionic contaminants. Dai et al.[299] electrospun polymeric nanofibers for the removal of model polycyclic aromatic hydrocarbons anthracene, benz[α]anthracene, and benzo[α]pyrene from wastewater. Best absorption capacity of $4112.3 \pm 35.5\ \mu g \cdot g^{-1}$ for anthracene on PCL nanofibers, and $1338.8 \pm 16.9\ \mu g \cdot g^{-1}$ for benz[α]anthracene and $712.1 \pm 7.8\ \mu g \cdot g^{-1}$ for benzo[α]pyrene on PLCL nanofibers were obtained. Absorption mechanisms were found to be mainly hydrophobic interaction, hydrogen bonding, π–π interactions and pore-filling between hydrocarbon molecules and polymer nanofibers. Chen et al.[305] surface-coated carbon nanofibers with *β*-cyclodextrin (β-CD) and found that they were able to remove ≈100% of phenolphthalein from an ethanol/water mixture in 5 min and $132.43\ mg \cdot g^{-1}$ of fuchsin acid compared to $34.2\ mg \cdot g^{-1}$ in activated carbon.

Incorporating catalysts that break down contaminants into nanofiber filter membranes can help prevent membrane fouling due to accumulation of contaminant molecules on the fiber surfaces, a common phenomenon observed in molecular filter membranes that leads to decreased filtering efficiency, low flux, and high-pressure drop.[220] Ceramic or metal nanoparticles are usually incorporated into nanofiber filter membranes to catalytically degrade molecular contaminants. Demir et al.[280] synthesized Ag-nanoparticle-coated poly[acrylonitrile-*co*-(glycidyl methacrylate)] (P(AN-GMA)) and poly(glycidyl methacrylate) (PGMA) nanofibers and found that they could completely reduce Methylene Blue in 11 min in the presence of $NaBH_4$. Ceramic nanofibers can also be employed for the same purpose. Li et al.[285] electrospun CeO_2–ZnO nanofibers and found that they could photocatalytically degrade 98% of Rhodamine B in 3 h. Besides molecular contaminants, bacteria also cause membrane fouling. Integrating anti-bacterial materials such as Ag nanoparticles[306] or chemical biocides[317] into nanofiber filter membranes can reduce the amount of bacteria in both filtrate and membrane and help prevent/delay membrane biofouling.[318]

Nanofibers have also been applied in product purification as separation and affinity membranes. Peng and Ichinose[313] fabricated MnOOH nanofibers and used them to separate various compounds. Selectivity factor of 4.9 was obtained for ethanol/water separation and 26.7 for CO_2 separation from air, with 93% rejection for 5 nm Au nanoparticles (NPs) and 94% absorption for Cytochrome C after 2 min 40 s in separate tests. Yoshimatsu et al.[319] synthesized PET nanofibers containing propranolol-imprinted nanoparticles. The nanofibers showed high selectivity toward propranolol (80%) compared to other structural analogs (<50%) and stability in various solvent systems.

Different nanofiber-based membranes have been synthesized for filtration and separation of various substances. Performance in the functionalities of interest have

Table 5. Nanofibers for filtration and separation.

Function	Nanofiber fabrication technique	Nanofiber used[a)]
catalytic degradation of organic compounds	electrospinning	Fe NPs-coated PAA/PVA NFs;[276–278] Fe_3O_4 NPs in PANCAA NFs;[279] Ag NPs-coated P(AN-GMA) and PGMA NFs;[280] SiO_2 NFs containing Ag NPs;[281] Cu or Fe NPs supported on CNFs[282]
photocatalytic degradation of organic compounds	electrospinning, hydrothermal synthesis, sol/gel synthesis, template synthesis	TiO_2 NPs-coated PSEI NFs;[283] polymer NFs containing short TiO_2 NFs;[284] Ag NPs-doped zeolite Y particles on Al_2O_3 NFs;[220] CeO_2–ZnO NFs;[285] TiO_2 NFs;[286] hydrogen TiO_2 NFs;[286,287] TiO_2 NPs-coated TiO_2 NFs;[288] anatase-coated TiO_2(B) NFs;[289] TiO_2-coated CNFs[290]
ion absorption	CCVD, electrospinning, hydrothermal synthesis, re-precipitation, sol/gel synthesis	Nylon-6 or PCL NFs containing AlOOH NPs;[291] SiO_2 and PVA/SiO_2 NFs;[292,293] dithizone NFs;[294] SiO_2 NFs;[295,296] $Na_2Ti_3O_7$ and $Na_{1.5}H_{0.5}Ti_3O_7$ NFs;[297] CNFs in Ba^{2+}-alginate-coated vesicles[298]
hydrocarbon absorption	electrospinning, hydrothermal synthesis	PCL, PDLLA, PLACL, PLGA, and MPEG-PLGA NFs;[299] PMMA/PNIPAM NFs;[300] Azido phenyl-carbomylated or phenyl-carbomylated β-CD/PMMA NFs;[301] PS NFs containing α-, β-, or γ-CD;[302] DNA-CTMA NFs containing Fe_3O_4 NPs;[303] CNFs;[304] β-CD-coated CNFs[305]
pathogen removal	electrospinning	Ag NPs-coated PA, PAA, PEI and PSU NFs;[306] chlorinated *m*-aramide NFs;[307] Nylon-6,6 NFs containing various biocides;[308] Ag NPs-containing CA, PAN and PVC NFs[309]
multi-functional membranes	electrospinning, hydrothermal synthesis, solution aging with aminoethanol	poly(MMA-*co*-NAAP) NFs;[310] chitosan/PEO NFs;[311] TiO_2 NPs-coated polyamide-1,1 NFs;[312] MnOOH NFs;[313] TiO_2 nanofibers[314]
affinity membrane	rlectrospinning	Cibacron Blue F3GA-coated cellulose NFs;[315] PET NFs containing propranolol-imprinted NPs[316]

[a)]CA, cellulose acetate; CD, cyclodextrin; CNFs, carbon nanofibers; CTMA, cetyltrimethylammonium; MMA, methyl methacrylate; MPEG, methoxypoly(ethylene glycol); NAAP, : *N*-allyl-4,5-di[(2-picolyl)amino]-1,8-naphthalimide; NFs, nanofibers; NPs, nanoparticles; PA, polyamide; PAA, poly(acrylic acid); PAN, polyacrylonitrile; PANCCA, poly[acrylonitrile-*co*-(acrylic acid)]; P(AN-GMA), poly[acrylonitrile-*co*-(glycidyl methacrylate)]; PCL, poly(ε-caprolactone); PDLLA, poly(D,L-lactide); PEI, polyethyleneimine; PEO, poly(ethylene oxide); PET, poly(ethylene terephthalate); PGMA, poly(glycidyl methacrylate); PLACL, poly(lactide-*co*-caprolactone); PLGA, poly[D,L-lactic acid)-*co*-(glycolic acid)]; PMMA, poly(methyl methacrylate); PNIPAM, poly(*N*-isopropylacrylamide); PS, polystyrene; PSEI, polydimethylsiloxane-*block*-polyetherimide; PSU, polysulfone; PVA, poly(vinyl alcohol); PVC, poly(vinyl chloride).

been evaluated and found to be promising or even better than the membranes currently in use. Fabrication techniques used depends on the architecture of nanofiber design while characterization techniques employed depends on the performance of interest in the application that the nanofibers have been designed for. Many reported studies used model compounds such as dyes to study the chemical degradation performance of nanofiber membranes. For further development in the intended application, chemical degradation performance against the original compounds would need to be assessed and validated. Furthermore, different functionalities in multi-functional nanofiber membranes had mostly been evaluated independently. A better assessment of multi-functionality and potential for the intended application is to study the performance of all functionalities simultaneously in field trials or under realistically simulated experimental conditions. Relevant factors of interest in the design and evaluation of nanofiber-

based membranes include working capacity, selectivity, leaching, stability under different working conditions, mechanical integrity, ease of regeneration, working/storage life, and environmental compatibility.

4.7. Chemical Protection and Decontamination

Chemical protection and decontamination represents a niche application for nanofibers that combines their excellent filtration property, high-fluid flux, and large specific surface area which can support catalysts, molecules, and chemical reactions. Research in this area has focused mainly on the application of nanofibers for the development of permeable wearable protective systems for military use such as gas masks and chemical protective suits.[320,321] However, such systems also find useful potential applications in personnel protection in environmental remediation and chemical processing industries, and also in the decontamination of the environment, facilities, and equipment exposed to toxic chemicals. Table 6 provides a summary of nanofibers that have been investigated for use in chemical protection and decontamination.

Degradation of toxic chemicals by nanofiber membranes have been achieved through various means. Incorporating metal or metal oxide nanoparticles into nanofiber membranes to catalytically degrade toxic chemicals is a common technique.[321] Krogman et al.[323] fabricated TiO_2-nanoparticle-coated nylon-6,6 composite nanofibers that could photocatalytically degradation 74% of chloroethylethylsulfide (CEES), a stimulant for mustard gas, while maintaining a water vapor flux of 14.2 $kg \cdot m^{-2} \cdot d^{-1}$ compared to 12.1 $kg \cdot m^{-2} \cdot d^{-1}$ in a US army cotton battle-dress uniform. Catalytic metal oxide nanofibers

Table 6. Nanofibers for chemical protection and decontamination.

Application	Nanofiber fabrication technique	Nanofiber used[a)]
photocatalytic degradation of allyl alcohol	electrospinning	TiO_2 NP-coated PAN, PEO, PMMA, PS and PSEI NFs[322]
photocatalytic degradation of CEES	electrospinning	TiO_2 NP-coated nylon-6,6 NFs[323]
photocatalytic degradation of CEPS	electrospinning	TiO_2 NP-coated PANI/PEO and PVC NFs[324]
photocatalytic degradation of CEPS	electrospinning	TiO_2 Ns-coated PSU NFs[325]
catalytic hydrolysis of DFP	electrospinning	PAAO-coated PAN NFs and PAAO NFs[326]
catalytic hydrolysis of PNPA	electrospinning	PAAO NFs[327]
catalytic hydrolysis of paraoxon	electrospinning	PVC, PVDF, and PSU NFs containing MgO or Al_2O_3 NPs[328]
catalytic hydrolysis of paraoxon	electrospinning	PVC NFs containing IBA and β-CD[329]
catalytic hydrolysis of CEES, DMMP and paraoxon	electrospinning	ZnO/TiO_2 NFs[330]
catalytic hydrolysis of DMCP and paraoxon	electrospinning	TiO_2 NP-coated nylon-6/PEI NFs and nylon-6/PEI NFs[331]
catalytic hydrolysis of DFP; antimicrobial activity against aqueous *E. coli* and *S. aureus*	electrospinning	PU NFs containing glucose oxidase, horseradish peroxidise and copolymers based on DMAA-MA and 4-PAM[332]
absorption of topically applied octylmethoxycinnamate	electrospinning	PU NFs containing absorbent particles[333]

[a)]4-PAM, : *N*-alkyl-4-pyridiniumaldoxime; CD, cyclodextrin; CEES, chloroethylethylsulfide; CEPS, 2-chloroethylphenylsulfide; DFP, diisopropyl fluorophosphates; DMAA-MA, dimethylacrylamide methacrylate; DMCP, dimethyl chlorophosphate; DMMP, dimethylmethyl phosphonate; IBA, : *o*-iodosobenzoic acid; NFs, nanofibers; NPs, nanoparticles; PAAO, polyacrylamidoxime; PAN, polyacrylonitrile; PANI, polyaniline; PEI, polyethyleneimine; PEO, poly(ethylene oxide); PMMA, poly(methyl methacrylate); PNPA, *p*-nitrophenyl acetate; PS, polystyrene; PSEI, polydimethylsiloxane-*block*-polyetherimide; PSU, polysulfone; PU, polyurethane; PVC, poly(vinyl chloride); PVDF, poly[(vinylidene fluoride)-*co*-(hexafluoropropylene)].

Macromol. Mater. Eng. 2012, DOI: 10.1002/mame.201200143

can also be used directly to decompose toxic compounds.[321] Ramaseshan and Ramakrishna[330] fabricated $ZnO-TiO_2$ nanofibers with different Ti and Zn ratios and found that nanofibers synthesized with 40% Ti had the best hydrolytic activity, achieving 91% decomposition of paraoxon, a stimulant for organo-phosphorus compounds, in 50 min, and 69% decomposition of CEES in 10 min. While $ZnO-TiO_2$ nanofibers are not likely to be use in protective clothing due to their brittleness, they can be mounted onto stiff substrates to be used in filter canisters in facemasks.

Polymeric materials with reactive functional groups that can degrade toxic compounds have also been fabricated into nanofiber membranes. Chen et al.[326] functionalized the surfaces of electrospun polyacrylonitrile (PAN) nanofibers with oxime groups for the hydrolysis of diisopropyl fluorophosphates (DFP), an organo-phosphorous nerve agent. It was found that reaction increased by as much as 80-fold compared to PAN nanofibers. Molecular catalysts for the decomposition of toxic chemicals can be synthesized and integrated into nanofiber membranes as well. Ramaseshan et al.[329] synthesized a detoxification catalyst β-CD + *o*-iodosobenzoic acid (IBA) and incorporated it into poly(vinyl chloride) (PVC) nanofibers. The resulting PVC/β-CD + IBA blended nanofibers was found to be 11.5 times faster in the hydrolysis of paraoxon compared to activated charcoal and 2–10 times faster than PVC/β-CD, PVC/IBA, and PVC/IBA/β-CD blended nanofibers.

For direct exposure of skin to chemical contaminants, nanofibers can offer decontamination solutions. Vigorous washing and scrubbing of exposed skin massages it and increases transport of contaminants into hair follicles. As hair follicles are long-term reservoirs for topically applied substances, harmful effects of contaminants may extend for long periods of time without detection and elimination. The use of absorbents is a better way to remove topical contaminants. Lademann et al.[333] developed electrospun PU nanofiber films containing absorbent particles trapped within their matrices and found that they were able to remove more topically applied sunscreen from skin (65%) compared to washing (40%).

Nanofibers have proven to be suitable carriers for catalysts in chemical protection and decontamination, and could even be made from the catalysts themselves. Chemical degradation performance of these nanofiber-based catalyst systems had mostly been evaluated against model compounds in place of more dangerous ones. While this allows for safer research and evaluation of materials in the laboratory for further development, the chemical degradation efficacy of these catalysts still requires validation against the original compounds. Degradation performances of nanofiber-based catalysts were also typically evaluated under closed or static conditions, which exhibited poor fidelity to the working conditions of intended use. Potential for practical applications could be more accurately assessed with field trials or under realistically simulated experimental conditions. For instance, Lee et al.[322] evaluated the degradation and penetration of allyl alcohol in TiO_2-coated nanofibers under continuous flow, which more accurately represents the working conditions of intended use. Chemical degradation performances of nanofiber-based catalysts were also frequently evaluated independently against individual compounds. It would be interesting to know how degradation performance of these catalysts would fare in the presence of multiple agents of similar and/or different chemical types. Such information are of importance since it is difficult to predict in advance the compounds that require decontamination or protection against. In addition, a more comprehensive assessment against various pertinent factors which could significantly impact the chemical degradation performance of nanofiber-based catalysts is required, such as reactant concentration, environmental contaminants, catalyst poisons, working conditions, repeated usage, and wear.

4.8. Textiles and Cosmetics

The applications of nanofibers in textiles and cosmetics are indicated in Table 7. Natural fibers such as cotton have been used traditionally for clothing because they impart comfort due to their softness, high absorbency, and high-fluid flux. However, their uses in non-clothing applications such as sporting equipment and upholsteries are restricted due to low strength, low durability, ease of soiling, and flammability. Synthetic polymer fibers are strong and dirt-resistant but they lack the flexibility and comfort of their natural counterparts.[334] Fabricating and using synthetic polymers nanofibers as textiles/fabrics could serve to overcome these short-comings. The thin diameters of nanofibers provide them with flexibility comparable to that of natural fibers while their open, porous morphologies ensure high-fluid fluxes. Mechanical strength of nanofiber mats/films can be reinforced by depositing/laminating them onto conventional textiles/fabrics or synthetic polymer substrates.[335]The resulting composite textiles/fabrics could maintain their desirable characteristics such as mechanical strength, nanofiber morphology, fluid flux, and thermal conductivity after repeated laundering.[336,337]

Incorporating functional materials into nanofiber textiles/fabrics during synthesis can endow them with many useful properties such as resistance to liquid penetration,[365–368] magnetism,[369] and electrical conductivity[370,371] that are difficult to realize with natural fabrics. This facilitates the development of functional textiles/fabrics with applications in personnel protec-

Table 7. Nanofibers for textiles and cosmetics.

Application/ Function	Nanofiber fabrication technique	Nanofiber used[a)]
textiles		
UV protection	electrospinning	PU NFs containing ZnO NPs[338]
anti-bacterial	electrospinning	CA NFs containing C1-BTMP;[339] PU NFs containing 5,10,15,20-tetraphenylporphyrin[340]
self cleaning	electrospinning	CA NFs containing TiO_2 NPs;[341] PAN NFs containing 1,4-*bis*(*o*-cyanostyryl)benzene or 1-(*o*-cyanostyryl)-4-(*p*-cyanostyryl)benzene[342]
color change	electrospinning	PEDOT NFs coated with thermochromic inks;[343] polyimide NFs containing *cis*-DATPP[344]
energy storage	electrospinning	PVDF-PEG 1000 NFs containing fumed silica[345]
environmental remediation	electrospinning	activated carbon cloths from lyocell-based regenerated cellulose nanofiber fabrics;[346] carbonized PAN NFs on activated carbon microfibers[347]
multi-functional textiles	electrospinning extrusion/extraction sol/gel synthesis	PVA-*co*-PE NFs coated with 2-AQS, 2,6-AQS or 2,7-AQS;[348] PU NFs containing ZnO NPs;[349] TiO_2-coated PAN NFs;[350] Nylon-6 NFs containing TiO_2 NPs[351]
cosmetics		
fragrance	electrospinning	PS NFs containing α-, β- or γ-CD and menthol[352]
topical delivery	electrospinning, extraction	collagen NFs containing Au NPs, L-ascorbic acid, retinoic acid and β-CD;[353] CA NFs containing retinoic acid and α-tocopherol; [354] PAN NFs containing L-ascorbic acid 2-phosphate and α-tocopherol acetate;[355] Silk NFs containing 2-phospho-L-ascorbic acid;[356] BC NFs (Biocellulose™ and NanoMasque™);[357–359] self-dissolving patch;[360,361] chitin nanofibrils[362–364]

[a)]2-AQS, anthraquinone-2-sulfonic acid; 2,6-AQS, anthraquinone-2,6-disulfonic acid; 2,7-AQS, anthraquinone-2,7-disulfonic acid; BC, bacteria cellulose; C1-BTMP, : *bis*(*N*-chloro-2,2,6,6-tetramethyl-4-piperidinyl) sebacate; CA, cellulose acetate; CD, cyclodextrin; NFs, nanofibers; NPs, nanoparticles; PAN, polyacrylonitrile; PCL, poly(ε-caprolactone); PEDOT, poly-3,4-ethylenedioxythiophene; PEG, poly(ethylene glycol); PLGA, poly[(lactic acid)-*co*-(glycolic acid)]; PS, polystyrene; PU, polyurethane; PVA, poly(vinyl alcohol); PVA-*co*-PE, poly[(vinyl alcohol)-*co*-ethylene]; PVDF, poly(vinylidene fluoride).

tion,[365,366,372] environmental remediation,[346,347] magnetic shielding,[373] anti-counterfeit tagging,[369] and wearable electronics/energy storage.[345,374–376] Chemical functionalities in textiles/fabrics can be enhanced with the use of nanofibers. For instance, nanofiber textiles/fabrics containing anti-microbial/anti-fungal agents showed greater activity and better performance compared to cast films as their dense, narrow but open pores and high-specific surface areas which could trap bacteria better and increase their exposure to the anti-microbial/anti-fungal agents.[339,340] Similarly, depositing a thin layer of polyurethane nanofibers containing UV-blocking ZnO nanoparticles onto textiles/fabrics could impart them with UV protection factor >40 for both UV-A and UV-B radiation while maintaining air and water vapor fluxes through the composite material due to the dense nanofiber mesh and its porous morphology.[338] Nanofiber fabrics had also been employed as sensor materials; their high-specific surface areas ensured excellent sensor/environment interactions resulting in shorter response/recovery times and higher sensitivities.[344,372]

The large specific surface area of nanofibers finds useful application in cosmetics products as well, usually as masks/patches for topical delivery/application of cosmetics/therapeutic substances.[377] Nanofiber facial masks, such as Biocellulose™,[358] NanoMasque™,[359]

and the Self-Dissolving Patch™ [361] are already commercial available for topical delivery/application of a wide variety of cosmeceuticals. Formulating cosmeceuticals into nanofibers also helps to improve their stability against environmental degradation. For instance, it was found that incorporating menthol into polystyrene nanofibers as cyclodextrin/menthol complexes could improve its release and stability up to 350 °C.[352] Integrating Vitamin A and C into collagen nanofiber facial masks enhanced their stability against oxidation as these masks need only be moisten before use. In contrast, commercial cotton facial masks that are pre-moistened led to oxidation and degradation of their active ingredients before use. The high-specific surface area of the collagen nanofiber facial masks also helped ensure optimum contact between mask and skin to enhance penetration of active ingredients into the skin for maximum effect.[353]

Nanofiber-based textiles with different functionalities have been developed for a variety of applications. Performance in the functions of interest have been investigated and found to be satisfactory or even better than that of traditional bulk textile materials. However, other material properties of nanofiber-based textiles that are relevant to their intended applications also need to be assessed. For instance, while air and moisture permeabilities are routinely evaluated for nanofibers developed for clothing applications, mechanical integrity, which is equally important, is not always investigated. Conventional tensile tests that are used to examine material strength and stiffness are insufficient to characterize clothing material; tests for other mechanical properties such as pliability, tear, bending, compression, or peel strength would be more relevant and useful.[335,337] Other material properties that are pertinent to clothing, such as water repellency, thermal conductivity, and touch, may also need to be assessed.[336] For skin-contacting applications, cell viability, and biocompatibility should to be evaluated. Investigations into the performance of nanofiber-based textiles after prolonged usage, wear, and under different working conditions are also required. Field studies could be conducted to evaluate the performance of the nanofiber-based textiles in order to better understand the effects of practical use and identify opportunities for improvements. Where necessary, safety issues relating to the use of nanomaterials in nanofiber-based textiles, such as toxicity and leaching, must be addressed.

4.9. Chemical Sensing

Chemical sensors are typically based on property changes in their sensing materials due to chemical interactions with analyte molecules. Sensor performance thus depends very much on the speed and magnitude with which the material property is modified. Traditional chemical sensors use thin films to speed up their interactions with analyte molecules. However, their performance remains unsatisfactory due to slow sensor/analyte interactions, resulting in long response/recovery times, low sensitivities, and high limits of detection. Recently, nanofibers have been investigated as sensing materials for chemical sensors. Their thin fibers, high-specific surface areas and porous morphology enable swift sensor/analyte interactions that produce faster response/recovery, higher sensitivities, and lower limits of detection.[378] Table 8 provides a summary of the nanofibers that have been investigated for use in chemical sensing.

Conducting polymers such as poly(3,4-ethylenedioxythiophene) (PEDOT), polypyrrole, and polyaniline are commonly used in chemical sensors.[378] Interaction between polymer and analyte molecules changes the conductivity of the polymer, which is measured and used to quantify the amount of analyte present. Kaner and co-workers synthesized a series of polyaniline-based nanofibers and investigated their use as sensing materials.[385,386] Results showed that nanofibers outperformed thin films in chemical sensing in terms of response/recovery times, sensitivity, and limit of detection. For example, polyaniline-nanofiber-based sensors had a response time of 2 s and >20% resistance change in the presence of 20 000 ppm methanol compared to 33 s and <15% resistance change in film-based sensors. HCl sensing produced similar results. Polyaniline nanofibers-based sensors had a response time of ≈2 s compared to ≈30 s in film-based sensors in the presence of 100 ppm HCl (Figure 5).[410] Chemical sensing in polyaniline occurs through various means including doping, de-doping, reduction, swelling, and polymer chain conformation changes. For analytes that do not interact significantly with polyaniline, the polymer can be doped, coated, or composited with other materials during nanofiber synthesis to induce resistance change in the presence of the analyte. The high specific surface area, porosity, and thin diameter of nanofibers mean faster diffusion of analyte molecules into the polymer to effect these changes, leading to better sensor performance. Besides conducting polymers, other conducting materials such as ceramic nanofibers and carbon nanofibers have also been used in chemical sensing. Santangelo et al.[398] fabricated VO_x-coated carbon nanofibers and applied them to the detection of NO_2 in air. Performance of the sensor was found to be dependent on the crystal structure of VO_x. Beside resistance, other material properties such as current,[381] fluorescence,[379,380] color,[344] surface acoustic wave (SAW),[399,400] and reflectance[382] can also be measured and used for chemical sensing.

When functionalized with biomolecules, nanofibers can act as effective biosensors. Tang et al.[406] immobilized glucose oxidase onto TiO_2 nanofibers with chitosan and

Table 8. Nanofibers for chemical sensing.

Chemical sensor	Nanofiber fabrication technique	Nanofiber used[a)]
gas sensors		
colorimetric/fluorescence	electrospinning	Polyimide NFs containing *cis*-DATPP[344]
fluorescence	electrospinning	PU NFs containing PAA-PM;[379] PS NFs containing a fluorescent sensing polymer (porous/solid)[380]
current	electrospinning, chemical oxidative polymerization	PANI/TiO_2 composite NFs[381]
reflectance	polymerization	CNFs[382]
resistance	electrospinning,CCVD, rapidly initiated polymerization,interfacial polymerization, chemical deposition, vapor deposition, polymerization, atomic layer, deposition	MWCNT-coated nylon-6,6 NFs;[383] MWCNT-coated nylon-6 NFs and nylon-6 NFs containing MWCNTs;[384] PANI NFs;[385–388] PANI NFs modified with $CuCl_2$;[386,389] PANI NFs modified with $CuBr_2$;[390] amine-coated PANI NFs;[22] PDADMAC-coated APTS-BH/PEO/PANI NFs;[391] PANI NFs containing CNTs;[392] PPy NFs;[393,394] PMMA/BPO core PPy shell NFs;[395] PEDOT:PSS/PVP NFs;[396] CNFs;[397] VO_x-coated CNFs[398]
SAW	rapidly initiated polymerization	PANI NFs;[399] PPy NFs[400]
ion sensors		
fluorescence	electrospinning	PU NFs containing PAA-PM[379]
biosensors		
fluorescence	electrospinning	H-PURET-coated CA NFs[401]
current	rapidly initiated polymerization	Au NPs-coated PANI NFs coated with DNA[402]
electrogenerated chemiluminescence	in carbon paste	Cholesterol oxidase immobilized on CNF/CdS hollow sphere composite[403]
amperometric	electro-polymerization, bacteria, electrospinning, polyol reduction	HRP immobilized on PANI-PVS NFs;[404] HRP immobilized on Au NPs-coated BC NFs;[405] glucose oxidase immobilized on TiO_2 NFs with chitosan;[406] CNFs;[407] Glucose oxidase immobilized on CNFs;[408] Pt NPs-coated CNFs;[409] streptavidin immobilized on Au NPs-coated CNFs[386]

[a)]APTS, 3-aminopropyltriethoxysilane; BC, bacteria cellulose; BH, 1-bromohexane; BPO, benzoyl peroxide; CA, cellulose acetate; CCVD, catalytic chemical vapor decomposition; CNFs, carbon nanofibers; *cis*-DATPP, 5,10-*bis*(4-aminophenyl)-15,20-diphenylporphyrin; H-PURET, hydrolyzed poly[2-(3-thienyl)ethanolbutoxycarbonylmethylurethane]; HRP, horseradish peroxidase; MWCNTs, multi-walled carbon nanotubes; NFs, nanofibers; NPs, nanoparticles; PAA-PM, poly(acrylic acid)-poly(pyrene methanol); PANI, polyaniline; PDADMAC, poly(diallyldimethylammonium chloride); PEDOT, poly(3,4-ethylenedioxythiophene); PEO, poly(ethylene oxide); PMMA, poly(methyl methacrylate); PPy, polypyrrole; PS, polystyrene; PSS, poly(styrenesulfonate); PU, polyurethane; PVP, poly(*N*-vinyl-2-pyrrolidone); PVS, poly(vinyl sulfonate).

used them for H_2O_2 and glucose sensing. The composite nanofibers were able to detect H_2O_2 within 5 s in the concentration range of 18–72 $\times 10^{-6}$ M and glucose within 10 s in the concentration range of 0.01–6.98 $\times 10^{-3}$ M. Although voltammetry is usually employed in biosensing, other forms of material changes such as current,[402] fluorescence,[401] and electrogenerated chemiluminescence[403] can also be utilized.

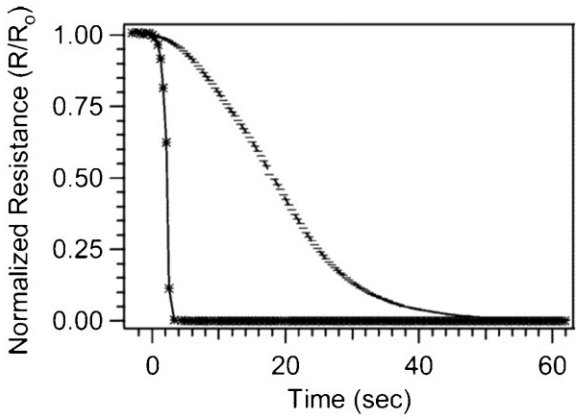

Figure 5. Response of 0.3 μm nanofiber (–) and conventional polyaniline (---) thin films to 100 ppm HCl (Reprinted from ref.,[410] Copyright 2004, with permission from American Chemical Society).

A good chemical sensor should have short response and recovery times, high selectivity and sensitivity, low-detection limit, large working range, ease of regeneration/recovery, temporal and thermal stability, and robustness. Nanofibers have proven to be better chemical sensors compared to conventional film- and ceramic-based sensors in terms of shorter response times, higher sensitivities, and lower detection limits. Nevertheless, there are still opportunities for further development. It is observed, for instance, with the exception of a few cases, that recovery times of nanofiber-based gas sensors are usually much longer than their response times. Furthermore, extensive flushing with air, nitrogen, or sometimes even a neutralizing gas is required to return the response of these sensors to their original states. No explanation has been given to account for their long recovery times. However, for practical applications, recovery times of nanofiber-based gas sensors needs to be shorten and sensor regeneration made more convenient. While some nanofiber-based gas sensors have been developed with selectivity for a particular analyte through the use of target-specific ligands, others made from materials such as polyaniline (PANI), multi-walled carbon nanotubes (MWCNT)-nylon 6, polypyrrole (Ppy), and PEDOT-poly(styrene sulfonate) (PSS)-polyvinyl-pyridine (PVP) exhibited response to various chemicals. This highlights the need to understand and evaluate the response of nanofiber-based gas sensors to the presence of multiple gases in the sensing environment, which so far have focused mainly on a single analyte under controlled conditions. Sensor performance also has to be assessed under different environmental conditions since it has been shown to be affected by humidity[388] and other environmental factors such as temperature. Concurrently, selectivity to the target analyte needs to be enhanced and sensitivity to environmental changes reduced. The potential of a nanofiber-based chemical sensor for an intended application is best evaluated under conditions that most closely resemble its working environment. Extensive cyclic evaluations are also essential to assess the robustness, stability, and working life of the sensors.

5. Electronics

5.1. The Need for Nanofibers

Rapid advancement in science and technology in recent years and the quest for miniaturization of devices and circuits for better performance and cost benefits have led to an emerging interest in nanostructured materials. These nanostructures, which are confined to nanometer dimensions, exhibit unique and dissimilar properties compared to their bulk counterparts. The limited motion of electrons in these confined systems and the quantum effects produced by nanostructures are the main driving criteria for extensive research in this field.[411] In this regard, 1D nanostructures, especially nanofibers and nanowires, have attracted the attention of many researchers of diverse disciplines due to their novel properties and applications.[412,413] One major area in nanomaterials in which the potential of one-dimensionality is widely explored is in the application of inorganic semiconducting metal oxides.[414,415] The ability to apply the unique properties of these materials in practical applications demands better understanding and further development of current technology. The impact of one-dimensionality in physical and electrical properties have been observed in many nanomaterials including enhanced photon absorption and emission,[416] improved ballistic transport characteristics[417] and metal to insulator transition in materials.[418] A large variety of materials have been synthesized in 1D and incorporated into devices, proving their intriguing potentials.[418–421] The present review focuses on the electronic properties of metal oxide nanofibers and applications of metal oxide nanofibers with few aspects of nanowires for comparison.

5.2. Significance of 1D Nanofibers

One of the most significant aspects of nanofibers is their 1D aspect ratio. Their thin diameters put the radial dimension of these structures at or below the characteristic length scale of various interesting and fundamental solid state phenomena: the exciton Bohr radius, wavelength of light, phonon mean free path, critical size of magnetic domains, exciton diffusion length, and others.[422] Figure 6 shows the guided electron transport pathways in nanofibers compared to that in conventional nanoparticles. In

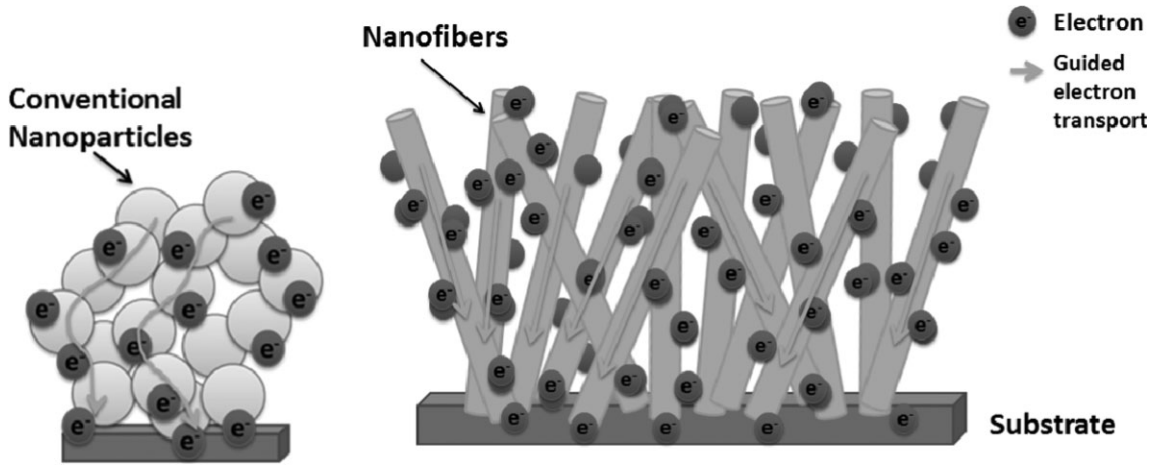

Figure 6. The guided electron transport pathway in nanofibers compared to that in conventional nanoparticle system.

nanofibers, the mean free path of the electrons is shorter, giving rise to the intriguing properties for electronic applications. Low Debye lengths and large surface area to volume ratios dominate charge transport in these nanostructures. The expression for Debye length can be written as:

$$L_D = \sqrt{\left(\frac{\varepsilon_0}{e^2}\frac{\varepsilon k_B}{n_d}T\right)}$$

where k_B is Boltzmann's constant, ε the dielectric constant, ε_0 the permittivity of free space, T the operating temperature, e the electron charge and n_d the carrier concentration. Surface properties which are altered in this regard modify the nanofibers' conductivity, which affects their charge transport and which in turn, has direct implication on device performance.[423] Formation of surface localized acceptor states particularly in metal oxides results in charge transfer between bulk and surface in order to establish thermal equilibrium. Thus a non-neutral region within the semiconductor bulk is formed, resulting in a surface space charge region.[411] In general, conventional MOS nanoparticles, which are widely used as gas sensors, exhibit high sensitivity for gas detection but their sensing properties degrade with the growth of aggregates among the nanoparticles under repeated operations at higher working temperatures.[424] One-dimensional nanofibers, with their high-aspect ratios, large surface areas, and quantum size effects, have become a favorable candidate for overcoming this issue. This property is largely applied in gas sensing since the addition or depletion of majority charge carriers due to absorption of gas molecules leads to measurable changes in nanofiber conductivity. The electron density in these nanostructures depends on the concentration of surface oxygen vacancies which in turn varies as a function of oxygen adsorption and desorption.[425] Oxygen vacancies acts as donor states in metal oxides such as ZnO and SnO_2, attributed to the semiconducting nature of the material.[426] Modifying the diameter of these nanofibers to the depletion layer thickness facilitates complete control of carrier transport. In polycrystalline metal oxide sensors, the charge carriers need to overcome the energy barrier formed at the interface of adjacent grains by thermionic emission to maintain their movement from one grain to another. Hence, in these 1D nanostructures, current flows parallel to the surface via carriers which are thermally activated from surface states. Doping of nanofibers further enhances their electrical properties. Materials such as Al, Ga, and In are used as dopants for ZnO.[427,428] Sb and In are widely used as dopants for SnO_2.[429,430] Dopants in this case help increase the stability of nanofibers in maintaining their conductivity by inducing more charge carriers thereby reducing the Debye length, providing better air stability for the devices. Doping also facilitates tailoring of the depletion/space-charge layer by introducing defect states. In this case, to enhance sensitivity, different promoters such as Pd, Pt, Ru, Cu, etc. have been used. These promoters aid in the catalytic activities of the metals during oxidation of inflammable gases. One of the main factors affecting carrier transport between nanofiber networks is the formation of depletion regions at contacts which act as a hindrance for electron transfer from one nanofiber to another.[415] Moreover, adsorbents on the surface of these nanofibers tend to form a positive space charge due to accumulation of electrons which widen the depletion layer further.[431] The change in electronic properties is due to interaction between metal (Ti)–ZnO nanowire of Schottky barrier at the metal/nanowire interface. This causes an increase in resistivity due to alterations in Fermi-level pinning and an increase in barrier heights

for electron transfer.[432,433] Similarly, the use of nanofibers allows the formation of a direct conduction path for photogenerated carriers to the electrode whereas in conventional nanoparticle structure based solar cells, conduction is limited by several charge-hopping events between individual particles. Using nanofibers ensures that the mobility of the electrons in the solar cells is much higher than that in nanoparticle-based solar cells with improvement in device efficiency since recombination is highly reduced.[434] Moreover, the nano-dimensional diameters of these nanofibers allows the formation of depletion regions at the surface leading to interfacial band bending. This band bending also assists in sweeping electrons away from the surface of the nanowires thereby reducing recombination in these devices. Thus, the nano dimensionality exhibits interesting electronic properties which are entirely distinct from their bulk counterparts. The nanofibers also improve the effective electron diffusion length which aids in efficient collection of electrons thereby reducing recombination.[434]

5.3. Nanofiber-Based Sensors

Diverse applications of nanofibers in gas sensors are demonstrated in Table 9. The fundamental concept of gas sensors is based on changes on the surface of the active material upon which its electrical or optical properties depend. The absorbed species trigger these effects causing a change in the local charge carrier density leading to variations in conductivity which can be detected.[435] The active material is chosen in specific interest to the species to be detected. As discussed earlier, the high-surface area of 1D nanofibers enable better detection of target species due to enhanced electronic properties as a benefit of confined electron transport.[435,436] Electrical responses were shown to increase with decreasing nanofiber diameters due to the scaling effect.[437] These nanostructures offer various advantages such as superior stability due to high crystallinity, very large surface area to volume ratios, high sensitivity, and selectivity, dimensions comparable to the Debye length and surface space charge region. These nanofibers can also be extended for mass production for large-scale fabrication using the simpler methods as mentioned earlier. Metal oxides are widely used as active materials in gas detectors due to their potential to ionosorb oxygen at temperatures above 100 °C.[438] Metal oxide nanofibers are usually produced by electrospinning the precursor solution containing metal ions along with the polymer-solution mixture. The nanofibers are then calcined at high temperatures to remove the polymer and to

Table 9. Application of electrospun nanofibers in gas sensing.

Material	Principle	Fiber dimension (nm)	Detected	Detection limit	Operating temperature	Reference
TiO_2	resistive	120–850	CO, NO_2	50 ppb	300–400 °C	[452]
TiO_2/ZnO	resistive	250	O_2	5.1×10^{-3} Torr	300 °C	[453]
TiO_2	resistive	200–500	NO_2	500 ppb	150–400 °C	[454]
LiCl/TiO_2	resistive	150–260	H_2O	11%	room temp.	[455]
SnO_2	resistive	100	C_2H_5OH	10 ppb	330 °C	[456]
SnO_2	resistive	80–160	toluene	10 ppm	350 °C	[457]
MWCNT/SnO_2	resistive	300–800	CO	47 ppm	room temp,	[458]
ZnO/SnO_2	resistive	100–200	toluene	10 ppm	200–400 °C	[459]
Fe–SnO_2	resistive	60–150	C_2H_5OH	10 ppm	300 °C	[460]
In_2O_3	resistive	30	NO_2	500 ppb	400 °C	[461]
In_2O_3	FET	10	NO_2	20 ppb	room temp.	[462]
Ag/In_2O_3	resistive	60–130	HCHO	5 ppm	115 °C	[463]
ZnO	resistive	100–200	H_2S	4 ppm	room temp.	[464]
ZnO	FET	40	O_2	10 ppm	room temp.	[465]
Pt/In_2O_3	resistive	60–100	H_2S	50 ppm	140–300 °C	[466]
WO_3	resistive	20–140	NH_3	50 ppm	350 °C	[467]
$SrTi_xFe_{0.2}O_{3-x}$	resistive	<100	CH_3OH	5 ppm	400 °C	[468]
SnO_2	resistive	<200	H_2O	1500 ppm	180 °C	[469,470]
SnO_2	resistive	<300	H_2	10 ppm	200 °C	[471]
SnO_2–Ru	resistive	<500	NO_2	250 ppm	room temp.	[472]

enhance the crystallinity of the metal oxide fibers thus produced. Reports have shown that the absorbed NO_2 molecules on the surface increase the resistance of the metal oxide nanofibers thereby altering its conductivity due to interactions between the electrons and absorbed NO_2 ions.[439] Moreover, NO_2 molecules adsorb onto SnO_2 surface oxygen vacancies with certain desorption energies.[440,441] Therefore, metal oxide sensors are generally operated at temperatures above 150 °C which ensures fast molecular desorption as well as full recovery of the initial sensor surface.[442] Nanofibers employed for detecting target species of gas molecules in field-effect transistor (FET) type gas sensors are shown in Figure 7. Metal oxides such as TiO_2, WO_3, ZnO, SnO_2 and MoO_3 are widely used for detecting trace concentrations.[443,444] Metal oxide nanofibers made of Molybdenum oxide (MoO_3) is used for detecting ammonia.[445] Wang et al. demonstrated that electrospun WO_3 nanofibers exhibited rapid response and high sensitivity to various concentrations of ammonia due to the high purity of the material, larger surface-to-volume ratio and increased porosity of the surface providing better exposure of the gas to the sensing material.[446] Cobalt-doped ZnO nanofibers were also employed as photoelectric oxygen sensors due to their faster response to the variation in surface states w.r.t oxygen adsorption.[447] TiO_2 nanofibers are used for detecting NO_2 and H_2.[448] Electrospun TiO_2 non-woven mats were found to exhibit ultra-high sensitivity to NO_2 with a detection limit estimated of about 1 ppb (parts per billion).[448] Electrospun nanofibers can also serve as effective supporting substrate for other sensing materials like nanoparticles of noble metals. TiO_2 membranes loaded with Pd nanoparticles resulted in increased sensitivity and fast response.[449] The response times in this case varies as a function of nanofiber diameter.[450] Higher specific surface area of the nanowires/nanofibers combined with high-porosity results in higher sensor selectivity and it also enables rapid transport of target molecules.[448] Craighead et al. fabricated gas sensors based on the PANI/PEO composite nanofibers by electrospinning which also exhibited rapid and reversible resistance change on exposure to ammonia gas. Similarly, carbon nanotubes/poly(vinylidene fluoride) (PVdF) composite nanofibers showed 35 times increase in sensing threshold than that of the film counterpart.[451]

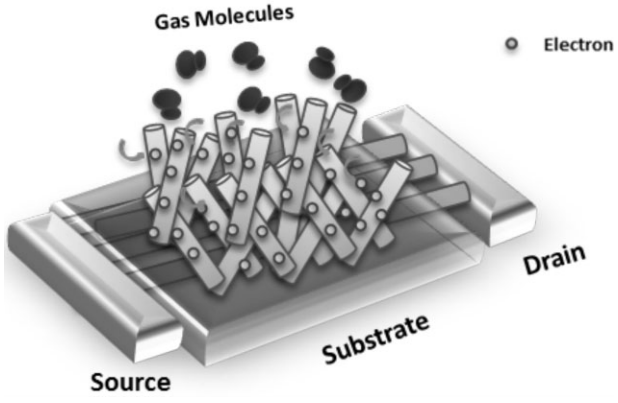

Figure 7. Application of nanofibers as sensor material for gas detection in gas sensors.

Ultra-sensitive metal oxide gas sensors made from nanofibers especially by electrospinning has high-aspect ratio with long nanofiber lengths varying from 10 to several 100 nm. Though these nanofibers can be produced in large scale with much ease by electrospinning compared to other 1D nanostructure fabrication techniques, reproducibility and uniformity of nanofiber dimension is yet to be achieved for sensor applications. A slight variation in the dimension and porosity of nanofibers could affect the sensitivity of the gas sensors. Hence in order to overcome this issue focused research has to be carried out not only in finding new materials for gas sensors but also in developing optimized fabrication protocols for even well studied nanofiber materials to transcend them from lab results to the industrial applications.

5.4. Nanofibers for Photovoltaics/Solar Cells

This field of research is intensely focused on capturing the energy that is freely available from sunlight and convert it into electric power. Photovoltaics follow the principle of impinging the photons onto the pre-tailored semiconducting junctions favorable for formation of electron-hole pair upon light absorption. This creates an electric potential across the interface driving the charges to its appropriate electrodes. Typical solar cells use junctions between two inorganic solids (P-N junctions) for energy harvesting. In the similar fashion, excitonic solar cells such as dye-sensitized solar cells (DSSCs); a kind of photochemical cell uses the liquid solid combination which is well reviewed elsewhere.[473] The main function of a highly efficient photoelectrode for DSSCs is to provide expedient features such as fast electron transporting pathway, slow interfacial electron recombination network and enhanced dye absorption by large specific surface area. The anodes used in the case of DSSC are usually made of sintered films of nanostructured metal oxides such as TiO_2, ZnO, SnO_2, and Nb_2O_5. The nanoparticle films provide large surface to interact with the dye or chromophore. The electron-hole pair disassociates at this interface with electrons injected into the semiconductor layer. These injected electrons need to pass through a large number of traps and grain boundaries present in the nanoparticle film before reaching the collecting electrode. The holes on the other hand move toward the Pt electrode which is later reduced by redox reaction in the electrolyte. The purpose of using NPs is

mainly for the ease of fabrication and large surface area. By replacing the NP layer with nanofibers or single crystalline nanowire, the charge collection efficiency and electron diffusion co-efficient can be increased to a large extent owing to minimized losses due to traps and grain boundaries. One main drawback in this case is the reduced surface area for dye absorption which subsequently reduces the energy conversion efficiency. ZnO photoelectrodes made of electrospun nanofibers with tunable thicknesses is reported. The DSSCs with this photoelectrode showed power conversion efficiency of about 3% which is achieved under irradiation of AM 1.5 with power density of 100 $mW \cdot cm^{-2}$.[474] ZnO nanofibers thus obtained after calcination resulted in high crystallinity with pure wurtzite phase. The improved performance of these ZnO nanofibers can be attributed to high porosity enabling efficient permeability of electrolytes and high-surface area enhancing the dye absorption on the photoelectrode surface. In comparison, Law et al. demonstrated the use of nanowires in DSSC with solution grown ZnO nanowires giving an efficiency of 1.5% even though the charge transport properties are highly enhanced. The cause of low performance is attributed to the decreased surface area and low-dye loading onto the nanowire surface.[475] The importance of the surface area in the nanowire based devices are compared with other nanostructures such as dendritic wires.[434,476] High-surface area and close packing of the nanofibers enables enrichment of the light harvesting and the reduction of the electron back-reaction on the transparent conducting oxide surface without significantly sacrificing electron transport.

The application of nanofibers and its significant performance characteristics in DSSCs is listed in Table 10. Electrospun TiO_2 nanofibers or nanorods are most widely used as photoelectrode for DSSCs for their high-surface area and high porosity leading to increased adsorption of dye sensitizers.[477–479] Figure 8 indicates the improvement of electron diffusion and reduction of recombination in DSSCs by incorporating electrospun TiO_2 nanowires as photoanodes. Figure 9 shows the application of metal oxide nanofibers as photoelectrodes serving as chief electron transport layer in DSSCs. Song et al. used the porous electrospun TiO_2 nanofibers in the quasi-solid state DSSCs achieving high-photocurrent generation.[474,480,481] Transient absorption spectroscopy studies performed at the dye/semiconductor interface for nanofibers showed improved kinetics of charge transfer.[482] Kim and co-workers used high-molecular-weight poly(vinyl acetate) (PVAc) to induce phase separation, which resulted in the formation of TiO_2 nanorods of size 15–30 nm within sintered nanofibers

Table 10. Application of nanofibers in DSSC and its significance.

Material	Nanofiber diameter [nm]	Significance	Efficiency [%]	Reference
TiO_2	100–150	high electron diffusion coefficient	4.2	[434]
TiO_2	150–200	high electron diffusion coefficient and low charge recombination	9.52	[476]
TiO_2 nanoparticles/nanofibers	120	nanofibers as a light-harvesting layer, increased IPCE	10.3	[489]
nanoporous TiO_2	200	high porosity, high sensitizer absorption	5.02	[490]
TiO_2(solid-state DSSC)	20	enhanced penetration of polymer gel electrolyte	3.8	[491]
TiO_2 nanofiber/nanoparticle composite	200–300	improved light harvesting, lower series resistance and large shunt resistance	8.8	[492]
TiO_2	150	increased photocurrent	4.14	[493]
TiO_2 multi-core	200	high surface area and increased photocurrent	5.77	[494]
ZnO	500	efficient electron conducting pathway	3.1	[495]
ZnO	200–500	high surface activity, relatively improved photocurrent	1.34	[496]
Al-doped ZnO	40–150	high surface adhesion and less tensile stress under calcinations	0.55	[497]

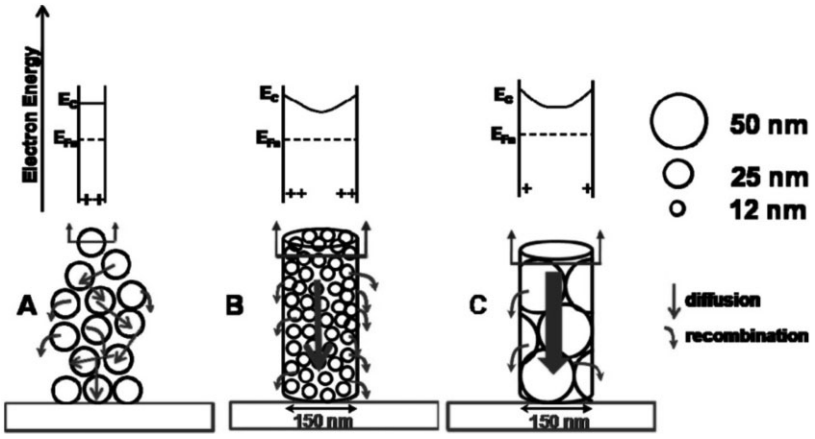

Figure 8. Schematics showing the difference in diffusion process and recombination process in nanoparticle and nanofiber systems in DSSCs. The bottom and top panel shows the morphologies and energy levels, respectively. Diffusion is improved in nanofibers with enhanced particle size due to reduction of the space charge region within the volume of the nanofibers (Reprinted from ref.,[434] Copyright 2009, with permission from American Chemical Society).

of diameter 60 nm having higher specific surface area of about 123 $m^2 \cdot g^{-1}$. The resultant dye loading (8.59×10^{-8} mol $\cdot$ mg^{-1}) was 2.5 times greater than that reported for TiO2 nanoparticles (3.44×10^{-8} mol $\cdot$ mg^{-1}). This innovative combination resulted in efficiencies of 9–11% similar to the highest efficiencies reported using TiO_2 nanoparticles.[483] Furthermore, electrospun nanofibers also facilitates longer electron lifetimes, and increase effective electron diffusion coefficients (D_{eff}), thereby resulting in improved carrier collection and device performance efficiencies.[484] Recent reports have also shown that photoelectrodes made of TiO_2 nanofibers exhibit better efficiency than TiO_2 nanoparticles since the former provides a better electron transport pathway reducing the trapping and detrapping events during the process of charge collection.[485] SnO_2 nanofibers are also obtained by electrospinning which on calcination at 500 °C results in polycrystalline nanofibers with high-aspect ratios. These fibers employed as photoanodes result in increased charge mobility and electron lifetime. But it also had a drawback of increased recombination resulting in low-poor conversion efficiency of about 1% due to poor dye loading as a function of reduced surface area. Recently it has been demonstrated that increasing the Sn concentration in the precursor solution used for electrospinning could result in highly crystalline nanostructures with enhanced dye loading, high-electron mobility and increased charge lifetime. These nanostructures also exhibit high-open circuit voltage of about 700 mV and photovoltaic power conversion efficiency (PCE) of about 3% which is higher than any other pure tin oxide photoelectrodes.[486] Recently SnO_2—TiO_2 core-shell nanofibers are also produced by electrospinning to overcome the drawbacks existing in pure SnO_2 devices. This core-shell system is designed to meet the present state of the art research requirements for DSSCs by combining the beneficial properties of both the materials by means of a single fabrication process. Power conversion efficiency of about 5.1% by employing this is achieved which is five times higher than pure SnO_2 nanofiber or nanotube architecture.[487] P-type materials such as CuO nanofibers are also obtained by electrospinning copper acetate/poly(vinyl alcohol)/water solution followed by calcination at 500 °C. These fibers exhibited enhanced crystallinity as a function of dwelling time under calcination. The dwell time is found to affect the crystallite size proportionately thereby altering the bandgap of the material as a result of quantum confinement. These CuO nanofibers are used as blocking layer in conjunction with ZnO photoelectrodes which resulted in 25% increase in the current density as compared to plain ZnO photoelectrodes.[488]

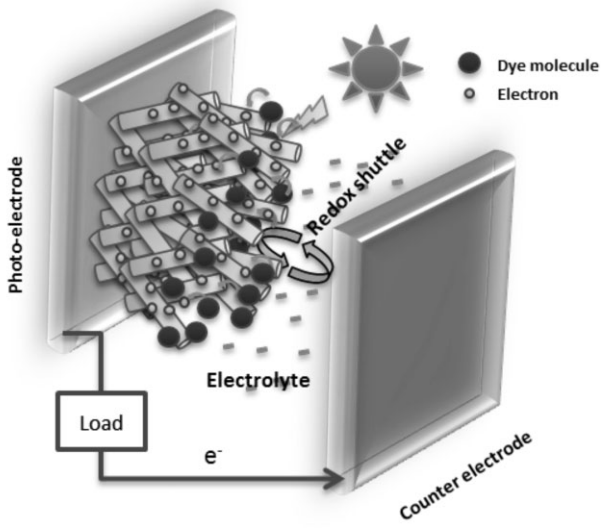

Figure 9. Application of nanofibers as photo-electrodes in DSSC.

The application of nanofibers as a replacement for nanoparticles as photoelectrodes in DSSCs is still an open debate among the researchers. One of the main reasons is the scalability issue. Even though electrospinning method of producing nanofibers is highly scalable and cost effective compared to other techniques, achieving nanofibers of uniform diameter (<50 nm) is still a major challenge which is yet to be addressed. Since the nanofiber diameter

directly plays a major role is determining the specific surface area which in turn determines the amount of dye loading onto the photoelectrode. Hence it has a direct implication on the performance of DSSCs. Even though many other quasi 1D structures such as nanoflowers, nanospheres, and so on are reported, there is a trade-off between low-production rate, surface area, and performance. Moreover vertically aligned nanofibrous photoelectrode with high-specific surface area is not yet achieved in any of the methods which is really a need of the hour for improving the efficiency of DSSCs. Future research in the direction of nanofibers should be able to address these existing issues by concentrating simultaneously on both material as well as charge transport perspective in these devices.

5.5. Energy Storage (Lithium Ion Batteries)

The main factor for future energy needs and application of alternative energy sources are effective storage media, such as batteries. Generally, the capacity loss in batteries often arises from the volume change in charging and discharging reactions leading to stress-induced material failure. Therefore, nanostructures with high-surface-to-volume ratio, which additionally contribute to higher conduction values, are promising anode materials for lithium ion battery. For the effective incorporation of Li in the electrode material, reduction and formation of metallic species is highly required. Therefore, the formed metal reacts with the reduced Lithium atoms in order to form an alloy which serves as the storage medium. The process of battery discharging (Li inserted) and charging (Li released) at room temperature takes place at anode electrode. Considering the above mentioned factors electrospun nanofibers serve as effective electrode materials since these materials possess shorter charge diffusion path compared to that of the nanoparticles. Moreover these nanofibers also exhibit faster intercalation kinetics due to their high-surface area/mass ratio. Electrospun nanofibers also plays a major role in reducing the charge transfer resistance between the electrolyte and the active electrode materials since these fibers have unique property of possessing large number of lithium insertion sites. Thus the use of nanofibers as electrode materials in Li-ion batteries has become indispensable.

Some of the applications of nanofibers as anode, cathode, and separator materials in Li ion batteries are listed in Table 11. Electronic conductivity of the nanofibers play a major role in reducing the resistance, thereby, improving

Table 11. Application of nanofibers in batteries and its significance.

Materials	Functionality	Significance	Reference
MnO_x/C	anode	high porosity, large surface area, and high conductivity	[504,505]
Fe_3O_4/C	anode	highly reversible and large volume changed during conversion reaction	[506]
Co/C	anode	Li-ion diffusion distance is reduced	[507]
Sn/C	anode	Sn parking density is higher	[508]
		increased surface area and improved interfacial electrode electrolyte contact	[509]
Si/C	anode	large reversible capacity, cyclic performance is relatively higher and Li ion diffusion distance is short	[510]
		high surface area and increase in reversible capacity	[511]
Cu/C	anode	improved ionic transfer and high electronic conductivity	[512]
Ni/C	anode	high electronic conductivity and higher rate capacity	[513]
porous C	anode	smaller pore size, high surface area, and enhanced stability in cycling performance	[514]
$LiCoO_2$	cathode	three-dimensional structure, higher rate capacity, and improved reversibility	[515]
		rapid Li ion diffusion	[516]
$LiCoO_2$/MgO	cathode	core/shell structure, high reversibility, and impedance growth is lower	[517]
Al-doped $LiNi_{1/3}Co_{1/3}Mn_{1/3}O_2$	cathode	superior rate capacity and better cycling performance	[518]
PVDF	separator	cycling capability is higher and capacity loss is less	[519]
PVDF-HFP	separator	enhanced electrochemical stability, high-cycling capacity	[520]
SiO_2/PAN	separator	stable cycling performance with improved electrolyte uptake	[521]

the Faradaic reaction through enhanced ionic transfer. The application of electrospun nanofibers as anode materials in Li batteries exhibits superior electrochemical properties compared to its nanopowder counterparts. Kim et al.[483] employed electrospun carbon fibers in lithium ion batteries achieving a reversible capacity of up to 500 $mA \cdot h \cdot g^{-1}$. The employment of nanofibers as cathode and anode materials in Li ion batteries is described in Figure 10. Chen and co-workers[484] synthesized C/Co composite nanofibers using electrospinning which when employed in Li ion batteries showed higher order of capacity retention and improved electrical conductivity. The electrospun C/Co composite nanofibers thus produced exhibits large reversible capacity of about 800 $mA \cdot h \cdot g^{-1}$ and good cycling performance. Electrospun $LiCoO_2$ nanofibers with diameters about 500 nm exhibited a high-initial charge and discharge capacity.[498] However, the formation of crystalline Li_2CO_3 and CoF_2 impurities due to the dissolution of cobalt and lithium cations from $LiCoO_2$ leads to large loss for the electrode retention capacity. This problem was solved by fabricating $LiCoO_2$/MgO coaxial nanofibers using electrospinning. These core/shell fibers exhibited excellent reversibility and smaller impedance growth.[499] Fu and co-workers[500] observed that single-walled nanotube (SWNT)/NiO composite nanofibers synthesized by electrospinning improved the rate capability when compared with pure NiO nanofibers. It also exhibited better cycling performance at large charge and discharge current densities with a noticeable improvement in durability. Fan et al. prepared Mn_3O_4 nanofibers by electrospinning. These nanofibers exhibited excellent electrochemical capacity which exceeded 450 $mA \cdot h \cdot g^{-1}$ for at least 50 cycles.[501] Sun et al.[502] also applied electrospun Mn oxides nanofibers to Li cells and obtained a high-reversible discharge capacity of 160 $mA \cdot h \cdot g^{-1}$. Recently, nitridated electrospun TiO_2 hollow nanofibers were synthesized by Hyungkyu et al.[503] These fibers exhibited an excellent rate performance with discharge capacity of about 85 $mA \cdot h \cdot g^{-1}$ which was nearly two times higher than that of pristine TiO_2 nanofibers 45 $mA \cdot h \cdot g^{-1}$. The significant improvement in the rate capability is due to the hollow geometry and conducting shell layer of these nanofibers which provides a shorter Li ion diffusion length and a high electronic conductivity along the surface. Thus the nanofibers play a significant role in altering the electronic properties of these materials resulting in better performance compared to its nanoparticle counterparts.

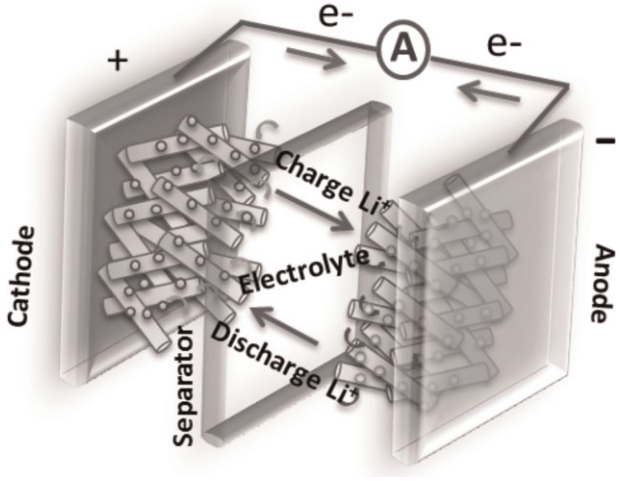

Figure 10. Application of nanofibers as cathode and anode materials in Li ion batteries.

High-performance nanofibrous mats employed as anodes, cathodes, and separators has promising potential for replacing commercially used nanoparticle based systems for lithium-ion batteries. Though these nanofibers exhibit material homogeneity and porosity suitable for energy storage applications, low-production rate, high cost of producing ternary metal oxide composites and nanostructure/performance relationship entities of these novel nanofibers are not well understood. Development of multistacked morphology from nanofibrous mats with high-surface area, porosity, and good surface activity is needed without leveraging the production rate and homogeneity. Furthermore recent advances in electrospinning for producing aligned and bridged nanofibers could also provide simple solution for maintaining fiber integrity and composition of ceramic nanofiber networks.

6. Conclusion

With advances in the fabrication techniques, many types of nanofibers with different morphologies and functional properties can be fabricated to satisfy various requirements in specific applications. During the past two decades, studies on nanofibers have shown their significant advantages in the treatment of tissue/organ failures as well as chemical and electrical processes. In medicine, the regeneration of bone, cartilage, skin, heart, and blood vessels, etc. has been facilitated when they have been treated with nanofiber-based scaffolds as shown by successes in small-to-large animal studies and clinical trials. Besides, nanofibers have provided greater efficiency in catalytic reactions; higher efficiency and flux in filtration and separation processes; as well as fast response and higher sensitivity in chemical sensors compared to other micro- to macro-size materials. Similarly, higher sensitivity, improved efficiency and high-rate capability have been achieved in the applications of nanofibers in sensors, solar cells, and lithium ion batteries, respectively. However, further efforts in the modification of nanofibrous structures and functions should be done to bring them into the marketplace.

Amongst the fabrication methods, electrospinning is the solely method which can fabricate various nanofibers for all of the three applications, medicine, chemistry, and electronics. In medicine, electrospinning has been shown to be the most successfully used method compared to self-assembly and phase separation in in vivo studies. Chemical applications also achieved significant outcomes by using nanofibers from electrospinning. In electronics, electrospinning is a very convenient way to precisely control the hydrolysis rate of ceramic materials, which is crucial for preparing well-defined ceramic nanostructures. This technology is to generate new nanostructures by digesting the as-spun inorganic/polymer nanofibers, followed by a hydrothermal reaction. This is a novel aspect of electrospun ceramic nanofibers. And researchers might hopefully acquire other ceramic nanocrystals with exciting and well-defined shapes in this way, and bring to this method some more powerful features. There is no doubt that electrospinning has become one of the most favored techniques for fabricating 1D ceramic nanofibers in a cost-effective and controllable fashion.

7. Future Perspectives

Science and engineering of nano-dimensional structures are expected to make a significant contribution in the field of health and biomedical sciences. Further modifications of nanofibers should be done to closely mimic the 3D hierarchical structure and mechanical properties of native ECM of targeted tissues/organs. This is expected to significantly facilitate the regeneration of damaged tissues/organs. Besides, detail biological mechanisms on the interactions between cells and nanofibrous matrix should be addressed to clearly understand the influence of nano-dimensional fibers at cellular level, especially their role in directing the differentiation of stem cells. Novel engineering of ''smart and designer'' scaffolds that offer release of biomolecules for effective differentiation of stem cells could be aimed at therapeutic level favoring patient care. Another prolific direction would be to study on the fundamental design of nanofibers that might systematically delivery multiple bioactives and target the specific compartments of the body, promote tissue regeneration including blood-brain barrier crossing. Collective efforts of biologists, engineers, and clinicians to improve the life quality of patients using stem cell/biomaterial approach requires thorough investigation and understanding on the mechanism of stem cell differentiation on nanofibrous topographies. Moreover, in vivo assessment of stem cell/biomaterials and their therapeutic potential need to be more thoroughly investigated on a long-term basis. This would lay a solid foundation to design excellent scaffolds for medical treatments. Moreover, further large animal studies and clinical trials of nanofiber-based scaffolds would be performed to bring these scaffolds into real clinical treatments of diverse targeted tissues/organs. The efficacies obtained from these preliminary evaluated nanofibers together with the development of advanced technologies will further lead to new therapeutic methods in the near future. However, the future of nanotechnology at large depends on the material design and tools following the detailed evaluation and understanding of the biological processes rather than applying various materials in vogue.

In chemical processes, current research on the use of nanofibers has focused largely on developing nanofibers with single new functionalities. Looking forward, multi-functional nanofiber membranes/films may be preferred for practical applications due to the unpredictable and complex nature of their chemical processes. For instance, multi-functionality is highly desired in protection and decontamination since it is not possible to predict for certain which or how many agent users would need protection against. Multi-functionality could be achieved by integrating multiple/multi-functional compounds or functional groups into nanofibers during synthesis. Amitai et al.[332] reported on the fabrication of multi/functional composite polymer nanofibers that were able to detoxify 85% of DFP in 30 min with anti-bacteria activity against *Escherichia. coli* and *Staphylococcus aureus*. Multi-functional membranes that could remove various types of pollutants from wastewater had also been synthesized.[312,314]

In electronics, taking a future perspective, it can be considered that the advances in the capability to control the structural/compositional complexity of nanofibers leads to the development of unique nanosystems including electronic, optoelectronic circuits, systems for harnessing, and storage of energy. The key factor will be in the exploitation of the science behind the controlling factors of producing the nanofibers which determines the functionality of the device. Appropriate selection of materials combined with the right nanostructure with precise organization to form a complete device could result in novel outcomes capable of changing the technologies of the coming years. For instance, technology which could produce hydrogen directly from sunlight can be rendered possible by meticulous engineering of these nanofibers from both materials as well as from nano-dimensional point of view.

Received: April 22, 2012; Revised: June 26, 2012; Published online:
DOI: 10.1002/mame.201200143

Keywords: applications; chemistry; electronics; fabrication; medicine; nanofibers

[1] F. Klaessig, M. Marrapese, S. Abe, "Current Perspectives in Nanotechnology Terminology and Nomenclature," in *Nanotechnology Standards*, (Eds., V. Murashov, J. Howard), Springer Verlag, New York **2011**, p. 260.
[2] M. Endo, H. W. Kroto, *J. Phys. Chem.* **1992**, *96*, 6941.
[3] W. E. Teo, S. Ramakrishna, *Nanotechnology* **2006**, *17*, R89.
[4] W. E. Teo, R. Inai, S. Ramakrishna, *Sci. Tech. Adv. Mater.* **2011**, *12*, 013002.
[5] J. D. Hartgerink, E. Beniash, S. I. Stupp, *Proc. Natl. Acad. Sci. USA* **2002**, *99*, 5133.
[6] P. Berndt, G. Fields, M. Tirrell, *J. Am. Chem. Soc.* **1995**, *117*, 9515.
[7] P. X. Ma, R. Zhang, *J. Biomed. Mater. Res.* **1999**, *46*, 60.
[8] P. Ma, J. Choi, *Tissue Eng.* **2001**, *7*, 23.
[9] J. Huang, S. Virji, B. H. Weiller, R. B. Kaner, *J. Am. Chem. Soc.* **2003**, *125*, 314.
[10] J. Huang, R. B. Kaner, *J. Am. Chem. Soc.* **2004**, *126*, 851.
[11] J. Huang, R. B. Kaner, *Angew. Chem. Int. Ed.* **2004**, *43*, 5817.
[12] D. Li, J. Huang, R. B. Kaner, *Acc. Chem. Res.* **2009**, *42*, 135.
[13] T. S. Mintz, Y. V. Bhargava, S. A. Thorne, R. Chopdekar, V. Radmilovic, Y. Suzuki, T. M. Devine, *Electrochem. Solid-State Lett.* **2005**, *8*, D26.
[14] X. Liu, Y. Zhou, *Appl. Phys. A: Mater. Sci. Process.* **2005**, *81*, 685.
[15] N. Wang, Y. Cai, R. Zhang, *Mater. Sci. Eng. R* **2008**, *60*, 1.
[16] A. Vomiero, M. Ferroni, E. Comini, G. Faglia, G. Sberveglieri, *Cryst. Growth Des.* **2010**, *10*, 140.
[17] D. Zheng, S. Sun, W. Fan, H. Yu, C. Fan, G. Cao, Z. Yin, X. Song, *J. Phys. Chem. B* **2005**, *109*, 16439.
[18] J. Zhang, Z. Liu, C. Lin, J. Lin, *J. Cryst. Growth* **2005**, *280*, 99.
[19] D. Li, Y. Xia, *Nano Lett.* **2004**, *4*, 933.
[20] X. Liu, X. Jin, P. X. Ma, *Nat. Mater.* **2011**, *10*, 398.
[21] G. Wei, Q. Jin, W. V. Giannobile, P. X. Ma, *Biomaterials* **2007**, *28*, 2087.
[22] S. Virji, R. Kojima, J. D. Fowler, J. G. Villanueva, R. B. Kaner, B. H. Weiller, *Nano Res.* **2009**, *2*, 135.
[23] S. Xu, Y. Wei, M. Kirkham, J. Liu, W. Mai, D. Davidovic, R. L. Snyder, Z. L. Wang, *J. Am. Chem. Soc.* **2008**, *130*, 14958.
[24] P. Yang, H. Yan, S. Mao, R. Russo, J. Johnson, R. Saykally, N. Morris, J. Pham, R. He, H. J. Choi, *Adv. Funct. Mater.* **2002**, *12*, 323.
[25] B. Liu, E. S. Aydil, *J. Am. Chem. Soc.* **2009**, *131*, 3985.
[26] A. Frenot, I. Chronakis, *Curr. Opin. Colloid Interface Sci.* **2003**, *8*, 64.
[27] M. Demira, I. Yilgorb, E. Yilgorb, B. Ermana, *Polymer* **2002**, *43*, 3303.
[28] R. Nirmalaa, K. T. Namb, S. J. Parkb, Y. S. Shinc, R. Navamathavand, H. Y. Kimb, *Appl. Surf. Sci.* **2010**, *256*, 6318.
[29] P. Gupta, G. L. Wilkes, *Polymer* **2003**, *44*, 6353.
[30] H. Zhouab, T. B. Greenc, Y. L. Jooa, *Polymer* **2006**, *47*, 7497.
[31] J. J. Stankus, L. Soletti, K. Fujimoto, Y. Hong, D. A. Vorp, W. R. Wagner, *Biomaterials* **2007**, *28*, 2738.
[32] S. Zhang, T. C. Holmes, C. M. DiPersio, R. O. Hynes, X. Su, A. Rich, *Biomaterials* **1995**, *16*, 1385.
[33] N. B. Malkar, J. L. Lauer-Fields, D. Juska, G. B. Fields, *Biomacromolecules* **2003**, *4*, 518.
[34] J. D. Hartgerink, E. Beniash, S. I. Stupp, *Science* **2001**, *294*, 1684.
[35] H. Hosseinkhani, M. Hosseinkhani, F. Tian, H. Kobayashi, Y. Tabata, *Biomaterials* **2006**, *27*, 4079.
[36] M. Shin, H. Abukawa, M. J. Troulis, J. P. Vacanti, *J. Biomed. Mater. Res. A* **2008**, *84*, 702.
[37] A. Kolmakov, *Int. J. Nanotechnol.* **2008**, *5*, 450.
[38] M. Zheng, L. Zhang, G. Li, W. Shen, *Chem. Phys. Lett.* **2002**, *363*, 123.
[39] C. T. Kresge, *Nature* **1992**, *359*, 710.
[40] A. Corma, *Chem. Rev.* **1997**, *97*, 2373.
[41] R. Wagner, W. Ellis, *Appl. Phys. Lett.* **1964**, *4*, 89.
[42] V. Kuznetsov, I. Kuzmina, I. Sylvestrova, *Bull. Mater. Sci.* **1984**, *6*, 177.
[43] M. Vergés, A. Mifsud, C. Serna, *J. Chem. Soc., Faraday Trans.* **1990**, *86*, 959.
[44] L. Dai, X. Chen, J. Jian, M. He, T. Zhou, B. Hu, *Appl. Phys. A: Mater. Sci. Process.* **2002**, *75*, 687.
[45] P. Mendes, M. Moreira, S. Tebcherani, M. Orlandi, J. Andrés, M. Li, N. Diaz-Mora, J. Varela, E. Longo, *J. Nanopart. Res.* **2012**, *14*, 750.
[46] P. D. A. Rabenau, *Angew. Chem. Int. Ed. Engl.* **1985**, *24*, 1026.
[47] A. Persidis, *Nat. Biotechnol.* **1999**, *17*, 508.
[48] R. Langer, J. P. Vacanti, *Science* **1993**, *260*, 920.
[49] Y. Ikada, *J. R. Soc. Interface* **2006**, *3*, 589.
[50] Life Science Intelligence, "*Worldwide Markets and Emerging Technologies for Tissue Engineering and Regenerative Medicine*," Medical Device Market Research, Huntington Beach, CA.
[51] L. G. Griffith, *Science* **2002**, *295*, 1009.
[52] Frost & Sullivan, "Advances in Replacement Organs and Tissue Engineering (Technical Insights) (D12E-01-00-00-00)." San Antonio, TX, 2008, p. 99.
[53] A. Atala, R. Lanza, J. A. Thomson, "*Principles of Regenerative Medicine*," 2nd edition, Academic Press, New York **2010**, p. 1182.
[54] Y. Naito, T. Shinoka, D. Duncan, N. Hibino, D. Solomon, M. Cleary, A. Rathore, C. Fein, S. Church, C. Breuer, *Adv. Drug Deliv. Rev.* **2011**, *63*, 312.
[55] C. Y. Xu, R. Inai, M. Kotaki, S. Ramakrishna, *Biomaterials* **2004**, *25*, 877.
[56] R. A. Neal, S. G. McClugage, M. C. Link, L. S. Sefcik, R. C. Ogle, E. A. Botchwey, *Tissue Eng. Part C, Methods* **2009**, *15*, 11.
[57] J. Meng, H. Kong, Z. Han, C. Wang, G. Zhu, S. Xie, H. Xu, *J. Biomed. Mater. Res. A* **2009**, *88*, 105.
[58] C. P. Barnes, S. A. Sell, E. D. Boland, D. G. Simpson, G. L. Bowlin, *Adv. Drug. Deliv. Rev.* **2007**, *59*, 1413.
[59] P. Malafaya, G. Silva, E. Baran, R. Reis, *Curr. Opin. Solid State Mater. Sci.* **2002**, *6*, 283.
[60] P. B. Malafaya, G. A. Silva, R. L. Reis, *Adv. Drug Deliv. Rev.* **2007**, *59*, 207.
[61] W. Li, Y. Jiang, R. Tuan, *Tissue Eng.* **2006**, *12*, 1775.
[62] M. M. Stevens, J. H. George, *Science* **2005**, *310*, 1135.
[63] D. D. Schlaepfer, C. R. Hauck, D. J. Sieg, *Prog. Biophys. Mol. Biol.* **1999**, *71*, 435.
[64] K. A. DeMali, K. Wennerberg, K. Burridge, *Curr. Opin. Cell. Biol.* **2003**, *15*, 572.
[65] S. Y. Chew, R. Mi, A. Hoke, K. W. Leong, *Biomaterials* **2008**, *29*, 653.
[66] B. Geiger, J. P. Spatz, A. D. Bershadsky, *Nat. Rev. Mol. Cell. Biol.* **2009**, *10*, 21.
[67] L. T. Nguyen, S. Liao, S. Ramakrishna, C. K. Chan, *Nanomedicine* **2011**, *6*, 961.
[68] R. M. Salasznyk, R. F. Klees, W. A. Williams, A. Boskey, G. E. Plopper, *Exp. Cell Res.* **2007**, *313*, 22.

[69] M. J. Dalby, M. O. Riehle, H. Johnstone, S. Affrossman, A. S. G. Curtis, *Cell Biol. Int.* **2004**, *28*, 229.
[70] M. J. Dalby, N. Gadegaard, P. Herzyk, D. Sutherland, H. Agheli, C. D. W. Wilkinson, A. S. G. Curtis, *J. Cell Biochem.* **2007**, *102*, 1234.
[71] K. M. Woo, V. J. Chen, P. X. Ma, *J. Biomed. Mater. Res. A* **2003**, *67*, 531.
[72] E. K. F. Yim, K. W. Leong, *Nanomedicine* **2005**, *1*, 10.
[73] N. S. Binulal, M. Deepthy, N. Selvamurugan, K. T. Shalumon, S. Suja, U. Mony, R. Jayakumar, S. V. Nair, *Tissue Eng. Part A* **2010**, *16*, 393.
[74] T. Kaully, K. Kaufman-Francis, A. Lesman, S. Levenberg, *Tissue Eng. Part B: Rev.* **2009**, *15*, 159.
[75] S. Ghanaati, M. J. Webber, R. E. Unger, C. Orth, J. F. Hulvat, S. E. Kiehna, M. Barbeck, A. Rasic, S. I. Stupp, C. J. Kirkpatrick, *Biomaterials* **2009**, *30*, 6202.
[76] H. Cao, K. Mchugh, S. Y. Chew, J. M. Anderson, *J. Biomed. Mater. Res. Part A* **2010**, *93*, 1151.
[77] E. D. Boland, T. A. Telemeco, D. G. Simpson, G. E. Wnek, G. L. Bowlin, *J. Biomed. Mater. Res.* **2004**, *71B*, 144.
[78] T. H. Ying, D. Ishii, A. Mahara, S. Murakami, T. Yamaoka, K. Sudesh, R. Samian, M. Fujita, M. Maeda, T. Iwata, *Biomaterials* **2008**, *29*, 1307.
[79] S. Wang, Y. Zhang, H. Wang, Z. Dong, *Int. J. Biol. Macromol.* **2011**, *48*, 345.
[80] Y. Gui-Bo, Z. You-Zhu, W. Shu-Dong, S. De-Bing, D. Zhi-Hui, F. Wei-Guo, *J. Biomed. Mater. Res. Part A* **2010**, *93*, 158.
[81] S. Srouji, T. Kizhner, E. Suss-Tobi, E. Livne, E. Zussman, *J. Mater. Sci. Mater. Med.* **2008**, *19*, 1249.
[82] M. Casper, J. Fitzsimmons, J. Stone, A. Meza, Y. Huang, T. Ruesink, S. W. O'Driscoll, G. G. Reinholz, *Osteoarthritis Cartilage* **2010**, *18*, 981.
[83] J. Stankus, D. Freytes, S. Badylak, W. Wagner, *J. Biomater. Sci. Polym. Ed.* **2008**, *19*, 635.
[84] K. A. Blackwood, R. McKean, I. Canton, C. O. Freeman, K. L. Franklin, D. Cole, I. Brook, P. Farthing, S. Rimmer, J. W. Haycock, A. J. Ryan, S. MacNeil, *Biomaterials* **2008**, *29*, 3091.
[85] T. Telemeco, C. Ayres, G. Bowlin, G. Wnek, E. Boland, N. Cohen, C. M. Baumgarten, J. Mathews, D. G. Simpson, *Acta Biomater.* **2005**, *1*, 377.
[86] K. T. Kurpinski, J. T. Stephenson, R. R. R. Janairo, H. Lee, S. Li, *Biomaterials* **2010**, *31*, 3536.
[87] J. L. Ifkovits, K. Wu, R. L. Mauck, J. A. Burdick, C. Egles, *PLOS one* **2010**, *5*, e15717.
[88] J. Henry, K. Burugapalli, P. Neuenschwander, A. Pandit, *Acta Biomater.* **2009**, *5*, 29.
[89] H. G. Sundararaghavan, R. B. Metter, J. A. Burdick, *Macromol. Biosci.* **2010**, *10*, 265.
[90] M. F. Leong, M. Z. Rasheed, T. C. Lim, K. S. Chian, *J. Biomed. Mater. Res. A* **2009**, *91*, 231.
[91] Q. P. Pham, U. Sharma, A. G. Mikos, *Biomacromolecules* **2006**, *7*, 2796.
[92] J. Nam, Y. Huang, S. Agarwal, J. Lannutti, *Tissue Eng.* **2007**, *13*, 2249.
[93] Y. Zhang, H. Ouyang, T. Chwee, S. Ramakrishna, Z. M. Huang, *J. Biomed. Mater. Res. Part B Appl. Biomater.* **2005**, *72*, 156.
[94] Y. Song, Y. Li, Q. Zheng, *J. Wuhan Univ. Technol. Mater. Sci. Ed.* **2010**, *25*, 803.
[95] Q. Jin, G. Wei, Z. Lin, J. V. Sugai, S. E. Lynch, P. X. Ma, W. V. Giannobile, M. Isalan, *PloS one* **2008**, *3*, e1729.
[96] H. Hosseinkhani, M. Hosseinkhani, A. Khademhosseini, *Yakhteh Med. J.* **2006**, *8*, 204.
[97] E. A. Phelps, A. J. García, *Curr. Opin. Biotechnol.* **2010**, *21*, 704.
[98] H. Sun, K. Feng, J. Hu, S. Soker, A. Atala, P. X. Ma, *Biomaterials* **2010**, *31*, 1133.
[99] E. Seyedjafari, M. Soleimani, N. Ghaemi, I. Shabani, *Biomacromolecules* **2010**, *11*, 3118.
[100] A. Nandakumar, L. Yang, P. Habibovic, C. van Blitterswijk, *Langmuir* **2010**, *26*, 7380.
[101] X. Yang, F. Yang, X. F. Walboomers, Z. Bian, M. Fan, J. A. Jansen, *J. Biomed. Mater. Res. A* **2010**, *93*, 247.
[102] B. Chan, R. Wong, B. Rabie, *Int. J. Oral. Maxillofac. Surg.* **2011**, *40*, 612.
[103] X. B. Yang, R. S. Bhatnagar, S. Li, R. O. C. Oreffo, *Tissue Eng.* **2004**, *10*, 1148.
[104] Y. C. Fu, H. Nie, M. L. Ho, C. K. Wang, C. H. Wang, *Biotechnol. Bioeng.* **2008**, *99*, 996.
[105] H. Nie, M. L. Ho, C. K. Wang, C. H. Wang, Y. C. Fu, *Biomaterials* **2009**, *30*, 892.
[106] T. Osathanon, M. L. Linnes, R. M. Rajachar, B. D. Ratner, M. J. Somerman, C. M. Giachelli, *Biomaterials* **2008**, *29*, 4091.
[107] T. Osathanon, C. M. Giachelli, M. J. Somerman, *Biomaterials* **2009**, *30*, 4513.
[108] E. Luong-Van, L. Grøndahl, S. Song, V. Nurcombe, S. Cool, *J. Mol. Histol.* **2007**, *38*, 459.
[109] H. Hosseinkhani, M. Hosseinkhani, F. Tian, H. Kobayashi, Y. Tabata, *Tissue Eng.* **2007**, *13*, 11.
[110] M. Shin, H. Yoshimoto, J. Vacanti, *Tissue Eng.* **2004**, *10*, 33.
[111] A. Mata, Y. Geng, K. J. Henrikson, C. Aparicio, S. R. Stock, R. L. Satcher, S. I. Stupp, *Biomaterials* **2010**, *31*, 6004.
[112] T. D. Sargeant, M. O. Guler, S. M. Oppenheimer, A. Mata, R. L. Satcher, D. C. Dunand, S. I. Stupp, *Biomaterials* **2008**, *29*, 161.
[113] Y. M. Kolambkar, K. M. Dupont, J. D. Boerckel, N. Huebsch, D. J. Mooney, D. W. Hutmacher, R. E. Guldberg, *Biomaterials* **2011**, *32*, 65.
[114] J. D. Boerckel, Y. M. Kolambkar, K. M. Dupont, B. A. Uhrig, E. A. Phelps, H. Y. Stevens, A. J. García, R. E. Guldberg, *Biomaterials* **2011**, *32*, 5241.
[115] K. Woo, V. Chen, H. Jung, T. Kim, H. Shin, J. Baek, H. M. Ryoo, P. X. Ma, *Tissue Eng. Part A* **2009**, *15*, 2155.
[116] W. J. Cho, J. H. Kim, S. H. Oh, H. H. Nam, J. M. Kim, J. H. Lee, *J. Biomed. Mater. Res. A* **2009**, *91*, 400.
[117] E. K. Ko, S. I. Jeong, N. G. Rim, Y. M. Lee, H. Shin, B. K. Lee, *Tissue Eng. Part A* **2008**, *14*, 2105.
[118] J. H. Jo, E. J. Lee, D. S. Shin, H. E. Kim, H. W. Kim, Y. H. Koh, J. H. Jang, *J. Biomed. Mater. Res. B Appl. Biomater.* **2009**, *91*, 213.
[119] E. Pişkin, I. A. Işog˘lu, N. Bölgen, I. Vargel, S. Griffiths, T. Cavuşog˘lu, P. Korkusuz, E. Güzel, S. Cartmell, *J. Biomed. Mater. Res. A* **2009**, *90*, 1137.
[120] K. S. Hong, E. C. Kim, S. H. Bang, C. H. Chung, Y. I. Lee, J. K. Hyun, H. H. Lee, J. H. Jang, T. I. Kim, H. W. Kim, *J. Biomed. Mater. Res. A* **2010**, *94*, 1187.
[121] Y. Z. Cai, L. L. Wang, H. X. Cai, Y. Y. Qi, X. H. Zou, H. W. Ouyang, *J. Biomed. Mater. Res. A* **2010**, *95*, 49.
[122] S. Shin, H. Park, K. Kim, M. Lee, Y. Choi, Y. Park, Y. M. Lee, Y. Ku, I. C. Rhyu, S. B. Han, *J. Periodontol.* **2005**, *76*, 1778.
[123] K. H. Kim, L. Jeong, H. N. Park, S. Y. Shin, W. H. Park, S. C. Lee, T. I. Kim, Y. J. Park, Y. J. Seol, Y. M. Lee, Y. Ku, I. C. Rhyu, S. B. Han, C. P. Chung, *J. Biotechnol.* **2005**, *120*, 327.
[124] Y. Kang, K. Kim, Y. Seol, S. Rhee, *Acta Biomater.* **2009**, *5*, 462.
[125] Y. J. Seol, K. H. Kim, Y. M. Kang, I. A. Kim, S. H. Rhee, *J. Biomed. Mater. Res. B Appl. Biomater.* **2009**, *90B*, 679.
[126] O. D. Schneider, F. Weber, T. J. Brunner, S. Loher, M. Ehrbar, P. R. Schmidlin, W. J. Stark, *Acta Biomater.* **2009**, *5*, 1775.
[127] S. A. Steigman, A. Ahmed, R. M. Shanti, R. S. Tuan, C. Valim, D. O. Fauza, *J. Pediatr. Surg.* **2009**, *44*, 1120.

[128] J. D. Klein, C. G. Turner, A. Ahmed, S. A. Steigman, D. Zurakowski, D. O. Fauza, *J. Pediatr. Surg.* **2010**, *45*, 1354.
[129] J. S. Park, D. G. Woo, H. N. Yang, H. J. Lim, K. M. Park, K. Na, K. H. Park, *J. Biomed. Mater. Res. A* **2010**, *92*, 988.
[130] X. F. Zheng, S. B. Lu, W. G. Zhang, S. Y. Liu, J. X. Huang, Q. Y. Guo, *Biotechnol. Bioprocess. Eng.* **2011**, *16*, 593.
[131] J. P. Chen, C. H. Su, *Acta Biomater.* **2011**, *7*, 234.
[132] W. J. Li, H. Chiang, T. F. Kuo, H. S. Lee, C. C. Jiang, R. S. Tuan, *J. Tissue Eng. Regen. Med.* **2009**, *3*, 1.
[133] S. Ho, D. Hutmacher, A. Ekaputra, D. Hitendra, J. Hui, *Tissue Eng. Part A* **2009**, *16*, 1123.
[134] Z. Yin, X. Chen, J. L. Chen, W. L. Shen, T. M. Hieu Nguyen, L. Gao, H. W. Ouyang, *Biomaterials* **2010**, *31*, 2163.
[135] Y. O. Kang, I. S. Yoon, S. Y. Lee, D. D. Kim, S. J. Lee, W. H. Park, S. M. Hudson, *J. Biomed. Mater. Res. B Appl. Biomater.* **2010**, *92*, 568.
[136] I. Han, K. J. Shim, J. Y. Kim, S. U. Im, Y. K. Sung, M. Kim, I. K. Kang, J. C. Kim, *Artif. Organs* **2007**, *31*, 801.
[137] S. S. Scherer, G. Pietramaggiori, J. Matthews, S. Perry, A. Assmann, A. Carothers, M. Demcheva, R. C. Muise-Helmericks, A. Seth, J. N. Vournakis, R. C. Valeri, T. H. Fischer, H. B. Hechtman, D. P. Orgill, *Ann. Surg.* **2009**, *250*, 322.
[138] J. G. Merrell, S. W. McLaughlin, L. Tie, C. T. Laurencin, A. F. Chen, L. S. Nair, *Clin. Exp. Pharmacol. Physiol.* **2009**, *36*, 1149.
[139] H. S. Kim, H. S. Yoo, *J. Controlled Release* **2010**, *145*, 264.
[140] J. S. Choi, K. W. Leong, H. S. Yoo, *Biomaterials* **2008**, *29*, 587.
[141] J. S. Choi, S. H. Choi, H. S. Yoo, *J. Mater. Chem.* **2011**, *21*, 5258.
[142] K. S. Rho, L. Jeong, G. Lee, B. M. Seo, Y. J. Park, S. D. Hong, S. Roh, J. J. Cho, W. H. Park, B. M. Min, *Biomaterials* **2006**, *27*, 1452.
[143] J. Chen, G. Chang, *Colloid Surf. A* **2008**, *313-314*, 183.
[144] S. J. Liu, Y. C. Kau, C. Y. Chou, J. K. Chen, R. C. Wu, W. L. Yeh, *J. Membr. Sci.* **2010**, *355*, 53.
[145] X. Liu, T. Lin, J. Fang, G. Yao, H. Zhao, M. Dodson, X. Wang, *J. Biomed. Mater. Res. A* **2010**, *94*, 499.
[146] K. Zhang, Y. Qian, H. Wang, L. Fan, C. Huang, A. Yin, X. Mo, *J. Biomed. Mater. Res. A* **2010**, *95*, 870.
[147] H. Meng, L. Chen, Z. Ye, S. Wang, X. Zhao, *J. Biomed. Mater. Res. B Appl. Biomater.* **2009**, *89B*, 379.
[148] K. Ma, S. Liao, L. He, J. Lu, S. Ramakrishna, C. K. Chan, *Tissue Eng. Part A* **2011**, *17*, 1413.
[149] P. Lochman, J. Páral, J. Kočí, *J. Appl. Biomed.* **2011**, *9*, 143.
[150] P. Lochman, M. Plodr, J. Páral, K. Smejkal, *Surg. Infect. (Larchmt)* **2010**, *11*, 29.
[151] R. Uppal, G. N. Ramaswamy, C. Arnold, R. Goodband, Y. Wang, *J. Biomed. Mater. Res. B Appl. Biomater.* **2011**, *97*, 20.
[152] W. Wang, S. Itoh, A. Matsuda, S. Ichinose, K. Shinomiya, Y. Hata, J. Tanaka, *J. Biomed. Mater. Res. A* **2008**, *84*, 557.
[153] W. Wang, S. Itoh, K. Konno, T. Kikkawa, S. Ichinose, K. Sakai, T. Ohkuma, K. Watabe, *J. Biomed. Mater. Res. A* **2009**, *91A*, 994.
[154] T. B. Bini, S. Gao, T. C. Tan, S. Wang, A. Lim, L. B. Hai, S. Ramakrishna, *Nanotechnology* **2004**, *15*, 1459.
[155] S. Panseri, C. Cunha, J. Lowery, U. Del Carro, F. Taraballi, S. Amadio, A. Vescovi, F. Gelain, *BMC Biotechnol.* **2008**, *8*, 39.
[156] I. P. Clements, Y. T. Kim, A. W. English, X. Lu, A. Chung, R. V. Bellamkonda, *Biomaterials* **2009**, *30*, 3834.
[157] Y. Zhu, A. Wang, S. Patel, K. Kurpinski, E. Diao, X. Bao, G. Kwong, W. L. Young, S. Li, *Tissue Eng. Part C: Methods* **2011**, *17*, 705.
[158] W. Wang, S. Itoh, A. Matsuda, T. Aizawa, M. Demura, S. Ichinose, K. Shinomiya, J. Tanaka, *J. Biomed. Mater. Res. A* **2008**, *85*, 919.
[159] S. Y. Chew, R. Mi, A. Hoke, K. W. Leong, *Adv. Funct. Mater.* **2007**, *17*, 1288.
[160] H. S. Koh, T. Yong, W. E. Teo, C. K. Chan, M. E. Puhaindran, T. C. Tan, A. Lim, B. H. Lim, S. Ramakrishna, *J. Neural Eng.* **2010**, *7*, 046003.
[161] A. M. McGrath, L. N. Novikova, L. N. Novikov, M. Wiberg, *Brain Res. Bull.* **2010**, *83*, 207.
[162] A. Wang, Z. Tang, I. H. Park, Y. Zhu, S. Patel, G. Q. Daley, S. Li, *Biomaterials* **2011**, *32*, 5023.
[163] S. Meiners, I. Ahmed, A. S. Ponery, N. Amor, S. L. Harris, V. Ayres, Y. Fan, Q. Chen, R. Delgado-Rivera, A. N. Babu, *Polym. Int.* **2007**, *56*, 1340.
[164] D. Cigognini, A. Satta, B. Colleoni, D. Silva, M. Donegà, S. Antonini, F. Gelain, S. Zhang, *PloS One* **2011**, *6*, e19782.
[165] J. Guo, H. Su, Y. Zeng, Y. X. Liang, W. M. Wong, R. G. Ellis-Behnke, K. F. So, W. Wu, *Nanomedicine* **2007**, *3*, 311.
[166] F. Gelain, S. Panseri, S. Antonini, C. Cunha, M. Donega, J. Lowery, F. Taraballi, G. Cerri, M. Montagna, F. Baldissera, A. Vescovi, *ACS nano* **2011**, *5*, 227.
[167] Y. X. Liang, S. W. H. Cheung, K. C. W. Chan, E. X. Wu, D. K. C. Tay, R. G. Ellis-Behnke, *Nanomedicine* **2011**, *7*, 351.
[168] M. J. Webber, X. Han, S. N. Prasanna Murthy, K. Rajangam, S. I. Stupp, J. W. Lomasney, *J. Tissue Eng. Regen. Med.* **2010**, *4*, 600.
[169] V. F. Segers, T. Tokunou, L. J. Higgins, C. MacGillivray, J. Gannon, R. T. Lee, *Circulation* **2007**, *116*, 1683.
[170] J. M. Singelyn, J. A. DeQuach, S. B. Seif-Naraghi, R. B. Littlefield, P. J. Schup-Magoffin, K. L. Christman, *Biomaterials* **2009**, *30*, 5409.
[171] X. Cui, H. Xie, H. Wang, H. Guo, J. Zhang, C. Wang, Y. Z. Tan, *Tohoku J. Exp. Med.* **2010**, *222*, 281.
[172] H. D. Guo, G. H. Cui, H. J. Wang, Y. Z. Tan, *Biochem. Biophys. Res. Commun.* **2010**, *399*, 42.
[173] Y. D. Lin, M. L. Yeh, Y. J. Yang, D. C. Tsai, T. Y. Chu, Y. Y. Shih, M. Y. Chang, Y. W. Liu, A. C. L. Tang, T. Y. Chen, C. Y. Luo, K. C. Chang, J. H. Chen, H. L. Wu, T. K. Hung, P. C. H. Hsieh, *Circulation* **2010**, *122*, S132.
[174] J. Hu, X. Sun, H. Ma, C. Xie, Y. E. Chen, P. X. Ma, *Biomaterials* **2010**, *31*, 7971.
[175] M. J. Webber, J. Tongers, M. A. Renault, J. G. Roncalli, D. W. Losordo, S. I. Stupp, *Acta Biomater.* **2010**, *6*, 3.
[176] S. Lepidi, G. Abatangelo, V. Vindigni, G. Deriu, B. Zavan, C. Tonello, R. Cortivo, *FASEB J.* **2006**, *20*, 103.
[177] F. Innocente, D. Mandracchia, E. Pektok, B. Nottelet, J. C. Tille, S. de Valence, G. Faggian, A. Mazzucco, A. Kalangos, R. Gurny, M. Moeller, B. H. Walpoth, *Circulation* **2009**, *120*, S37.
[178] Y. Hong, S. H. Ye, A. Nieponice, L. Soletti, D. A. Vorp, W. R. Wagner, *Biomaterials* **2009**, *30*, 2457.
[179] M. Mutsuga, Y. Narita, A. Yamawaki, M. Satake, H. Kaneko, Y. Suematsu, A. Usui, Y. Ueda, *J. Thorac. Cardiovasc. Surg.* **2009**, *137*, 703.
[180] M. Kapadia, L. Chow, N. Tsihlis, S. Ahanchi, J. Eng, J. Murar, J. Martinez, D. Popowich, Q. Jiang, J. Hrabie, *J. Vasc. Surg.* **2008**, *47*, 173.
[181] C. K. Hashi, Y. Zhu, G. Y. Yang, W. L. Young, B. S. Hsiao, K. Wang, B. Chu, S. Li, *Proc. Natl. Acad. Sci. USA* **2007**, *104*, 11915.
[182] W. He, Z. Ma, W. E. Teo, Y. X. Dong, P. A. Robless, T. C. Lim, S. Ramakrishna, *J. Biomed. Mater. Res. A* **2009**, *90*, 205.
[183] B. W. Tillman, S. K. Yazdani, S. J. Lee, R. L. Geary, A. Atala, J. J. Yoo, *Biomaterials* **2009**, *30*, 583.
[184] M. Kim, J. Kim, G. Yi, S. Lim, Y. Hong, D. Chung, *Macromol. Res.* **2008**, *16*, 345.

[185] K. Kuraishi, H. Iwata, S. Nakano, S. Kubota, H. Tonami, M. Toda, N. Toma, S. Matsushima, K. Hamada, S. Ogawa, W. Taki, *J. Biomed. Mater. Res. B Appl. Biomater.* **2009**, *88*, 230.
[186] N. Navarro-Alvarez, A. Soto-Gutierrez, Y. Chen, J. Caballero-Corbalan, W. Hassan, S. Kobayashi, Y. Kondo, M. Iwamuro, K. Yamamoto, E. Kondo, *J. Hepatol.* **2010**, *52*, 211.
[187] T. Yamamoto, N. Navarro-Alvarez, A. Soto-Gutierrez, T. Yuasa, M. Iwamuro, Y. Kubota, M. Seita, H. Kawamoto, S. M. Javed, E. Kondo, H. Noguchi, S. Kobayashi, S. Nakaji, N. Kobayashi, *Cell Transplant* **2010**, *19*, 799.
[188] R. Hashizume, K. L. Fujimoto, Y. Hong, N. J. Amoroso, K. Tobita, T. Miki, B. B. Keller, M. S. Sacks, W. R. Wagner, *Biomaterials* **2010**, *31*, 3253.
[189] Y. Hong, K. Fujimoto, R. Hashizume, J. Guan, J. J. Stankus, K. Tobita, W. R. Wagner, *Biomacromolecules* **2008**, *9*, 1200.
[190] N. Bölgen, I. Vargel, P. Korkusuz, Y. Z. Mencelog˘lu, E. Pişkin, *J. Biomed. Mater. Res. B Appl. Biomater.* **2007**, *81*, 530.
[191] H. Tian, S. Bharadwaj, Y. Liu, P. Ma, A. Atala, Y. Zhang, *Tissue Eng. Part A* **2010**, *16*, 1769.
[192] A. Zajicova, K. Pokorna, A. Lencova, M. Krulova, E. Svobodova, S. Kubinova, E. Sykova, M. Pradny, J. Michalek, J. Svobodova, M. Munzarova, V. Holan, *Cell Transplant* **2010**, *19*, 1281.
[193] N. Navarro-Alvarez, J. Rivas-Carrillo, A. Soto-Gutierrez, T. Yuasa, T. Okitsu, H. Noguchi, S. Matsumoto, J. Takei, N. Tanaka, N. Kobayashi, *Cell Transplant.* **2008**, *1*, 111.
[194] Z. Luo, S. Wang, S. Zhang, *Biomaterials* **2011**, *32*, 2013.
[195] K. Mi, G. Wang, Z. Liu, Z. Feng, B. Huang, X. Zhao, *Macromol. Biosci.* **2009**, *9*, 437.
[196] S. H. Ranganath, Y. Fu, D. Y. Arifin, I. Kee, L. Zheng, H. S. Lee, P. K. H. Chow, C. H. Wang, *Biomaterials* **2010**, *31*, 5199.
[197] E. L. Bakota, Y. Wang, F. R. Danesh, J. D. Hartgerink, *Biomacromolecules* **2011**, *12*, 1651.
[198] H. Karmouty-Quintana, F. Tamimi, T. K. McGovern, L. M. Grover, J. G. Martin, J. E. Barralet, *Biomaterials* **2010**, *31*, 6050.
[199] W. Hu, Z. M. Huang, *Polym. Int.* **2010**, *59*, 92.
[200] W. Hu, Z. M. Huang, X. Y. Liu, *Nanotechnology* **2010**, *21*, 315104.
[201] K. Pawlowski, S. Rittgers, S. Schmidt, G. Bowlin, *Front Biosci.* **2004**, *9*, 1412.
[202] S. Y. Silva, L. C. Rueda, M. López, I. D. Vélez, C. F. Rueda-Clausen, D. J. Smith, G. Muñoz, H. Mosquera, F. A. Silva, A. Buitrago, H. Díaz, P. López-Jaramillo, *Trials* **2006**, *7*, 14.
[203] P. Lopez-Jaramillo, M. Y. Rincon, R. G. Garcia, S. Y. Silva, E. Smith, P. Kampeerapappun, C. Garcia, D. J. Smith, M. Lopez, I. D. Velez, *Am. J. Trop. Med. Hyg.* **2010**, *83*, 97.
[204] S. Y. Silva, L. C. Rueda, G. A. Márquez, M. López, D. J. Smith, C. A. Calderón, J. C. Castillo, J. Matute, C. F. Rueda-Clausen, A. Orduz, F. A. Silva, P. Kampeerapappun, M. Bhide, P. López-Jaramillo, *Trials* **2007**, *8*, 26.
[205] S. Jung, D. Day, *Am. Ceram. Soc. Bull.* **2011**, *90*, 25.
[206] S. Liao, C. K. Chan, S. Ramakrishna, *Front Mater. Sci. China* **2010**, *4*, 29.
[207] D. Li, Y. Xia, *Adv. Mater.* **2004**, *16*, 1151.
[208] K. De Jong, J. Geus, *Catal. Rev.* **2000**, *42*, 481.
[209] C. Kriegel, A. Arrechi, K. Kit, D. J. McClements, J. Weiss, *Crit. Rev. Food Sci. Nutr.* **2008**, *48*, 775.
[210] R. Gopal, Z. Ma, S. Kaur, S. Ramakrishna, *Top. Appl. Phys.* **2007**, *109*, 72.
[211] C. Huang, S. J. Soenen, J. Rejman, B. Lucas, K. Braeckmans, J. Demeester, S. C. de Smedt, *Chem. Soc. Rev.* **2011**, *40*, 2417.
[212] S. Agarwal, A. Greiner, J. H. Wendorff, *Adv. Funct. Mater.* **2009**, *19*, 2863.
[213] R. Ramaseshan, S. Sundarrajan, R. Jose, S. Ramakrishna, *J. Appl. Phys.* **2007**, *102*, 111101.
[214] S. Agarwal, J. H. Wendorff, A. Greiner, *Macromol. Rapid Commun.* **2010**, *31*, 1317.
[215] J. Delgado, D. Su, G. Rebmann, N. Keller, A. Gajovic, R. Schlogl, *J. Catal.* **2006**, *244*, 126.
[216] J. Delgado, R. Vieira, G. Rebmann, D. Su, N. Keller, M. Ledoux, R. Schlogl, *Carbon* **2006**, *44*, 809.
[217] J. H. Zhou, Y. Cui, J. Zhu, P. Li, T. J. Zhao, Y. C. Dai, W. K. Yuan, *Stud. Surf. Sci. Catal.* **2006**, *159*, 753.
[218] X. Fang, H. Ma, S. Xiao, M. Shen, R. Guo, X. Cao, X. Shi, *J. Mater. Chem.* **2011**, *21*, 4493.
[219] L. Chen, S. Hong, X. Zhou, Z. Zhou, H. Hou, *Catal. Commun.* **2008**, *9*, 2221.
[220] X. Ke, S. Ribbens, Y. Fan, H. Liu, P. Cool, D. Yang, H. Zhu, *J. Membr. Sci.* **2011**, *375*, 69.
[221] J. Armor, "What is catalysis or *Catalysis, so what*?". Available from http://www.nacatsoc.org/what.asp, last accessed 2012/08/20.
[222] R. Vieira, C. Pham-Huu, N. Keller, M. J. Ledoux, *Chem. Commun.* **2002**, *9*, 954.
[223] R. Vieira, D. Bastos-Netto, M. J. Ledoux, C. Pham-Huu, *Appl. Catal. A* **2005**, *279*, 35.
[224] R. Vieira, P. Bernhardt, M. J. Ledoux, C. Pham-Huu, *Catal. Lett.* **2005**, *99*, 177.
[225] M. A. Keane, P. M. Patterson, *Catal. Lett.* **2005**, *99*, 33.
[226] M. Demir, M. Gulgun, Y. Menceloglu, B. Erman, S. Abramchuk, E. Makhaeva, A. Khokhlov, V. Matveeva, M. Sulman, *Macromolecules* **2004**, *37*, 1787.
[227] M. Ruta, G. Laurenczy, P. J. Dyson, L. Kiwi-Minsker, *J. Phys. Chem. C* **2008**, *112*, 17814.
[228] W. Teunissen, A. A. Bol, J. W. Geus, *Catal. Today* **1999**, *48*, 329.
[229] M. L. Toebes, F. F. Prinsloo, J. H. Bitter, A. J. van Dillen, K. P. de Jong, *J. Catal.* **2003**, *214*, 78.
[230] J. Chen, X. Tang, J. Liu, E. Zhan, J. Li, X. Huang, W. Shen, *Chem. Mater.* **2007**, *19*, 4292.
[231] J. M. Nhut, R. Vieira, N. Keller, C. Pham-Huu, W. Boll, M. J. Ledoux, *Stud. Surf. Sci. Catal.* **2002**, *143*, 983.
[232] M. Zhiani, B. Rezaei, J. Jalili, *Int. J. Hydrogen Energy* **2010**, *35*, 9298.
[233] E. Formo, Z. Peng, E. Lee, X. Lu, H. Yang, Y. Xia, *J. Phys. Chem. C* **2008**, *112*, 9970.
[234] S. Perathoner, M. Gangeri, P. Lanzafame, G. Centi, *Kinet. Catal.* **2007**, *48*, 877.
[235] M. Li, G. Han, B. Yang, *Electrochem. Commun.* **2008**, *10*, 880.
[236] M. Khosravi, M. K. Amini, *Carbon* **2010**, *48*, 3131.
[237] B. K. Balan, S. M. Unni, S. Kurungot, *J. Phys. Chem. C* **2009**, *113*, 17572.
[238] C. L. Lee, Y. C. Ju, P. T. Chou, Y. C. Huang, L. C. Kuo, J. C. Oung, *Electrochem. Commun.* **2005**, *7*, 453.
[239] G. S. Chai, S. B. Yoon, J. S. Yu, *Carbon* **2005**, *43*, 3028.
[240] N. T. Xuyen, T. H. Kim, H. Z. Geng, I. H. Lee, K. K. Kim, Y. H. Lee, *J. Mater. Chem.* **2009**, *19*, 7822.
[241] S. H. Hong, M. S. Jun, I. Mochida, S. H. Yoon, "Selective Synthesis of Carbon Nanofibers as Better Catalyst Supports for Low-Temperature Fuel Cells," in *Catalysis for Sustainable Energy Production* (Ed.: P. Barbaro, C. Bianchini), Wiley-VCH Verlag GmbH, KGaA, Weinheim **2009**, p. 71–87.
[242] M. Tsuji, M. Kubokawa, R. Yano, N. Miyamae, T. Tsuji, M. S. Jun, S. Hong, S. Lim, S. H. Yoon, I. Mochida, *Langmuir* **2007**, *23*, 387.
[243] T. Maiyalagan, *Int. J. Hydrogen Energ.* **2009**, *34*, 2874.
[244] T. Maiyalagan, *J. Solid State Electrochem.* **2009**, *13*, 1561.

[245] H. Ogihara, M. Sadakane, Q. Wu, Y. Nodasaka, W. Ueda, *Chem. Commun.* **2007**, *39*, 4047.
[246] G. Mestl, N. I. Maksimova, N. Keller, V. V. Roddatis, R. Schlogl, *Angew. Chem. Int. Ed.* **2001**, *40*, 2066.
[247] D. S. Su, X. Chen, X. Liu, J. J. Delgado, R. Schlögl, A. Gajović, *Adv. Mater.* **2008**, *20*, 3597.
[248] A. Bauer, K. Lee, C. Song, Y. Xie, J. Zhang, R. Hui, *J. Power Sources* **2010**, *195*, 3105.
[249] S. Maldonado, K. J. Stevenson, *J. Phys. Chem. B* **2005**, *109*, 4707.
[250] S. Zhan, D. Chen, X. Jiao, C. Tao, *J. Phys. Chem. B* **2006**, *110*, 11199.
[251] S. Chuangchote, J. Jitputti, T. Sagawa, S. Yoshikawa, *ACS Appl. Mater. Interfaces* **2009**, *1*, 1140.
[252] T. Tamura, H. Kawakami, *Nano Lett.* **2010**, *10*, 1324.
[253] W. Li, M. Waje, Z. Chen, P. Larsen, Y. Yan, *Carbon* **2010**, *48*, 995.
[254] J. H. Lin, T. H. Ko, M. Y. Yen, *Energy Fuels* **2009**, *23*, 4042.
[255] E. Formo, M. S. Yavuz, E. P. Lee, L. Lane, Y. Xia, *J. Mater. Chem.* **2009**, *19*, 3878.
[256] H. Kim, Y. Choi, N. Kanuka, H. Kinoshita, T. Nishiyama, T. Usami, *Appl. Catal. A* **2009**, *352*, 265.
[257] T. Kim, T. Park, *Biotechnol. Prog.* **2006**, *22*, 1108.
[258] T. E. Herricks, S. H. Kim, J. Kim, D. Li, J. H. Kwak, J. W. Grate, S. H. Kim, Y. Xia, *J. Mater. Chem.* **2005**, *15*, 3241.
[259] J. Xie, Y. L. Hsieh, *J. Mater. Sci.* **2003**, *38*, 2125.
[260] J. P. Lindner, C. Roben, A. Studer, M. Stasiak, R. Ronge, A. Greiner, H. J. Wendorff, *Angew. Chem. Int. Ed.* **2009**, *48*, 8874.
[261] M. Stasiak, A. Studer, A. Greiner, J. H. Wendorff, *Chem. Eur. J.* **2007**, *13*, 6150.
[262] C. Röben, M. Stasiak, B. Janza, A. Greiner, J. Wendorff, A. Studer, *Synthesis* **2008**, *2008*, 2163.
[263] H. Jia, G. Zhu, B. Vugrinovich, W. Kataphinan, D. Reneker, P. Wang, *Biotechnol. Prog.* **2002**, *18*, 1027.
[264] X. J. Huang, Z. K. Xu, L. S. Wan, C. Innocent, P. Seta, *Macromol. Rapid Commun.* **2006**, *27*, 1341.
[265] Z. G. Wang, J. Q. Wang, Z. K. Xu, *J. Mol. Catal. B: Enzyme* **2006**, *42*, 45.
[266] Z. G. Wang, L. S. Wan, Z. M. Liu, X. J. Huang, Z. K. Xu, *J. Mol. Catal. B: Enzyme* **2009**, *56*, 189.
[267] S. Ramakrishna, R. Jose, P. S. Archana, A. S. Nair, R. Balamurugan, J. Venugopal, *J. Mater. Sci.* **2010**, *45*, 6283.
[268] P. Gibson, H. Schreuder-Gibson, D. Rivin, *Colloid Surf. A* **2001**, *187-188*, 469.
[269] K. M. Yun, A. B. Suryamas, F. Iskandar, L. Bao, H. Niinuma, K. Okuyama, *Sep. Purif. Technol.* **2010**, *75*, 340.
[270] R. Barhate, C. K. Loong, S. Ramakrishna, *J. Membr. Sci.* **2006**, *283*, 209.
[271] F. Cui, Y. Li, J. Ge, *Mater. Sci. Eng. R Rep.* **2007**, *57*, 1.
[272] R. S. Barhate, S. Sundarrajan, D. Pliszka, S. Ramakrishna, *Filtr. Sep.* **2008**, *45*, 32.
[273] S. Kaur, R. Gopal, W. J. Ng, S. Ramakrishna, T. Matsuura, *MRS Bull.* **2008**, *33*, 21.
[274] M. G. Hajra, K. Mehta, G. G. Chase, *Sep. Purif. Technol.* **2003**, *30*, 79.
[275] H. Ma, K. Yoon, L. Rong, Y. Mao, Z. Mo, D. Fang, Z. Hollander, J. Gaiteri, B. S. Hsiao, B. Chu, *J. Mater. Chem.* **2010**, *20*, 4692.
[276] S. Xiao, M. Shen, R. Guo, Q. Huang, S. Wang, X. Shi, *J. Mater. Chem.* **2010**, *20*, 5700.
[277] S. Xiao, M. Shen, R. Guo, S. Wang, X. Shi, *J. Phys. Chem. C* **2009**, *113*, 18062.
[278] S. Xiao, S. Wu, M. Shen, R. Guo, Q. Huang, S. Wang, X. Shi, *ACS Appl. Mater. Interfaces* **2009**, *1*, 2848.
[279] X. Y. Ye, Z. M. Liu, Z. G. Wang, X. J. Huang, Z. K. Xu, *Mater. Lett.* **2009**, *63*, 1810.
[280] M. M. Demir, G. Ugur, M. A. Gulgun, Y. Z. Menceloglu, *Macromol. Chem. Phys.* **2008**, *209*, 508.
[281] A. C. Patel, S. Li, C. Wang, W. Zhang, Y. Wei, *Chem. Mater.* **2007**, *19*, 1231.
[282] A. Rodríguez, G. Ovejero, M. Romero, C. Díaz, M. Barreiro, J. García, *J. Supercritical Fluids* **2008**, *46*, 163.
[283] J. A. Lee, Y. S. Nam, G. C. Rutledge, P. T. Hammond, *Adv. Funct. Mater.* **2010**, *20*, 2424.
[284] A. E. Deniz, A. Celebioglu, F. Kayaci, T. Uyar, *Mater. Chem. Phys.* **2011**, *129*, 701.
[285] C. Li, R. Chen, X. Zhang, S. Shu, J. Xiong, Y. Zheng, W. Dong, *Mater. Lett.* **2011**, *65*, 1327.
[286] A. Rezaee, M. T. Ghaneian, N. Taghavinia, M. K. Aminian, S. J. Hashemian, *Environ. Technol.* **2009**, *30*, 233.
[287] M. N. Chong, B. Jin, H. Zhu, C. Chow, C. Saint, *Chem. Eng. J.* **2009**, *150*, 49.
[288] S. Doh, C. Kim, S. Lee, S. Lee, H. Kim, *J. Hazard. Mater.* **2008**, *154*, 118.
[289] D. Yang, H. Liu, Z. Zheng, Y. Yuan, J. Zhao, E. R. Waclawik, X. Ke, H. Zhu, *J. Am. Chem. Soc.* **2009**, *131*, 17885.
[290] X. Liu, Y. Gu, J. Huang, *Chem. Eur. J.* **2010**, *16*, 7730.
[291] G. Hota, B. R. Kumar, W. J. Ng, S. Ramakrishna, *J. Mater. Sci.* **2008**, *43*, 212.
[292] S. Wu, F. Li, H. Wang, L. Fu, B. Zhang, G. Li, *Polymer* **2010**, *51*, 6203.
[293] Y. N. Wu, F. Li, Y. Wu, W. Jia, P. Hannam, J. Qiao, *Colloid Polym. Sci.* **2011**, *289*, 1253.
[294] Y. Takahashi, S. Danwittayakul, T. M. Suzuki, *Analyst* **2009**, *134*, 1380.
[295] K. Stenderup, J. Justesen, C. Clausen, M. Kassem, *Bone* **2003**, *33*, 919.
[296] S. Li, X. Yue, Y. Jing, S. Bai, Z. Dai, *Colloid Surf. A* **2011**, *380*, 229.
[297] D. J. Yang, Z. F. Zheng, H. Y. Zhu, H. W. Liu, X. P. Gao, *Adv. Mater.* **2008**, *20*, 2777.
[298] B. Fugetsu, S. Satoh, T. Shiba, T. Mizutani, Y. Nodasaka, K. Yamazaki, K. Shimizu, M. Shindoh, K. Shibata, N. Nishi, Y. Sato, K. Tohji, F. Watari, *Bull. Chem. Soc. Jpn.* **2004**, *77*, 1945.
[299] Y. Dai, J. Niu, L. Yin, J. Xu, Y. Xi, *J. Hazard. Mater.* **2011**, *192*, 1409.
[300] F. Song, X. L. Wang, Y. Z. Wang, *Eur. Polym. J.* **2011**, *47*, 1885.
[301] S. Kaur, M. Kotaki, Z. Ma, R. Gopal, S. Ramakrishna, *Int. J. Neurosci.* **2006**, *5*, 1.
[302] T. Uyar, R. Havelund, J. Hacaloglu, F. Besenbacher, P. Kingshott, *ACS Nano* **2010**, *4*, 5121.
[303] D. Navarathne, Y. Ner, M. Jain, J. G. Grote, G. A. Sotzing, *Mater. Lett.* **2011**, *65*, 219.
[304] G. Singh, D. Rana, T. Matsuura, S. Ramakrishna, R. M. Narbaitz, S. Tabe, *Sep. Purif. Technol.* **2010**, *74*, 202.
[305] P. Chen, H. W. Liang, X. H. Lv, H. Z. Zhu, H. B. Yao, S. H. Yu, *ACS Nano* **2011**, *5*, 5928.
[306] D. Bjorge, N. Daels, S. De Vrieze, P. Dejans, T. Van Camp, W. Audenaert, J. Hogie, P. Westbroek, K. de Clerck, S. W. H. Van Hulle, *Desalination* **2009**, *249*, 942.
[307] S. S. Kim, D. Jung, U. H. Choi, J. Lee, *Ind. Eng. Chem. Res.* **2011**, *50*, 8693.
[308] N. Daels, S. De Vrieze, B. Decostere, P. Dejans, A. Dumoulin, K. De Clerck, *Desalination* **2010**, *257*, 170.
[309] N. L. Lala, R. Ramaseshan, L. Bojun, S. Sundarrajan, R. Barhate, L. Ying-jun, *Biotechnol. Bioeng.* **2007**, *97*, 1357.
[310] W. Wang, Q. Yang, L. Sun, H. Wang, C. Zhang, X. Fei, M. Sun, Y. Li, *J. Hazard. Mater.* **2011**, *194*, 185.

[311] K. Desai, K. Kit, J. Li, P. Michael Davidson, S. Zivanovic, H. Meyer, *Polymer* **2009**, *50*, 3661.
[312] B. Y. Lee, K. Behler, M. E. Kurtoglu, M. A. Wynosky-Dolfi, R. F. Rest, Y. Gogotsi, *J. Nanopart. Res.* **2010**, *12*, 2511.
[313] X. Peng, I. Ichinose, *Adv. Funct. Mater.* **2011**, *21*, 2080.
[314] X. Zhang, T. Zhang, J. Ng, D. D. Sun, *Adv. Funct. Mater.* **2009**, *19*, 3731.
[315] Z. Ma, M. Kotaki, S. Ramakrishna, *J. Membr. Sci.* **2005**, *265*, 115.
[316] R. Barhate, S. Ramakrishna, *J. Membr. Sci.* **2007**, *296*, 1.
[317] N. Daels, S. De Vrieze, I. Sampers, B. Decostere, P. Westbroek, A. Dumoulin, P. Dejans, K. de Clerck, S. W. H. Van Hulle, *Desalination* **2011**, *275*, 285.
[318] M. Botes, T. Eugene Cloete, *Crit. Rev. Microbiol.* **2010**, *36*, 68.
[319] K. Yoshimatsu, L. Ye, J. Lindberg, I. S. Chronakis, *Biosens. Bioelectron.* **2008**, *23*, 1208.
[320] M. Boopathi, B. Singh, R. Vijayaraghavan, *The Open Textile J.* **2008**, *1*, 1.
[321] S. Sundarrajan, A. R. Chandrasekaran, S. Ramakrishna, *J. Am. Ceram. Soc.* **2010**, *93*, 3955.
[322] J. A. Lee, K. C. Krogman, M. Ma, R. M. Hill, P. T. Hammond, G. C. Rutledge, *Adv. Mater.* **2009**, *21*, 1252.
[323] K. C. Krogman, J. L. Lowery, N. S. Zacharia, G. C. Rutledge, P. T. Hammond, *Nat. Mater.* **2009**, *8*, 512.
[324] S. Neubert, D. Pliszka, V. Thavasi, E. Wintermantel, S. Ramakrishna, *Mater. Sci. Eng. B* **2011**, *176*, 640.
[325] M. Roso, S. Sundarrajan, D. Pliszka, S. Ramakrishna, M. Modesti, *Nanotechnology* **2008**, *19*, 285707.
[326] L. Chen, L. Bromberg, H. Schreuder-Gibson, J. Walker, T. Hatton, G. Rutledge, *J. Mater. Chem.* **2009**, *19*, 2432.
[327] L. Chen, L. Bromberg, T. A. Hatton, G. C. Rutledge, *Polymer* **2007**, *48*, 4675.
[328] S. Sundarrajan, S. Ramakrishna, *J. Mater. Sci.* **2007**, *42*, 8400.
[329] R. Ramaseshan, S. Sundarrajan, Y. Liu, R. S. Barhate, N. L. Lala, S. Ramakrishna, *Nanotechnology* **2006**, *17*, 2947.
[330] R. Ramaseshan, S. Ramakrishna, *J. Am. Ceram. Soc.* **2007**, *90*, 1836.
[331] S. Sundarrajan, A. Venkatesan, S. Ramakrishna, *Macromol. Rapid Commun.* **2009**, *30*, 1769.
[332] G. Amitai, H. Murata, J. D. Andersen, R. R. Koepsel, A. J. Russell, *Biomaterials* **2010**, *31*, 4417.
[333] J. Lademann, A. Patzelt, S. Schanzer, H. Richter, I. Gross, K. Menting, L. Frazier, W. Sterry, C. Antoniou, *Skin Pharmacol. Physiol.* **2011**, *24*, 87.
[334] A. Sawhney, B. Condon, K. Singh, S. Pang, G. Li, D. Hui, *Text. Res. J.* **2008**, *78*, 731.
[335] X. J. Han, Z. M. Huang, C. L. He, L. Liu, Q. S. Wu, *Polym. Compos.* **2008**, *29*, 579.
[336] S. Lee, D. Kimura, K. H. Lee, J. C. Park, I. S. Kim, *Text. Res. J.* **2009**, *80*, 99.
[337] S. Lee, D. Kimura, A. Yokoyama, K. H. Lee, J. C. Park, I. S. Kim, *Text. Res. J.* **2009**, *79*, 1085.
[338] S. Lee, *Fiber. Polym.* **2009**, *10*, 295.
[339] X. Sun, L. Zhang, Z. Cao, Y. Deng, L. Liu, H. Fong, Y. Sun, *ACS Appl. Mater. Interfaces* **2010**, *2*, 952.
[340] J. Mosinger, O. Jirsk, P. Kubt, K. Lang, B. Mosinger, *J. Mater. Chem.* **2006**, *17*, 164.
[341] N. M. Bedford, A. J. Steckl, *ACS Appl. Mater. Interfaces* **2010**, *2*, 2448.
[342] S. Wang, Q. Yang, J. Du, J. Bai, Y. Li, *J. Appl. Polym. Sci.* **2007**, *103*, 2382.
[343] A. Laforgue, *J. Mater. Chem.* **2010**, *20*, 8233.
[344] Y. Y. Lv, J. Wu, Z. K. Xu, *Sens. Actuators B* **2010**, *148*, 233.
[345] T. T. T. Nguyen, J. S. Park, *J. Appl. Polym. Sci.* **2011**, *121*, 3596.
[346] M. Ramos, P. Bonelli, A. Cukierman, M. Ribeiro Carrott, P. Carrott, *J. Hazard. Mater.* **2010**, *177*, 175.
[347] H. Katepalli, M. Bikshapathi, C. S. Sharma, N. Verma, A. Sharma, *Chem. Eng. J.* **2011**, *171*, 1194.
[348] D. Wang, N. Liu, W. Xu, G. Sun, *J. Phys. Chem. C* **2011**, *115*, 6825.
[349] S. Lee, *J. Appl. Polym. Sci.* **2009**, *114*, 3652.
[350] S. Dadvar, H. Tavanai, H. Dadvar, M. Morshed, F. E. Ghodsi, *J. Sol-Gel Sci. Technol.* **2011**, *59*, 269.
[351] H. R. Pant, M. P. Bajgai, K. T. Nam, Y. A. Seo, D. R. Pandeya, S. T. Hong, H. Y. Kim, *J. Hazard. Mater.* **2011**, *185*, 124.
[352] T. Uyar, J. Hacaloglu, F. Besenbacher, *React. Funct. Polym.* **2009**, *69*, 145.
[353] A. Fathi-Azarbayjani, L. Qun, Y. W. Chan, S. Y. Chan, *AAPS Pharm. Sci. Technol.* **2010**, *11*, 1164.
[354] P. Taepaiboon, U. Rungsardthong, P. Supaphol, *Eur. J. Pharm. Biopharm.* **2007**, *67*, 387.
[355] X. M. Wu, C. J. Branford-White, D. G. Yu, N. P. Chatterton, L. M. Zhu, *Colloids Surf. B* **2011**, *82*, 247.
[356] L. P. Fan, K. H. Zhang, X. Y. Sheng, C. L. He, J. Li, X. M. Mo, H. S. Wang, "A Novel Skin-Care Product Based on Silk Fibroin Fabricated by Electrospinning", in *4th International Conference on Bioinformatics and Biomedical Engineering*, IEEE eXpress Conference Publishing, Chengdu **2010**.
[357] D. Klemm, D. Schumann, F. Kramer, N. Heßler, M. Hornung, H. P. Schmauder, S. Marsch, *Adv. Polym. Sci.* **2006**, *205*, 49.
[358] "All-purpose bio-cellulose mask with Botolift™", available from http://www.drwu.com/english/02_products/products_details.php?fid=8&pid=17, last accessed 2012/08/20.
[359] K. Frankenfeld, "NanoMasque – From biotechnology to cosmetics", available from http://www.nanomasque.de/seiten/englisch/research.html, last accessed 2012/08/20.
[360] N. Golubovic-Liakopoulos, S. R. Simon, B. Shah, *Semin. Cutan. Med. Surg.* **2011**, *30*, 176.
[361] http://agigma.com/home.html, last accessed 2012/08/20.
[362] P. Morganti, *Clin. Cosmet. Investig. Dermatol.* **2010**, *3*, 5.
[363] P. Morganti, G. Morganti, *Clin. Dermatol.* **2008**, *26*, 334.
[364] P. Morganti, "Chitin nanofibrils and their derivatives as cosmeceuticals," in *Chitin, Chitosan, Oligosaccharides and Their Derivatives* (Ed., S.-K. Kim), CRC Press, Boca Raton **2011**, Chapter 37, pp. 531–541.
[365] S. Lee, S. K. Obendorf, *Text. Res. J.* **2007**, *77*, 696.
[366] Y. K. Kang, C. H. Park, J. Y. Kim, T. J. Kang, *Fiber Polym.* **2007**, *8*, 564.
[367] L. A. Smith, X. Liu, J. Hu, P. Wang, P. X. Ma, *Tissue Eng. Part A* **2009**, *15*, 1855.
[368] N. S. Binulal, M. Deepthy, N. Selvamurugan, K. T. Shalumon, S. Suja, U. Mony, R. Jayakumar, S. V. Nair, *Tissue Eng. Part A* **2010**, *16*, 393.
[369] C. Barrera, C. Rinaldi, M. Satcher, J. P. Hinestroza, "Electrospun Nanofibers with Magnetic Domains for Smart Tagging of Textile Products," in *Handbook of Nanoscience, Engineering and Technology*, (Eds: W. A. Goddard III, D. Brenner, S. E. Lyshevski, G. J. Iafrate), 2nd edition, CRC Press, Boca Raton, FL **2007**, Chapter 21.3, pp. 21/17-21/26.
[370] E. Gasana, P. Westbroek, J. Hakuzimana, K. Declerck, G. Priniotakis, P. Kiekens, *Surf. Coat. Technol.* **2006**, *201*, 3547.
[371] S. Cetiner, F. Kalaoglu, H. Karakas, A. S. Sarac, *Text. Res. J.* **2010**, *80*, 1784.
[372] H. L. Schreuder-Gibson, Q. Truong, J. E. Walker, J. R. Owens, J. D. Wander, W. E. Jones, Jr, *MRS Bull.* **2008**, *28*, 574.
[373] M. Sonehara, T. Sato, M. Takasaki, H. Konishi, K. Yamasawa, Y. Miura, *IEEE Trans. Magn.* **2008**, *44*, 3107.

[374] S. Sundarrajan, R. Murugan, A. S. Nair, S. Ramakrishna, *Mater. Lett.* **2010**, *64*, 2369.
[375] J. T. Yang, B. L. Bader, J. A. Kreidberg, M. Ullman-Culleré, J. E. Trevithick, R. O. Hynes, *Dev. Biol.* **1999**, *215*, 264.
[376] E. K. F. Yim, S. W. Pang, K. W. Leong, *Exp. Cell Res.* **2007**, *313*, 1820.
[377] M. F. Ashby, P. J. Ferreira, D. L. Schodek, "Nanomaterial Product Forms and Functions," in *Nanomaterials, Nanotechnologies and Design: An Introduction for Engineers and Architects*, (Eds., M. F. Ashby, P. J. Ferreira, D. L. Schodek), Elsevier, New York **2009**, Chapter 10, pp. 403–465.
[378] Y. Z. Long, M. M. Li, C. Gu, M. Wan, J. L. Duvail, Z. Liu, Z. Fan, *Prog. Polym. Sci.* **2011**, *36*, 1415.
[379] X. Wang, C. Drew, S. H. Lee, K. J. Senecal, J. Kumar, L. A. Samuelson, *Nano Lett.* **2002**, *2*, 1273.
[380] Y. Long, H. Chen, Y. Yang, H. Wang, Y. Yang, N. Li, K. Li, J. Pei, F. Liu, *Macromolecules* **2009**, *42*, 6501.
[381] Y. Li, J. Gong, G. He, Y. Deng, *Mater. Chem. Phys.* **2011**, *129*, 477.
[382] T. L. Kelly, T. Gao, M. J. Sailor, *Adv. Mater.* **2011**, *23*, 1776.
[383] J. Choi, E. J. Park, D. W. Park, S. E. Shim, *Synth. Met.* **2010**, *160*, 2664.
[384] N. L. Lala, V. Thavasi, S. Ramakrishna, *Sensors* **2009**, *9*, 86.
[385] J. Huang, S. Virji, B. H. Weiller, R. B. Kaner, *Chem. Eur. J.* **2004**, *10*, 1314.
[386] S. Virji, R. B. Kaner, B. H. Weiller, "Detection of Toxic Chemicals for Homeland Security Using Polyaniline Nanofibers," in *Anti-Terrorism and Homeland Defense*, (Eds., J. G. Reynolds, G. E. Lawson, C. J. Koester), Volume 980 in *ACS Symposium Series*, American Chemical Society, Washington **2007**, pp. 101–115.
[387] J. D. Fowler, S. Virji, R. B. Kaner, B. H. Weiller, *J. Phys. Chem. C* **2009**, *113*, 6444.
[388] F. W. Zeng, X. X. Liu, D. Diamond, K. T. Lau, *Sens. Actuators B* **2010**, *143*, 530.
[389] S. Virji, J. D. Fowler, C. O. Baker, J. Huang, R. B. Kaner, B. H. Weiller, *Small* **2005**, *1*, 624.
[390] S. Virji, R. Kojima, J. D. Fowler, R. B. Kaner, B. H. Weiller, *Chem. Mater.* **2009**, *21*, 3056.
[391] P. Li, Y. Li, B. Ying, M. Yang, *Sens. Actuators B* **2009**, *141*, 390.
[392] Y. Liao, C. Zhang, Y. Zhang, V. Strong, J. Tang, X. G. Li, K. Kalantar-zadeh, E. M. V. Hoek, K. L. Wang, R. B. Kaner, *Nano Lett.* **2011**, *11*, 954.
[393] H. D. Tran, K. Shin, W. G. Hong, J. M. D'Arcy, R. W. Kojima, B. H. Weiller, R. B. Kaner, *Macromol. Rapid Commun.* **2007**, *28*, 2289.
[394] L. Al-Mashat, H. D. Tran, W. Wlodarski, R. B. Kaner, K. Kalantar-Zadeh, *IEEE Sens. J.* **2008**, *8*, 365.
[395] H. Bai, L. Zhao, C. Lu, C. Li, G. Shi, *Polymer* **2009**, *50*, 3292.
[396] J. Choi, J. Lee, J. Choi, D. Jung, S. E. Shim, *Synth. Met.* **2010**, *160*, 1415.
[397] L. Spinelle, M. Dubois, J. Brunet, K. Guérin, V. Parra, C. Varenne, *J. Nanosci. Nanotechnol.* **2010**, *10*, 5653.
[398] S. Santangelo, G. Messina, G. Faggio, M. G. Willinger, N. Pinna, A. Donato, A. Arena, N. Donato, G. Neri, *Diamond Relat. Mater.* **2010**, *19*, 590.
[399] A. Z. Sadek, C. O. Baker, D. A. Powell, W. Wlodarski, R. B. Kaner, K. Kalantar-Zadeh, *IEEE Sens. J.* **2007**, *7*, 213.
[400] L. Al-Mashat, H. D. Tran, W. Wlodarski, R. B. Kaner, K. Kalantar-Zadeh, *Sens. Actuators B* **2008**, *134*, 826.
[401] X. Wang, Y. G. Kim, C. Drew, B. C. Ku, J. Kumar, L. A. Samuelson, *Nano Lett.* **2004**, *4*, 331.
[402] E. Spain, R. Kojima, R. B. Kaner, G. G. Wallace, J. O'Grady, K. Lacey, T. Barry, T. E. Keyes, R. J. Forster, *Biosens. Bioelectron.* **2011**, *26*, 2613.
[403] Q. Zhu, M. Han, H. Wang, L. Liu, J. Bao, Z. Dai, J. Shen, *Analyst* **2010**, *135*, 2579.
[404] P. M. Ndangili, T. T. Waryo, M. Muchindu, P. G. Baker, C. J. Ngila, E. I. Iwuoha, *Electrochim. Acta* **2010**, *55*, 4267.
[405] T. Zhang, W. Wang, D. Zhang, X. Zhang, Y. Ma, Y. Zhou, L. Qi, *Adv. Funct. Mater.* **2010**, *20*, 1152.
[406] H. Tang, F. Yan, Q. Tai, H. L. Chan, *Biosens. Bioelectron.* **2010**, *25*, 1646.
[407] D. Liu, Y. Liu, H. Hou, T. You, *J. Nanomater.* **2010**, *2010*, 1.
[408] V. Stavyiannoudaki, V. Vamvakaki, N. Chaniotakis, *Anal. Bioanal. Chem.* **2009**, *395*, 429.
[409] D. Rathod, C. Dickinson, D. Egan, E. Dempsey, *Sens. Actuators B* **2010**, *143*, 547.
[410] S. Virji, J. Huang, R. B. Kaner, B. H. Weiller, *Nano Lett.* **2004**, *4*, 491.
[411] C. Weisbuch, B. Vinter, "*Quantum Semiconductor Structures: Fundamentals and Applications*," Reprint edition, Elsevier, Amsterdam **1991**, pp. 252.
[412] Y. Xia, P. Yang, Y. Sun, Y. Wu, B. Mayers, B. Gates, Y. Yin, F. Kim, H. Yan, *Adv. Mater.* **2003**, *15*, 353.
[413] P. Pauzauskie, P. Yang, *Mater. Today* **2006**, *9*, 36.
[414] G. Patzke, F. Krumeich, R. Nesper, *Angew. Chem. Int. Ed.* **2002**, *41*, 2446.
[415] N. Mathews, B. Varghese, C. Sun, V. Thavasi, B. Andreasson, C. Sow, S. Ramakrishna, S. G. Mhaisalkar, *Nanoscale* **2010**, *2*, 1984.
[416] O. Hayden, R. Agarwal, C. M. Lieber, *Nat. Mater.* **2006**, *5*, 352.
[417] H. Ohnishi, *Nature* **1998**, *395*, 780.
[418] S. Barth, F. Hernandez-Ramirez, J. Holmes, A. Romano-Rodriguez, *Prog. Mater. Sci.* **2010**, *55*, 563.
[419] W. Lu, P. Xie, C. Lieber, *IEEE Trans. Electron. Dev.* **2008**, *55*, 2859.
[420] O. Hayden, R. Agarwal, W. Lu, *Nano Today* **2008**, *3*, 12.
[421] I. Gonzalez-Valls, M. Lira-Cantu, *Energy Environ. Sci.* **2009**, *2*, 19.
[422] A. Alivisatos, *Science* **1996**, *271*, 933.
[423] T. Wolkenstein, "*Electronic Processes on Semiconductor Surfaces during Chemisorption*," Plenum Publishing, New York **1991**, p. 444.
[424] N. Yamazoe, *Sens. Actuators B* **2005**, *108*, 22.
[425] M. Arnold, P. Avouris, Z. Pan, Z. Wang, *J. Phys. Chem. B* **2003**, *107*, 659.
[426] Ç. Kiliç, A. Zunger, *Phys. Rev. Lett.* **2002**, *88*, 955011.
[427] S. Bae, C. Na, J. Kang, J. Park, *J. Phys. Chem. B* **2005**, *109*, 2526.
[428] J. Chen, J. Wang, R. Zhuo, D. Yan, J. Feng, F. Zhang, P. X. Yan, *Appl. Surf. Sci.* **2009**, *255*, 3959.
[429] P. Nguyen, H. Ng, J. Kong, A. Cassell, R. Quinn, J. Li, J. Han, M. McNeil, M. Meyyappan, *Nano Lett.* **2003**, *3*, 925.
[430] Q. Wan, E. Dattoli, W. Lu, *Appl. Phys. Lett.* **2007**, *90*, 222107.
[431] R. Pohle, M. Fleischer, H. Meixner, *Sens. Actuators B* **2000**, *68*, 151.
[432] Q. Wan, E. Dattoli, W. Lu, *Small* **2008**, *4*, 451.
[433] S. Ju, K. Lee, M. H. Yoon, A. Facchetti, T. Marks, D. Janes, *Nanotechnology* **2007**, *18*, 1.
[434] P. Archana, R. Jose, C. Vijila, S. Ramakrishna, *J. Phys. Chem. C* **2009**, *113*, 21538.
[435] N. Ramgir, Y. Yang, M. Zacharias, *Small* **2010**, *6*, 1705.
[436] Y. Dai, W. Liu, E. Formo, Y. Sun, Y. Xia, *Polym. Adv. Technol.* **2011**, *22*, 326.

[437] F. Hernandez-Ramirez, J. Prades, R. Jimenez-Diaz, T. Fischer, A. Romano-Rodriguez, S. Mathur, J. R. Morante, *Phys. Chem. Chem. Phys.* **2009**, *11*, 7105.
[438] N. Barsan, U. Weimar, *J. Electroceram.* **2001**, *7*, 143.
[439] M. Batzill, *Prog. Surf. Sci.* **2005**, *79*, 47.
[440] J. Prades, *J. Electrochem. Soc.* **2007**, *154*, H675.
[441] J. Prades, *Sens. Actuators B* **2007**, *126*, 62.
[442] D. Kim, *Nano Lett* **2009**, *9*, 1984.
[443] R. van der Wal, G. Berger, M. Kulis, G. Hunter, J. Xu, L. Evans, *Sensors* **2009**, *9*, 7866.
[444] B. Ding, M. Wang, J. Yu, G. Sun, *Sensors* **2009**, *9*, 1609.
[445] P. Gouma, *Rev. Adv. Mater. Sci.* **2003**, *5*, 147.
[446] G. Wang, Y. Ji, X. Huang, X. Yang, P. I. Gouma, M. Dudley, *J. Phys. Chem. B* **2006**, *110*, 23777.
[447] M. Yang, T. Xie, L. Peng, Y. Zhao, D. Wang, *Appl. Phys. A: Mater. Sci. Process.* **2007**, *89*, 427.
[448] I. D. Kim, A. Rothschild, B. Lee, D. Kim, S. Jo, H. Tuller, *Nano Lett.* **2006**, *6*, 2009.
[449] W. Jia, L. Su, Y. Ding, A. Schempf, Y. Wang, Y. Lei, *J. Phys. Chem. C* **2009**, *113*, 16402.
[450] H. Liu, J. Kameoka, D. Czaplewski, H. Craighead, *Nano Lett.* **2004**, *4*, 671.
[451] N. J. K. Laxminarayana, *Text. Res. J.* **2005**, *75*, 670.
[452] O. Landau, A. Rothschild, E. Zussman, *Chem. Mater.* **2009**, *21*, 9.
[453] J. Park, S. W. Choi, J. W. Lee, C. Lee, S. Kim, *J. Am. Ceram. Soc.* **2009**, *92*, 2551.
[454] I. D. Kim, A. Rothschild, B. Lee, D. Kim, S. Jo, H. Tuller, *Nano Lett.* **2006**, *6*, 2009.
[455] Z. Li, H. Zhang, W. Zheng, W. Wang, H. Huang, C. Wang, A. G. MacDiarmid, Y. Wei, *J. Am. Chem. Soc.* **2008**, *130*, 5036.
[456] B. Ding, M. Wang, J. Yu, G. Sun, *Sensors* **2009**, *9*, 1609.
[457] Q. Qi, T. Zhang, L. Liu, X. Zheng, *Sens. Actuators B* **2009**, *137*, 471.
[458] A. Yang, X. Tao, R. Wang, S. Lee, C. Surya, *Appl. Phys. Lett.* **2007**, *91*, 133110.
[459] X. Song, Z. Wang, Y. Liu, C. Wang, L. Li, *Nanotechnology* **2009**, *20*, 075501.
[460] Z. X. Wang, L. Liu, *Mater. Lett.* **2009**, *63*, 917.
[461] A. Vomiero, S. Bianchi, E. Comini, G. Faglia, M. Ferroni, G. Sberveglieri, *Cryst. Growth Des.* **2007**, *7*, 2500.
[462] B. R. Prasad, M. A. Brook, T. Smith, S. Zhao, Y. Chen, H. Sheardown, R. D'souza, Y. Rochev, *Colloids Surf. B* **2010**, *78*, 237.
[463] J. Wang, B. Zou, S. Ruan, J. Zhao, Q. Chen, F. Wu, *Mater. Lett.* **2009**, *63*, 1750.
[464] W. Y. Wu, J. M. Ting, P. J. Huang, *Nanoscale Res. Lett.* **2009**, *4*, 513.
[465] Q. Li, Y. Liang, Q. Wan, T. Wang, *Appl. Phys. Lett.* **2004**, *85*, 6389.
[466] W. Zheng, X. Lu, W. Wang, Z. Li, H. Zhang, Z. Wang, X. Xu, S. Li, C. Wang, *J. Colloid Interface Sci.* **2009**, *338*, 366.
[467] G. Wang, Y. Ji, X. Huang, X. Yang, P. I. Gouma, M. Dudley, *J. Phys. Chem. B* **2006**, *110*, 23777.
[468] K. Sahner, P. Gouma, R. Moos, *Sensors* **2007**, *7*, 1871.
[469] Y. Chen, X. Xue, Y. Wang, T. Wang, *Appl. Phys. Lett.* **2005**, *87*, 233503.
[470] J. Prades, R. Jimenez-Diaz, F. Hernandez-Ramirez, S. Barth, A. Cirera, A. Romano-Rodriguez, S. Mathur, J. R. Morante, *Appl. Phys. Lett.* **2008**, *93*, 123110.
[471] B. Wang, L. Zhu, Y. Yang, N. Xu, G. Yang, *J. Phys. Chem. C* **2008**, *112*, 6643.
[472] N. Ramgir, I. Mulla, K. Vijayamohanan, *Sens. Actuat. B.* **2005**, *107*, 708.
[473] M. Song, D. Kim, K. Ihn, S. Jo, D. Kim, *Nanotechnology* **2004**, *15*, 1861.
[474] W. Zhang, R. Zhu, X. Liu, B. Liu, S. Ramakrishna, *Appl. Phys. Lett.* **2009**, *95*, 043304.
[475] M. Law, L. Greene, J. Johnson, R. Saykally, P. Yang, *Nat. Mater.* **2005**, *4*, 455.
[476] B. Lee, M. Song, S. Y. Jang, S. Jo, S. Y. Kwak, D. Kim, *J. Phys. Chem. C* **2009**, *113*, 21453.
[477] P. Joshi, L. Zhang, D. Davoux, Z. Zhu, D. Galipeau, H. Fong, Q. Qiao, *Energy Environ. Sci.* **2010**, *3*, 1507.
[478] H. Kokubo, B. Ding, T. Naka, H. Tsuchihira, S. Shiratori, *Nanotechnology* **2007**, *18*, 165604.
[479] K. Onozuka, B. Ding, Y. Tsuge, T. Naka, M. Yamazaki, S. Sugi, S. Ohno, M. Yoshikawa, S. Shiratori, *Nanotechnology* **2006**, *17*, 1026.
[480] S. Yun, S. Lim, *J. Solid State Chem.* **2011**, *184*, 273.
[481] I. D. Kim, J. M. Hong, B. Lee, D. Kim, E. K. Jeon, D. K. Choi, D. J. Yang, *Appl. Phys. Lett.* **2007**, *91*, 163109.
[482] M. S. Park, *Adv. Funct. Mater.* **2008**, *18*, 455.
[483] C. Kim, K. Yang, M. Kojima, K. Yoshida, Y. Kim, Y. Kim, M. Endo, *Adv. Funct. Mater.* **2006**, *16*, 2393.
[484] L. Wang, Y. Yu, P. C. Chen, C. H. Chen, *Scr. Mater.* **2008**, *58*, 405.
[485] J. Y. Liao, J. W. He, H. Xu, D. B. Kuang, C. Y. Su, *J. Mater. Chem.* **2012**, *22*, 7910.
[486] E. Naveen Kumar, R. Jose, P. Archana, C. Vijila, M. Yusoff, S. Ramakrishna, *Energy Environ. Sci.* **2012**, *5*, 5401.
[487] C. Gao, X. Li, B. Lu, L. Chen, Y. Wang, F. Teng, J. Wang, Z. Zhang, X. Pan, E. Xie, *Nanoscale* **2012**, *4*, 3475.
[488] R. Sahaya, J. Sundaramurthya, P. S. Kumara, V. Thavasib, S. Mhaisalkara, S. Ramakrishnab, *J. Solid State Chem.* **2012**, *186*, 261.
[489] S. Chuangchote, T. Sagawa, S. Yoshikawa, *Appl. Phys. Lett.* **2008**, *93*, 033310.
[490] M. Song, D. Kim, S. Jo, D. Kim, *Synth. Met.* **2005**, *155*, 635.
[491] M. Song, D. Kim, K. Ihn, S. Jo, D. Kim, *Synth. Met.* **2005**, *153*, 77.
[492] P. Joshi, L. Zhang, D. Davoux, Z. Zhu, D. Galipeau, H. Fong, Q. Qiao, *Energy Environ. Sci.* **2010**, *3*, 1507.
[493] K. Onozuka, B. Ding, Y. Tsuge, T. Naka, M. Yamazaki, S. Sugi, S. Ohno, M. Yoshikawa, S. Shiratori, *Nanotechnology* **2006**, *17*, 1026.
[494] H. Kokubo, B. Ding, T. Naka, H. Tsuchihira, S. Shiratori, *Nanotechnology* **2007**, *18*, 165604.
[495] W. Zhang, R. Zhu, X. Liu, B. Liu, S. Ramakrishna, *Appl. Phys. Lett.* **2009**, *95*, 043304.
[496] I. D. Kim, J. M. Hong, B. Lee, D. Kim, E. K. Jeon, D. K. Choi, D. J. Yang, *Appl. Phys. Lett.* **2007**, *91*, 163109.
[497] S. Yun, S. Lim, *J. Solid State Chem.* **2011**, *184*, 273.
[498] Y. Gu, D. Chen, X. Jiao, *J. Phys. Chem. B* **2005**, *109*, 17901.
[499] Y. Gu, D. Chen, X. Jiao, F. Liu, *J. Mater. Chem.* **2007**, *17*, 1769.
[500] H. W. Lu, D. Li, K. Sun, Y. S. Li, Z. W. Fu, *Solid State Sci.* **2009**, *11*, 982.
[501] P. Viswanathamurthi, N. Bhattarai, H. Kim, M. Khil, D. Lee, E. K. Suh, *J. Chem. Phys.* **2004**, *121*, 441.
[502] K. Sun, H. W. Lu, D. Li, W. Zeng, Y. S. Li, Z. W. Fu, *Wuji Cailiao Xuebao* **2009**, *24*, 357.
[503] H. Han, T. Song, J. Y. Bae, L. F. Nazar, H. Kim, U. Paik, *Energy Environ. Sci.* **2011**, *4*, 4532.
[504] L. Ji, A. Medford, X. Zhang, *J. Mater. Chem.* **2009**, *19*, 5593.
[505] L. Ji, X. Zhang, *Electrochem. Commun.* **2009**, *11*, 795.
[506] L. Wang, Y. Yu, P. Chen, D. Zhang, C. Chen, *J. Power Sources* **2008**, *183*, 717.
[507] L. Wang, Y. Yu, P. C. Chen, C. H. Chen, *Scr. Mater.* **2008**, *58*, 405.

[508] Y. Yu, L. Gu, C. Zhu, P. Van Aken, J. Maier, *J. Am. Chem. Soc.* **2009**, *131*, 15984.
[509] Y. Yu, L. Gu, C. Wang, A. Dhanabalan, P. Van Aken, J. Maier, *Angew. Chem. Int. Ed. Engl.* **2009**, *48*, 6485.
[510] L. Ji, K. H. Jung, A. Medford, X. Zhang, *J. Mater. Chem.* **2009**, *19*, 4992.
[511] X. Fan, L. Zou, Y. P. Zheng, F. Y. Kang, W. C. Shen, *Electrochem. Solid-State Lett.* **2009**, *12*, A199.
[512] L. Ji, Z. Lin, R. Zhou, Q. Shi, O. Toprakci, A. Medford, C. R. Millns, X. Zhang, *Electrochim. Acta* **2010**, *55*, 1605.
[513] L. Ji, Z. Lin, A. Medford, X. Zhang, *Chem. Eur. J.* **2009**, *15*, 10718.
[514] L. Ji, X. Zhang, *Nanotechnology* **2009**, *20*, 155705.
[515] H. W. Lu, L. Yu, W. Zeng, Y. S. Li, Z. W. Fu, *Electrochem. Solid State* **2008**, *11*, A140.
[516] Y. Gu, D. Chen, X. Jiao, *J. Phys. Chem. B* **2005**, *109*, 17901.
[517] Y. Gu, D. Chen, X. Jiao, F. Liu, *J. Mater. Chem.* **2007**, *17*, 1769.
[518] Y. Ding, P. Zhang, Z. Long, Y. Jiang, F. Xu, *J. Alloys Compd.* **2009**, *487*, 507.
[519] K. Gao, X. Hu, C. Dai, T. Yi, *Mater. Sci. Eng. B* **2006**, *131*, 100.
[520] S. Choi, J. Kim, S. Jo, W. Lee, Y. R. Kim, *J. Electrochem. Soc.* **2005**, *152*, A989.
[521] H. R. Jung, D. H. Ju, W. J. Lee, X. Zhang, R. Kotek, *Electrochim. Acta* **2009**, *54*, 3630.